



UNIVERSITEIT VAN PRETORIA  
UNIVERSITY OF PRETORIA  
YUNIBESITHI YA PRETORIA

# Aspects of facial features in a South African sample as applicable for facial approximations

by

Heléne Francia Dorfling

Dissertation submitted in fulfilment of the requirements for the degree of

**MASTER OF SCIENCES**

in the

**FACULTY OF HEALTH SCIENCES**

Department of Anatomy

University of Pretoria

2017

The Research Ethics Committee, Faculty Health Sciences, University of Pretoria complies with ICH-GCP guidelines and has US Federal wide Assurance.

- FWA 00002567, Approved dd 22 May 2002 and Expires 20 Oct 2016.
- IRB 0000 2235 IORG0001762 Approved dd 22/04/2014 and Expires 22/04/2017.



UNIVERSITEIT VAN PRETORIA  
UNIVERSITY OF PRETORIA  
YUNIBESITHI YA PRETORIA

Faculty of Health Sciences Research Ethics Committee

28/01/2016

**Approval Certificate  
New Application**

**Ethics Reference No.: 8/2016**

**Title:** Aspects of facial features in a South African sample as applicable for facial approximations

Dear Helene Dorfling

The **New Application** as supported by documents specified in your cover letter dated 5/01/2016 for your research received on the 5/01/2016, was approved by the Faculty of Health Sciences Research Ethics Committee on its quorate meeting of 27/01/2016.

Please note the following about your ethics approval:

- Ethics Approval is valid for 2 years
- Please remember to use your protocol number (**8/2016**) on any documents or correspondence with the Research Ethics Committee regarding your research.
- Please note that the Research Ethics Committee may ask further questions, seek additional information, require further modification, or monitor the conduct of your research.

**Ethics approval is subject to the following:**

- The ethics approval is conditional on the receipt of 6 monthly written Progress Reports, and
- The ethics approval is conditional on the research being conducted as stipulated by the details of all documents submitted to the Committee. In the event that a further need arises to change who the investigators are, the methods or any other aspect, such changes must be submitted as an Amendment for approval by the Committee.

We wish you the best with your research.

Yours sincerely

**Professor Werdie (CW) Van Staden**

MBChB MMed(Psych) MD FCPsych FTCL UPLM

Chairperson: Faculty of Health Sciences Research Ethics Committee

*The Faculty of Health Sciences Research Ethics Committee complies with the SA National Act 61 of 2003 as it pertains to health research and the United States Code of Federal Regulations Title 45 and 46. This committee abides by the ethical norms and principles for research, established by the Declaration of Helsinki, the South African Medical Research Council Guidelines as well as the Guidelines for Ethical Research: Principles Structures and Processes 2004 (Department of Health).*

## DECLARATION

I declare that the dissertation that I am hereby submitting to the University of Pretoria for the MSc degree in Anatomy is my own work and that I have never before submitted it to any other tertiary institution for any degree.

\_\_\_\_\_

Heléne Francia Dorfling

\_\_\_\_\_ day of \_\_\_\_\_ 2017

# CONTENTS

Summary .....	v
Acknowledgements.....	vii
List of tables.....	viii
List of figures .....	ix
<b>1. Introduction .....</b>	<b>1</b>
<b>1.1. Aim .....</b>	<b>4</b>
<b>2. Literature review .....</b>	<b>5</b>
<b>2.1. Applied osteology of the skull .....</b>	<b>5</b>
2.1.1. Anterior view .....	6
2.1.2. Lateral view.....	9
2.1.3. The Bony Orbits.....	9
<b>2.2. Anatomy of the facial features.....</b>	<b>12</b>
2.2.1. The Eyes .....	14
2.2.2. The Nose .....	16
2.2.3. The Lips .....	19
2.2.4. The External Ears.....	22
<b>2.3. Known guidelines for reconstructing facial features in a forensic setting .....</b>	<b>24</b>
2.3.1. The Eyes .....	24
2.3.2. The Nose .....	27
2.3.3. The Mouth.....	29
2.3.4. The Ears.....	30
<b>2.4. Possible shortcomings of established guidelines .....</b>	<b>32</b>
<b>3. Materials and methods.....</b>	<b>34</b>
<b>3.1. Sample.....</b>	<b>34</b>
<b>3.2. Ethical considerations.....</b>	<b>35</b>
<b>3.3. Methodology.....</b>	<b>35</b>
3.3.1. Orbital and ocular measurements .....	39
3.3.2. Nasal measurements .....	48

3.3.3.	Oral measurements .....	55
3.3.4.	Auricular measurements.....	59
<b>3.4.</b>	<b>Statistical analyses: Intra - and inter-observer repeatability testing .....</b>	<b>61</b>
<b>4.</b>	<b>Results .....</b>	<b>63</b>
4.1.	Intra-observer repeatability testing and standard deviations on individual measurements.....	63
4.2.	Inter-observer repeatability testing.....	64
4.3.	Variation between the sexes .....	68
4.4.	Dimensions obtained on facial features .....	68
4.4.1.	Orbital and ocular measurements .....	68
4.4.2.	Nasal Measurements .....	78
4.4.3.	Oral measurements .....	81
4.4.4.	Auricular measurements.....	88
<b>5.</b>	<b>Discussion.....</b>	<b>97</b>
5.1.	Intra- and inter-observer repeatability .....	97
5.2.	Orbital and ocular dimensions .....	98
5.3.	Nasal dimensions .....	103
5.4.	Oral measurements and relationships.....	103
5.5.	Auricular dimensions .....	105
5.6.	Limitations and shortcomings .....	106
5.6.1.	Sample size.....	106
5.6.2.	Inter-observer correlations .....	107
5.6.3.	Individual features .....	107
<b>6.</b>	<b>Conclusion .....</b>	<b>109</b>
<b>7.</b>	<b>References.....</b>	<b>111</b>
	<b>Appendix A .....</b>	<b>116</b>
	<b>Appendix B.....</b>	<b>117</b>
	<b>Appendix C.....</b>	<b>120</b>

## SUMMARY

Identification of unknown individuals remains a challenge in the South African context. When it is not possible to identify the unknown individual with primary identifiers, e.g. DNA comparisons, forensic facial approximations (FA) are often used. The aim of this study was to evaluate existing guidelines for FA on a sample of black South Africans (BSA). Facial features considered were the eyes, nose, mouth and ears. The study sample consisted of 49 cadavers (38 males and 11 females, mean age 47), 30 computer tomography (CT) scans (23 males, 7 females, mean age 42) and 30 cone beam computer tomography (CBCT) scans (17 males and 13 females, mean age 33) of BSA. Orbital measurements on dissections included the position of the canthi, the diameters and position of the eyeball and the derived height and width of the orbit. Multiplanar level ocular and orbital depth measurements were performed on CT and CBCT scans using MevisLab ([www.mevislab.de](http://www.mevislab.de)). The relationship between the features of the anterior nasal spine (ANS) and the shape of the nasal tip was evaluated on dissections. Gerasimov's two-tangent method for determining the position of the nasal tip was performed on lateral view photographs of the dissected nose. Dental predictors of the width of the mouth and the philtrum were evaluated. Previously published formulae for the prediction of ear length were tested and population specific formulae designed, taking sex and age into consideration. In general, repeatability tests were acceptable apart from those dimensions involving the orbital canal, medial orbital margin and the philtrum. The eyeball was found to be slightly larger than expected, oval-shaped and supero-laterally placed in a rectangular shaped orbit with an eye fissure sloping slightly downwards laterally. A non-projecting nose with a bulbous nasal tip was the most commonly observed, however, no clear association with the features of the ANS was found. The two-tangent method could also not consistently predict the nasal tip position. The cheilia most often corresponded to the canine/first-premolar junction, while the inter-canine width constituted 60% of the mouth width. No statistically significant correlation could be observed between the upper central incisor width and the flat/absent philtrum width. Therefore, facial approximations guidelines for BSA should include a slightly larger and oval shaped eyeball with an eye fissure sloping slightly downwards laterally and a non-projecting nose with a bulbous tip. A 60% instead of a 75% rule should be used when predicting the mouth width and the cheilia should then correspond

to the canine/first-premolar junction. A flat philtrum should be expected. A shorter ear should be used, and the possible influence of sex and age should be taken into consideration when using population specific formulae. With this study possible limitations of the existing guidelines for approximating facial features in BSA were investigated and adaptations suggested. By increasing the sample size, future studies might address the possible influence of sex and aging. Certain landmarks could be revised to improve repeatability and other methodologies should be explored to approximate the nose in BSA.

Keywords: Black South Africans; population specific guidelines; endocanthion; exocanthion; philtrum; cheilion; skull; anterior nasal spine; ears

## ACKNOWLEDGEMENTS

I would like to express my sincerest gratitude and respect to my supervisor Prof. Anna Oettlé for her invaluable acumen, guidance, infectious enthusiasm, motivation and boundless patience. Much appreciation also to my co-supervisor Prof. Maryna Steyn, for her valuable advice, insight and enthusiasm.

This project was only possible due to the support and guidance of the various people at the Departments of Anatomy at the University of Pretoria and Sefako Makgatho Health Sciences University. Additionally, I would like to thank Samantha Pretorius for her aid in the statistical analysis of the data.

Special thanks to AESOP for the opportunity and funding to study abroad at Liverpool John Moores University, and the staff at LJMU who greatly inspired me and made me feel at home, especially Dr Matteo Borrini, Sarah and Mark.

To my family, especially my parents and Deon Swanepoel: thank you for the support, understanding, optimism and love, which enabled me to persist in this endeavour.

## LIST OF TABLES

Table 2.1 Bony and other landmarks .....	13
Table 3.1 Interpretation of the ICC test.....	61
Table 4.1 Standard deviations calculated for all orbital and ocular measurements.....	65
Table 4.2 Standard deviations calculated for all oral and auricular measurements on cadaver samples.....	66
Table 4.3 Inter-observer repeatability testing by means of ICC or Fleiss's Kappa (level of agreement between observers). .....	67
Table 4.4 Variation between male and female parameters Investigated by means of non-parametric Wilcoxon Rank Sum Test (2-sided).....	69
Table 4.5 Occurrence of ANS shapes. ....	78
Table 4.6 Occurrence of nasal tip shapes. ....	79
Table 4.7 Probability of nasal tip shape predicted by ANS shape. ....	80
Table 4.8 Correlation between mouth width and inter-canine width. ....	84
Table 4.9 Correlation between philtrum width and upper central incisor width. ....	86
Table 4.10 Regression formulae utilised in this study (where age is chronological age in years and sex is a dummy variable (female = 0 and male = 1)).....	93

## LIST OF FIGURES

Figure 2.1 Osteology of the skull on an anterior view .....	8
Figure 2.2 The bony orbit .....	11
Figure 2.3 Anatomy of the eyelid.....	15
Figure 2.4 Anatomy of the external nose .....	17
Figure 2.5 Nasal tip shape variations and their relation to the underlying bony aperture structure.....	19
Figure 2.6 The external anatomy of the lips .....	21
Figure 2.7 The external anatomy of the ear .....	23
Figure 2.8 Eyeball located supero-laterally within the orbit according to the literature .....	25
Figure 2.9 Eyeball protrusion .....	26
Figure 2.10 Gerasimov's two-tangent method for predicting the position of the nasal tip ...	28
Figure 2.11 Measurements to be utilized in regression equations for prediction of the nasal morphology .....	29
Figure 2.12 The relationship between the orientation of the ear and the angle of the jaw ..	31
Figure 3.1. Statistical analyses work flow for quantitative data.....	37
Figure 3.2. Statistical analyses work flow for qualitative data .....	38
Figure 3.3: FHP and parallel reference plane.....	39
Figure 3.4: Orbital and optic measurements .....	41
Figure 3.5: Selecting the region of interest on MevisLab.....	43
Figure 3.6: Antero-posterior diameter of the eyeball .....	44
Figure 3.7: Medio-lateral diameter of the eyeball .....	45
Figure 3.8: Supero-inferior diameter of the eyeball.....	46
Figure 3.9: Orbital depth .....	47
Figure 3.10: Separating the skin from the nose.....	49
Figure 3.11: Visualising the ANS in an antero-superior view.....	50
Figure 3.12: Lateral view photograph of bisected nose .....	51
Figure 3.13: Reference shapes for ANS.....	52
Figure 3.14 Visualising the anterior nasals spine from antero-superiorly .....	53
Figure 3.15: Gerasimov's two tangent method .....	54
Figure 3.16: Correlating a specific tooth/tooth-junction to the cheilia.....	56

Figure 3. 17: Width of the mouth and inter-canine width .....	56
Figure 3.18 The philtrum width .....	57
Figure 3.19: The width of the upper central incisors.....	58
Figure 3.20: The length of the ear .....	60
Figure 4.1 Basic descriptive statistics for the measurements pertaining to the position of the canthi.....	70
Figure 4.2 Basic descriptive statistics for measurements pertaining to the position of the eyeball in the orbit in dissections .....	71
Figure 4.3 Basic descriptive statistics for measurements pertaining to the size of the eyeball in all three modalities .....	72
Figure 4.4 Radar plot of the orbital width and height .....	73
Figure 4.5 Orbital depth as measured from the cornea to the optic canal on CT and CBCT scans .....	74
Figure 4.6 Comparisons on the medio-lateral diameter of the eyeball between modalities by means of the Wilcoxon Rank Sum test (2-sided).....	76
Figure 4.7 Comparisons on the supero-inferior diameter of the eyeball between modalities by means of the Wilcoxon Rank Sum test (2-sided).....	77
Figure 4.8 Correctly or incorrectly predicted nasal tip from ANS shape .....	80
Figure 4.9 Gerasimov's two-tangent method predictions.....	81
Figure 4.10 Basic descriptive statistics for measurements pertaining to the mouth.....	82
Figure 4.11 Tooth position at left cheilio.....	83
Figure 4.12 Tooth position at right cheilion.....	83
Figure 4.13 Correlation between actual and predicted mouth widths .....	85
Figure 4.14 Accuracy of estimated mouth width as indicated by residuals versus actual mouth width .....	85
Figure 4.15 Correlation between actual and predicted philtrum widths .....	87
Figure 4.16 Accuracy of estimated philtrum width as indicated by residuals versus actual philtrum width .....	87
Figure 4.17 Basic descriptive statistics on auricular measurements .....	88
Figure 4.18 Non-statistically significant correlation between actual and estimated ear length utilising regression formula no. 1 .....	89

Figure 4.19 Accuracy of estimated ear length utilising regression formula 1 as indicated by residuals versus actual ear length.....	90
Figure 4.20 Mild statistically significant correlation between actual and estimated ear length utilising regression formula no. 2 .....	91
Figure 4.21 Accuracy of estimated ear length utilising regression formula 2 as indicated by residuals versus actual ear length.....	91
Figure 4.22 Linear relationship between age and ear length .....	92
Figure 4.23 Accuracy of estimated ear length utilising Guyomarc’h & Stephan RF1 as indicated by residuals versus actual ear length.....	93
Figure 4.24 Accuracy of estimated ear length utilising Guyomarc’h & Stephan RF2 as indicated by residuals versus actual ear length.....	94
Figure 4.25 Accuracy of estimated ear length utilising Guyomarc’h & Stephan RF7 as indicated by residuals versus actual ear length.....	94
Figure 4.26 Accuracy of estimated ear length utilising Guyomarc’h & Stephan RF8 as indicated by residuals versus actual ear length.....	95
Figure 4.27 Accuracy of estimated ear length utilising Guyomarc’h & Stephan RF10 as indicated by residuals versus actual ear length.....	95
Figure 4.28 Accuracy of estimated ear length utilising Guyomarc’h & Stephan RF12 as indicated by residuals versus actual ear length.....	96
Figure 4.29 Accuracy of estimated ear length utilising Guyomarc’h & Stephan RF18 as indicated by residuals versus actual ear length.....	96
Figure 5.1 Graphic illustration of a) the findings from the literature and b) the mean dimensions of this study sample.....	99

# 1. INTRODUCTION

Identification of unknown individuals remains a challenge in the South African context. In cases where there is a strong suspicion regarding the identity of the unknown individual and a close relative is implied, methods such as DNA comparison are utilised to make a personal identification. However, in the South African context, unidentified individuals for which no information is available are commonplace. There are many factors responsible for this, including the high crime rates and high incidence of migrant labour which is associated with the South African socio-political and mining history <sup>1</sup>. In these circumstances, it is not possible to identify the unknown individual with primary identifiers and therefore forensic facial reconstruction, or facial approximation (FA), is often used <sup>1-3</sup> as a possible means to promote recognition. FA can thus be seen as a form of criminal intelligence when it comes to the investigation of a crime <sup>3-5</sup>.

The term “face prediction” was first documented by Kollman and Büchly <sup>6</sup> when attempting to build a face from the skull, without prior knowledge of the individual’s facial appearance <sup>3</sup>. Since the emergence of face prediction, the field has developed and changed, with contributions made by scientists and artists alike, from many geographical regions including Russia (Gerasimov), Germany (Kollman, Ulrich), the USA (Wilder, Krogman, Snow, Gatcliff) and the UK (Neave), to only name a few. The purpose of building a face from the skull is to promote recognition, and an accurate approximation should thus be easily recognisable as the person to whom the skull belonged <sup>4,7</sup>.

Following on the term “facial prediction” many other terms including facial reconstruction /reconstitution /restoration /reproduction /sculpture / approximation <sup>4</sup> have been used as synonyms. The problem arose with the misleading term “reconstruction”, as the word implies a perfect replication of the face of a person from the skull alone <sup>3</sup>. In recent years, a distinction has been made between facial reconstructions and FAs <sup>3</sup>. Where facial reconstruction dismisses discrepancies in the results and repeatability of a reconstruction as practitioner mistakes, FA accepts the possibility (and probability) of method error - in other words, if a method is not metric or quantitatively verifiable, it should be discarded, and more

appropriate methods adopted in its place. Therefore, for the purpose of this study, the term “facial approximation” will be used throughout.

Different techniques exist for creating an approximation of a person’s facial features, depending on the available evidence <sup>5</sup> and include two-dimensional (2D) and three-dimensional (3D) methods. Three-dimensional methods include both manual and computerised techniques. Approximation techniques centre around knowledge of the anatomy (specifically facial musculature) and soft tissue depths <sup>5,8-10</sup>. The musculature and tissue depths play a distinctly important role in the accuracy of FAs. However, the accurate placement and depiction of facial features seems to be an area of concern (and much controversy) when considering the sheer amount of conflicting reports on methodology.

Many studies over the past few decades have highlighted inaccuracies in commonly used methods utilised in FAs <sup>4,7,11-13</sup>. In a survey done by Tyrrell et al., <sup>14</sup>, FA specialists and other biological or forensic anthropologists reached a consensus of opinion that even though FA techniques were useful it was not adequately reliable or accurate enough to serve as evidence in a court of law. Most of the scientists believed that insufficient research had been done on the topic of FAs. Some comments from the participants of the survey include: “there are too many unknown variables that cannot be taken into account”; “reconstructions cannot allow for fatty tissue, facial hair, wrinkles, hairline, ear size and shape, lip shape”; “problem areas are the nose, lips, chin and ears”. Although the survey may be outdated, it does bring across an important point: there was – and still is – much room for developing more appropriate and accurate guidelines for FAs. Since the publication of this survey, numerous research studies have been performed in an attempt to address the lack of empirical validation of FA methods <sup>12, 15-24</sup>. Many different guidelines were so formulated for the prediction of each facial feature<sup>13</sup>.

More specifically, guidelines for approximations of the orbital area include the location and size of the eye fissure <sup>25</sup> (although variations for the position of the canthi has been reported)<sup>19, 24, 26</sup>; the size of the eyeball <sup>9, 15, 22, 27</sup>; the position of the eyeball within the orbit <sup>19, 22, 24, 28-32</sup> and the projection of the eyeball <sup>12, 15, 33</sup>.

Various guidelines for predicting the nasal projection have been proposed <sup>7, 13</sup>, most notably by Krogman and İşcan <sup>34</sup>, Gerasimov <sup>35</sup>, Prokopec and Ubelaker <sup>36</sup> and George <sup>37</sup>. Other

guidelines concerning the nose include the relationship between the shape of the anterior nasal spine (ANS) and the shape of the nasal tip <sup>25,38</sup>, as well as an integrated method for predicting nasal morphology by Rynn et al., <sup>16</sup>.

Methods for estimating mouth width has also been researched to a great degree. Interpupil distance has been suggested as a predictor for mouth width <sup>39</sup>, while other studies link the width of the mouth to interlimbus distance <sup>18,20,40</sup>. Although still unproven, Fedosyutkin and Nainys <sup>25</sup> suggested that the width of the mouth corresponds to the distance between the mandibular second molars. Wilkinson et al. <sup>20</sup> proposed formulae for calculating lip thickness from the teeth (also see <sup>41</sup>), while Stephan and Henneberg <sup>17</sup> refined previously proposed guidelines <sup>18</sup> for estimating mouth width by prescribing the 75% rule – where the inter-canine width occupies 75% of the mouth width. Regarding the width of the philtrum, Fedosyutkin and Nainys <sup>25</sup> suggests that the width of the philtrum corresponds to the distance between the midpoints of the upper central incisors, although this relationship remains untested.

Although guidelines for approximations of the ear do exist, many of these have not been tested or empirically validated. Some of the existing guidelines include: the size of the ear approximately corresponds to the size of the nose <sup>9, 35</sup>; the external auditory meatus corresponds to the tragus, thus indicating the position of the ear <sup>35</sup>; and the direction in which the mastoid processes are pointing, determines if the earlobes are free or attached <sup>25,35</sup>.

As inter-population variation in facial features has been reported in the literature <sup>42-45</sup>, these guidelines created for and on other populations for FAs may not necessarily be applicable in the South African context. A great degree of variation in facial features regarding the orthognathic face, as compared to the prognathic face (as noted in South Africans), can be expected. Most approximation techniques have been developed on the orthognathic face, while the prognathic face is largely unexplored, except for a few studies on soft tissue thicknesses <sup>2, 46</sup>. It is postulated that these inter-population differences may have an enormous effect on FAs and its accuracy, as is often demonstrated in practice (Capt. T.M. Briers, personal communication, 2014).

## 1.1. Aim

This study aims to investigate the relationships between the hard and soft tissues of the face, in order to provide guidelines that can be used in cases where FAs are done on individuals of black South Africans. Facial features to be studied include the eyes, the nose and the mouth as well as the ears. Although the most significant features for recognition of familiar faces are the eyes, nose and mouth (representing the inner parts of the face)<sup>47</sup>, many researchers have found that external features such as the ears play an important part in recognising unfamiliar faces especially in profile<sup>48-50</sup>.

The specific objectives are:

- To explore the features of the eyes and eyelids in relation to the orbits
- To provide data on the size of the eye ball
- To evaluate current guidelines for determining nasal tip shape and position
- To explore the features of the mouth in relation to the teeth
- To evaluate the size of the ears
- To correlate the findings of this study with established guidelines in the literature and determine which of the published guidelines are applicable to this population group

The information gained in this study is envisaged to be useful in the design of population specific guidelines in the South African context, in an attempt to validate and improve upon existing methods of FAs.

## 2. LITERATURE REVIEW

In the following literature review the applicable anatomy of the facial features is reviewed, to aid in the understanding of the methods used in this study. Known guidelines for FAs are outlined as well.

### 2.1. Applied osteology of the skull

The skull consists of the cranium and the mandible and is composed of 28 separate bones. Most of these bones are paired, except for some single bones in the median plane. The cranium can be divided into the neurocranium, or the cranial vault, and the viscerocranium, or the facial skeleton. The neurocranium encloses the brain and meninges, while the viscerocranium contains the organs of special sense <sup>51</sup>.

When studying the skull as a whole, or even its individual bones, it is best to view it from standard views called *normae*. These standard views are based on the establishment of the Frankfort Horizontal Plane (FHP) for creating a standard reference position <sup>52</sup>. According to Wilkinson <sup>38</sup> the FHP “is reached when a horizontal line passes through the inferior border of the orbit (orbitale) and the external auditory meatus (porion) on both sides of the skull”. From this standard reference position, a few different *normae*, namely the *normae frontalis*, *lateralis*, *occipitalis*, *verticalis* and *basalis* <sup>52</sup> can be established. In this section, only the *norma frontalis* (anterior view), *norma lateralis* (lateral view) and *norma basalis* (inferior view) will be discussed as these provide the most significant information with regards to FAs and are essential when considering the facial features that will be measured.

The anterior and lateral views as well as the bony orbits are outlined by integrating the applicable information from *Craniofacial Identification in Forensic Medicine* <sup>52</sup> and *Gray’s Anatomy* <sup>51</sup>. These texts provide similar descriptions to most standard anatomy textbooks.

### 2.1.1. Anterior view

On an anterior or frontal view (Fig. 2.1), the skull is in general ovoid shaped, being wider at the top than the bottom. The frontal bone (orange) forms the upper part, contributing to the cranial vault above the superior orbital margins (SOMs) and articulates with the two nasal bones (red) at the frontonasal sutures. The depression where these bones meet, marks the nasal root while the nasion is the specific anthropometric landmark at which the frontonasal and internasal sutures meet. A low and curved ridge, or superciliary arch (brow ridge), is visible superior to the SOM with their medial ends meeting at another anthropometric landmark, namely the glabella. The glabella is a slight median elevation between the superciliary arches. The superciliary arches are usually more pronounced in males. Above each superciliary arch a slight elevation can be seen, namely the frontal eminence and this is usually more obvious in females.

The upper part of the viscerocranium consists of the bony orbits and the bridge (or root) of the nose. The bony orbits vary slightly in shape but are approximately quadrangular. The frontal bone forms the entire SOM. The frontal process of the zygomatic bone (light green) and the zygomatic process of the frontal bone form the lateral orbital margin (LOM). The inferior orbital margin (IOM) is formed by the maxilla (dark green) medially and the zygomatic bone laterally. Both the lateral and inferior orbital margins are quite sharp and palpable. The medial margin of the orbit (MOM) is formed superiorly by the frontal bone and inferiorly by the lacrimal crest of the frontal process of the maxilla.

The central part of the viscerocranium mainly consists of the two maxillae and is separated by the anterior nasal aperture, which is piriform in shape. The nasal bones bound the anterior nasal aperture superiorly, while the maxillae form the rest of the borders. The bony septum consisting of the perpendicular plate of the ethmoid bone (yellow) and the vomer (brown) can be seen inside the anterior nasal aperture. Nasal cartilages attach to the bones and help form two distinct nasal cavities. The anterior nasal spine (ANS) is a uniquely human characteristic amongst primates, and together with the nasal bones, its shape can accurately predict the shape of the cartilaginous nose. Each maxilla forms part of the upper jaw, the floor of the oral cavity, the lateral wall of the nose, the floor of the nasal aperture and the cheekbones. Medially the maxilla forms the nasal notch (the floor and inferolateral border of the anterior nasal aperture) and is surmounted by the ANS at the intermaxillary suture. Each

maxilla also articulates superiorly with the zygomatic bone at the zygomaticomaxillary suture via a short, thick zygomatic process.

The lower part of the viscerocranium is formed by the alveolar processes of the maxillae that bear the upper dentition, the body of the mandible (light purple) and the alveolar processes of the mandible that bear the lower dentition. In the midline, the mental protuberance of the mandible gives the chin its characteristic prominence.

It is also important to understand the anatomy of the mandible and teeth, especially when attempting to reconstruct the mouth and lips. The width of the mouth can be determined by analysing the teeth <sup>17</sup>.



*Figure 2.1 Osteology of the skull on an anterior view*

Dark blue: Parietal bones

Light blue: Temporal bones

Orange: Frontal bone

Light green: Zygomatic bones

Dark purple: Sphenoid bones

Yellow: Ethmoid bone

Pink: Lacrimal bones

Red: Nasal bones

Dark green: Maxillae

Brown: Vomer

Light purple: Mandible

### 2.1.2. Lateral view

The features on the lateral view are applicable for their contribution to the bony orbit discussed further in the proposal. Apart from the face (discussed in section 2.1.1 regarding the anterior view), the temporal region is also visible on a lateral view of the skull and is briefly discussed for its importance in FAs, although not directly applicable to this study.

The lateral view of the skull clearly shows the essential role of the zygomatic bone in connecting the viscerocranium to the temporal and frontal bones. The temporal region is divided by the zygomatic arch into the upper temporal fossa and lower infra-temporal fossa. The temporal fossa is thus continuous with the infra-temporal fossa deep to the zygomatic arch. The four bones forming the floor of the temporal fossa meet at an H-shaped sutural junction named the pterion.

Other structures also visible on a lateral view of the skull are the body and ramus of the mandible, the mandibular fossa and articular tubercle, the external acoustic meatus and the mastoid and styloid processes. The lateral view of the skull also shows a few important features relevant in FAs, namely the overall profile of the face, the degree of projection of the chin, the degree of orthognathism/prognathism, as well as the prominence of the nasal bones and ANS.

### 2.1.3. The Bony Orbits

The bony orbits are located on either side of the nasal root and house the eyes. They are approximately the shape of a quadrilateral pyramid with its base at the orbital opening and narrowing along a postero-medial axis to the apex of the orbit. The walls of the orbits protect the eyes from injury as well as provide attachment for the extraocular muscles. Each orbit has a medial wall, lateral wall, roof and floor. The eyeball occupies only about a fifth of the volume of the orbit, with vessels, nerves, the extraocular muscles, connective tissue and orbital fat filling up the peri-orbital space.

The bones comprising the orbit, as well as other major landmarks within the orbit are indicated in Figure 2.2. The medial walls are approximately 25 mm apart in adults and are nearly parallel. It is mostly formed by the orbital plate of the ethmoid bone (pink) and

articulates with the orbital plate of the frontal bone (gray) superiorly, the body of the sphenoid bone (blue) posteriorly and the lacrimal bone (green) anteriorly. The lacrimal bone contains the fossa (2) for the nasolacrimal sac that is bounded in front by the anterior lacrimal crest (3) on the frontal process of the maxilla (yellow) and behind by the posterior lacrimal crests (1) of the lacrimal bone. The medial palpebral ligament along with the lacrimal part of orbicularis oculi muscle attach to the posterior lacrimal crest. The upper part of the nasolacrimal canal is formed by a descending process of the lacrimal bone and completed by the maxilla.

The lateral wall is formed by the orbital surface of the greater wing of the sphenoid bone posteriorly and the frontal process of the zygomatic bone (red) anteriorly, which articulate at the sphenozygomatic suture. A palpable ridge, the malar (orbital) tubercle (4), gives attachment to the lateral palpebral ligament and lies just inside the midpoint of the LOM. The superior orbital fissure (5), which lies between the greater and lesser wings of the sphenoid and communicates with the middle cranial fossa, separates the lateral wall of the orbit from the roof of the orbit posteriorly, while anteriorly these are continuous.

The roof of the orbit is mostly formed by the orbital plate of the frontal bone. Anteriorly, the frontal sinus and shallow lacrimal fossa is located medially and laterally, respectively. The roof slopes down towards the apex of the orbit where the lesser wing of the sphenoid completes it.

The floor of the orbit consists mainly of the orbital plate of the maxilla and articulates with the zygomatic bone antero-laterally and palatine bone postero-medially. The floor curves slightly antero-laterally into the lateral wall but is separated posteriorly from the lateral wall by the inferior orbital fissure (6), which communicates with the pterygopalatine and infra-temporal fossae. The thin bone of the floor forms the roof of the maxillary sinus and slopes down from the apex towards the LOM where it is notched by the infra-orbital groove (which sinks into the floor to become the infra-orbital canal and opens on the face at the infra-orbital foramen (7)).

It is important to understand the anatomy of the bony orbit when considering FAs in order to correctly place the eye within the socket. The malar tubercle, also known as Whitnall's tubercle, specifically is of significance to the forensic anthropologist as it assists in the correct

placement of the eye fissure in forensic FAs and skull-photo superimpositions<sup>10, 25, 53-56</sup>. The location of the palpebral fissure is defined by a straight line connecting the malar tubercle and the base of the posterior lacrimal crest, where the lateral and medial palpebral ligaments attach respectively<sup>25</sup>. By extension, the endo- and exocanthion's positions are also determined by the attachments of these ligaments. The position of these points will be further explored in this study.

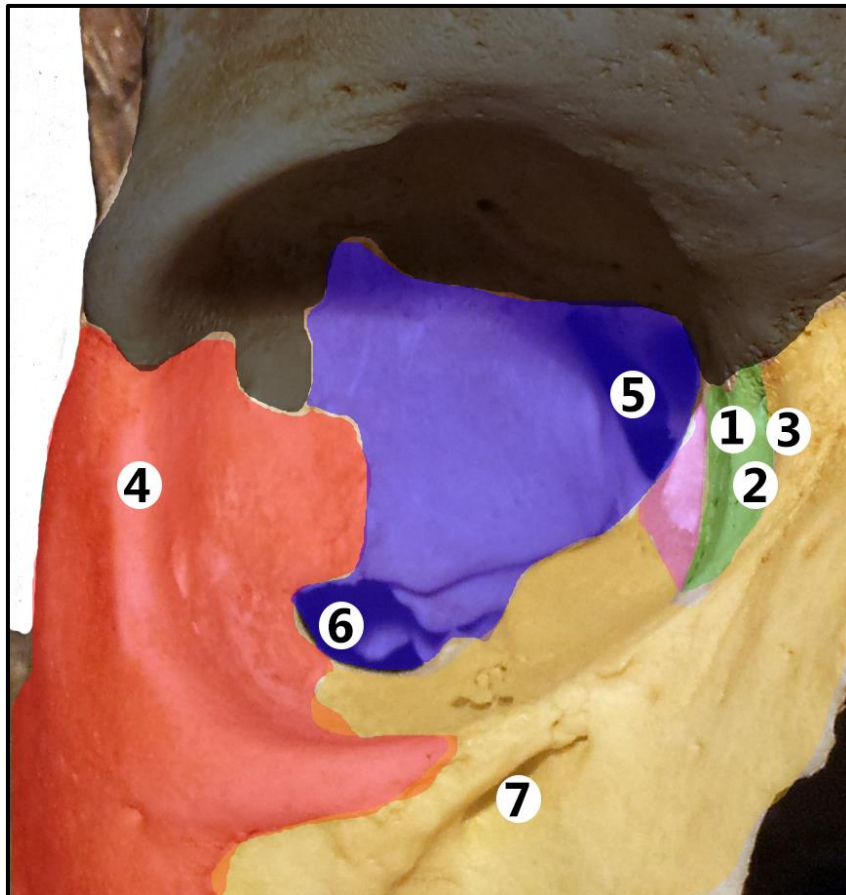


Figure 2.2 The bony orbit

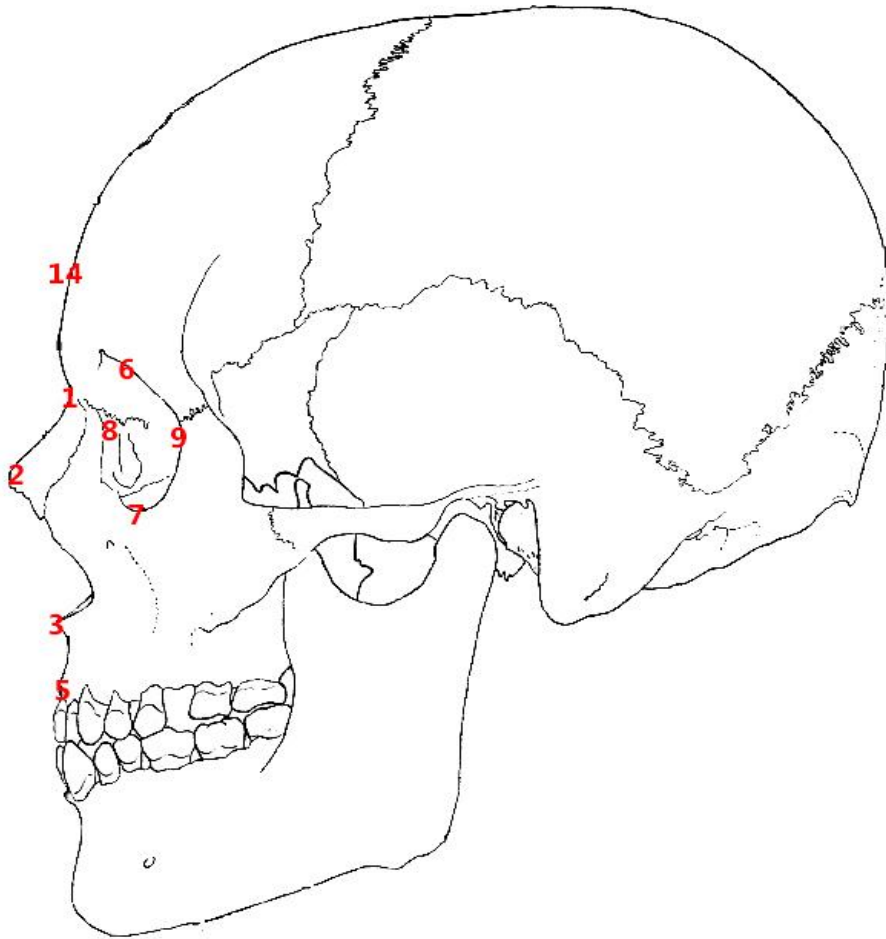
- |                             |                      |
|-----------------------------|----------------------|
| 1. Posterior lacrimal crest | Red: Zygomatic bone  |
| 2. Lacrimal fossa           | Blue: Sphenoid bone  |
| 3. Anterior lacrimal crest  | Gray: Frontal bone   |
| 4. Malar tubercle           | Pink: Ethmoid bone   |
| 5. Superior orbital fissure | Green: Lacrimal bone |
| 6. Inferior orbital fissure | Yellow: Maxilla      |
| 7. Infra-orbital foramen    |                      |

## 2.2. Anatomy of the facial features

The following sections are based on the descriptions in Clinically Oriented Anatomy <sup>57</sup> and Gray's Anatomy <sup>51</sup> in correspondence with other basic anatomy textbooks.

Landmarks relevant to this study are identified and defined in Table 2.1 and the relevant Figures (Fig. 2.3 – 2.7) in the rest of this section. These landmarks are to be used as points of reference throughout the following sections, as well as for all measurements involved in this study.

Table 2.1 Bony and other landmarks



1.	Nasion	Midpoint of the suture between the frontal and the two nasal bones <sup>56</sup>
2.	Rhinion	Anterior tip of the nasal bones, on the internasal suture <sup>56</sup>
3.	Anterior nasal spine (ANS) with acanthion	A bony protuberance on the inferior border of the nasal aperture, formed by the medial anterior surfaces of the maxillae <sup>51</sup> . The acanthion is defined as the tip of the ANS <sup>16</sup>
4.	Pronasale (see Fig. 2.4 no. 3)	Most protruding point of the tip of the nose <sup>56</sup>
5.	Supradentale	Point between the maxillary (upper) central incisors at the level of the cementum-enamel junction <sup>56</sup>
6.	Supraorbitale/ superior orbital margin (SOM)	Above the orbit, centred on the uppermost margin of the orbit <sup>56</sup>
7.	Infraorbitale/ inferior orbital margin (IOM)	Below the orbit, centred on the lowermost margin of the orbit <sup>56</sup>
8.	Medial orbital margin (MOM)	Point centred on the medial margin of the orbit
9.	Lateral orbital margin (LOM)	Point centred on the lateral margin of the orbit
10.	Endocanthion (see Fig. 2.3 no 2)	Point at the inner commissure of palpebral fissure <sup>56</sup>
11.	Exocanthion (see Fig. 2.3 no 1)	Point at the outer commissure of palpebral fissure <sup>56</sup>
12.	Cheilion (see Fig. 2.6 no 5)	Point located at each labial commissure <sup>56</sup>
13.	Philtrum (see Fig. 2.6 no 6)	The shallow groove superior to the tubercle of the upper lip and extending to the nasal septum <sup>57</sup>
14.	Glabella	Most prominent point between supraorbital ridges in midsagittal plane <sup>56</sup>
15.	Superaurale (see Fig. 2.7 no 15)	Highest point on the free margin of the auricle <sup>56</sup>
16.	Subaurale (see Fig. 2.7 no 16)	Lowest point on the free margin of the ear <sup>56</sup>
17.	Subspinale	Midline of the maxilla, as high as possible before the curvature of the ANS begins <sup>56</sup>

## 2.2.1. The Eyes

### *(i) The Eyelids*

When the upper and lower eyelids are closed, they cover the eyeball anteriorly. The eyelids have multiple functions, including protecting the eye from injury and excessive light, as well as keeping the cornea moist by spreading lacrimal fluid. These movable folds are covered externally by skin and internally by the palpebral conjunctiva, a transparent mucous membrane continuous with the bulbar conjunctiva covering the eyeball. The basic external anatomy of the eyelids is shown in Figure 2.3. The upper lid contains the superficial facial muscle levator palpebrae superioris, and is larger and more mobile than the lower lid. The lids are separated by the transverse palpebral fissure and meet at their medial and lateral extremities, namely the medial canthus (endocanthion) and lateral canthus (exocanthion). Most studies report the endocanthion to lie approximately 2 mm lower than the exocanthion. The distance from the canthi to the orbital margins will be measured during this study to determine their exact positions relative to the orbit. Located between the eyeball and the endocanthion is a small triangular space containing the lacrimal caruncle, which is mounted on a fold of conjunctiva named the plica semilunaris. When looking straight ahead, the upper lid covers the cornea by approximately 2-3 mm, and moves down to cover the entire cornea when closing the eyes. The lower lid extends to just below the corneo-scleral junction.

A dense band of connective tissue named the tarsal plate strengthens each lid. These bands of fibrous connective tissue are thin, elongated and crescent-shaped to provide support and determine the form of the eyelid. The shape of the tarsal plates is convex and conforms to the shape of the anterior surfaces of the eyes. The tarsal plates attach to the orbital margin via the orbital septum as well as the medial and lateral palpebral ligaments. The medial palpebral ligament passes from the medial ends of the two tarsal plates to the posterior lacrimal crest and the frontal process of the maxilla, while the lateral palpebral ligament passes from the lateral ends of the tarsal plates to the malar tubercle, located on the zygomatic bone within the orbital margin. The orbital septum spans from the tarsal plates to the margins of the orbit to become continuous with the periosteum.

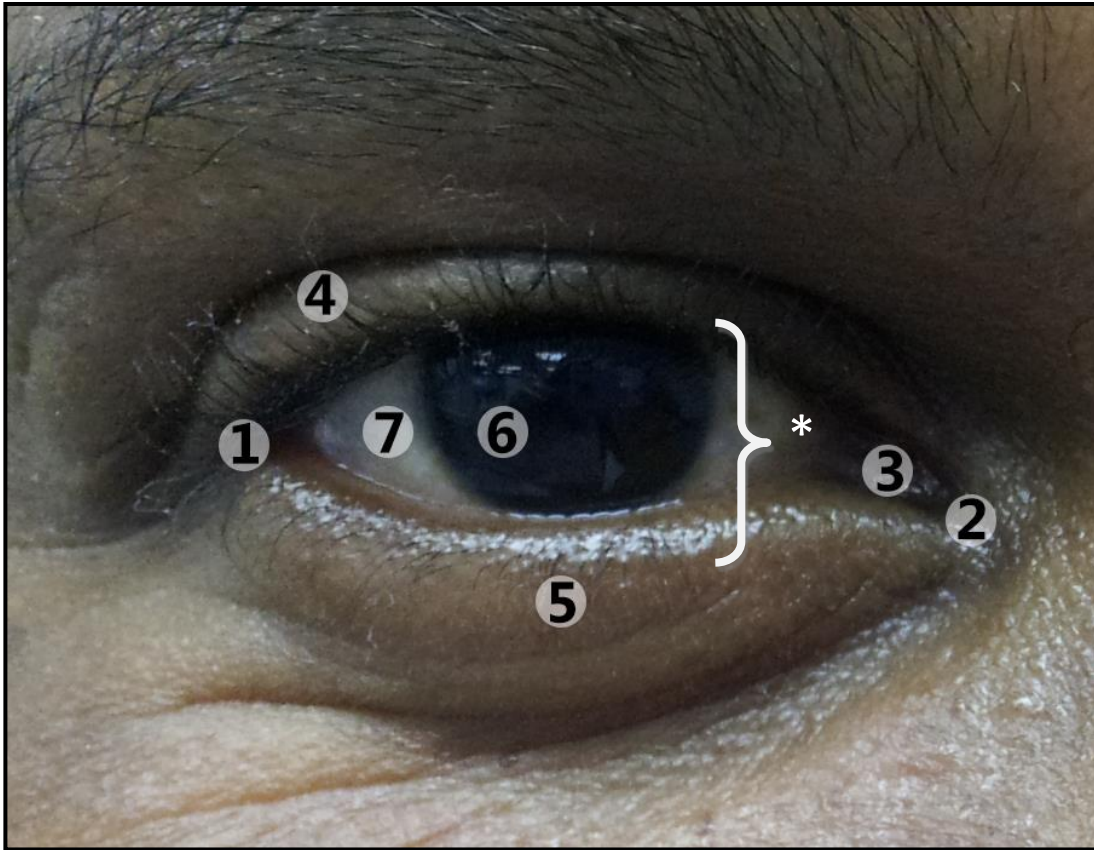


*Figure 2.3 Anatomy of the eyelid*

1. Exocanthion
2. Endocanthion
3. Lacrimal caruncle
4. Upper eyelid
5. Lower eyelid
6. Iris
7. Cornea

\*White bracket indicating palpebral fissure

### *(ii) The Eyeball*

The eyeball is only discussed very briefly as the internal structures and components hold no direct relevance to this study. The eyeball is a spherical structure containing the optical apparatus of the visual system and consists of three layers, as well an additional loose connective layer surrounding the eyeball. The three layers are from outside to inside: the

fibrous layer (sclera and cornea), the vascular layer (choroid, ciliary body and iris), and the inner layer (retina).

The eye is separated into three chambers filled with aqueous (vitreous) humour. The iris is a thin contractile diaphragm located on the anterior surface of the lens, with the pupil as a central aperture for light transmission. Vitreous humour maintains the shape of the eye, transmits light and holds the retina in place against the choroid.

### *(iii) The Extraocular muscles*

There are seven extraocular muscles, all working together synergistically and antagonistically to move the superior eyelids and eyeballs. These muscles are levator palpebrae superioris, the superior, inferior, medial and lateral recti, and the superior and inferior oblique muscles.

Levator palpebrae superioris is a thin, triangular muscle arising from the inferior aspect of the lesser wing of the sphenoid and expanding anteriorly in a wide aponeurosis. Some fibres attach onto the anterior surface of the upper tarsal plate, while the rest passes through orbicularis oculi to attach onto the skin of the upper eyelid. This muscle elevates the upper eyelid, an action that is opposed by the palpebral part of orbicularis oculi.

The four recti muscles are approximately strap-shaped. All the recti muscles originate from the common tendinous ring surrounding the optic canal and part of the superior orbital fissure and pass forward in the position implied by its respective name to insert on the sclera just posterior to the corneoscleral junction. The lateral and medial recti lie in the same horizontal plane while the superior and inferior recti lie in the same vertical plane.

## **2.2.2. The Nose**

The nose can be divided into the external nose and the internal nasal cavity. The external nose is the visible portion of the nose, which projects away from the face and opens anteriorly onto the face through the nostrils or nares (see Fig. 2.4). The dorsum of the nose extends from the root of the nose to the apex, or the nasal tip. The piriform nostrils are located on the lower surface of the nose, and bounded laterally by the alae. Hyaline cartilage and bone form the underlying skeleton of the nose.

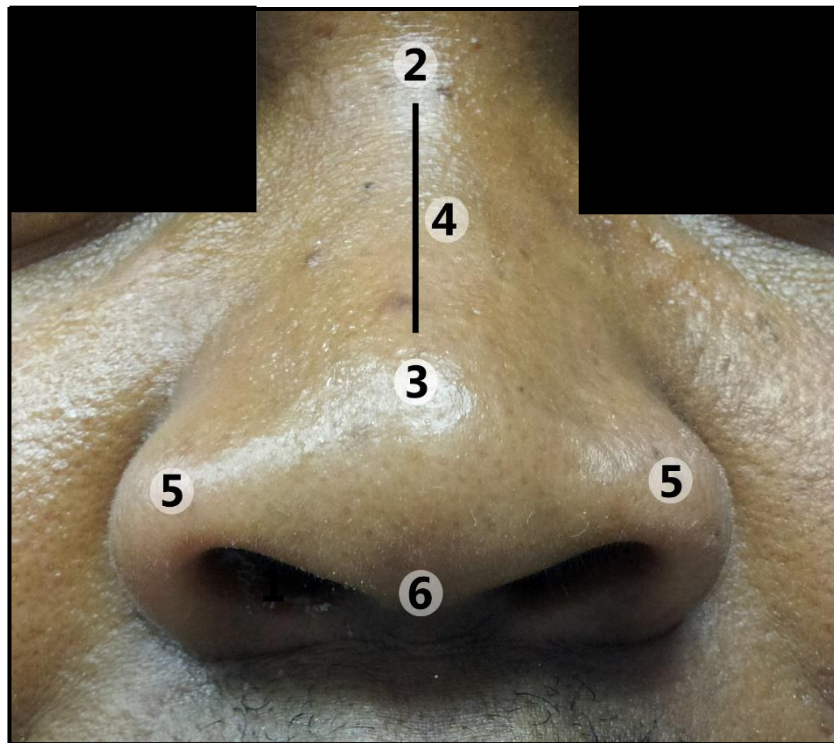


*Figure 2.4 Anatomy of the external nose*

1. Nostril
2. Root of the nose
3. Pronasale
4. Dorsum of the nose
5. Ala
6. Columella

The nasal bones, frontal processes of the maxillae, the nasal part of the frontal bone and its anterior nasal spine as well as the bony parts of the nasal septum all contribute to the bony part of the nose. The bony nose and nasal aperture has been discussed in section 2.1.1 under the anterior view of the skull.

The cartilaginous framework consists of five main cartilages and several minor cartilages: the paired lateral cartilages; the paired alar cartilages; one septal cartilage; and several minor alar cartilages. Due to this cartilaginous skeleton, the external nose can vary greatly in shape and size between individuals. The lateral cartilage is triangular with its anterior margin thicker than the posterior margin. It is continuous with the septal cartilage at its upper part, but might be separated from it antero-inferiorly by a thin fissure. Its superior margin is attached to the

nasal bone and frontal process of the maxilla, and its inferior margin is connected to the lateral crus of the major alar cartilage.

The internal nasal cavity is further divided into left and right cavities by the sagittally placed nasal septum. This septum is composed of a bony part and a mobile cartilage part. The bones contributing to the nasal septum is the perpendicular plate of the ethmoid bone forming the superior part, and the vomer and some small contributions by the nasal crests of the maxillary and palatine bones forming the postero-inferior part. The septal cartilage has a 'tongue-and-groove' articulation with the edges of the bony septum. Each nasal cavity has a roof, floor, medial and lateral wall. The roof consists of three parts, named for the bones forming each part: frontonasal, ethmoidal and sphenoidal. The roof is curved and narrow, except at its posterior end, where the nasal cavity opens posteriorly into the nasopharynx through the posterior nasal aperture or choanae. The floor is wider than the roof and formed by the palatine processes of the maxilla and the horizontal plates of the palatine bone. The medial wall consists of the nasal septum, while the lateral walls are irregular due to the three bony plates or conchae.

The shape of the external nose can vary greatly and all relates to the underlying bony structure. Rynn et al.,<sup>16</sup> describe a few variations of nasal tip shapes according to features of the bony aperture (see Fig. 2.5).

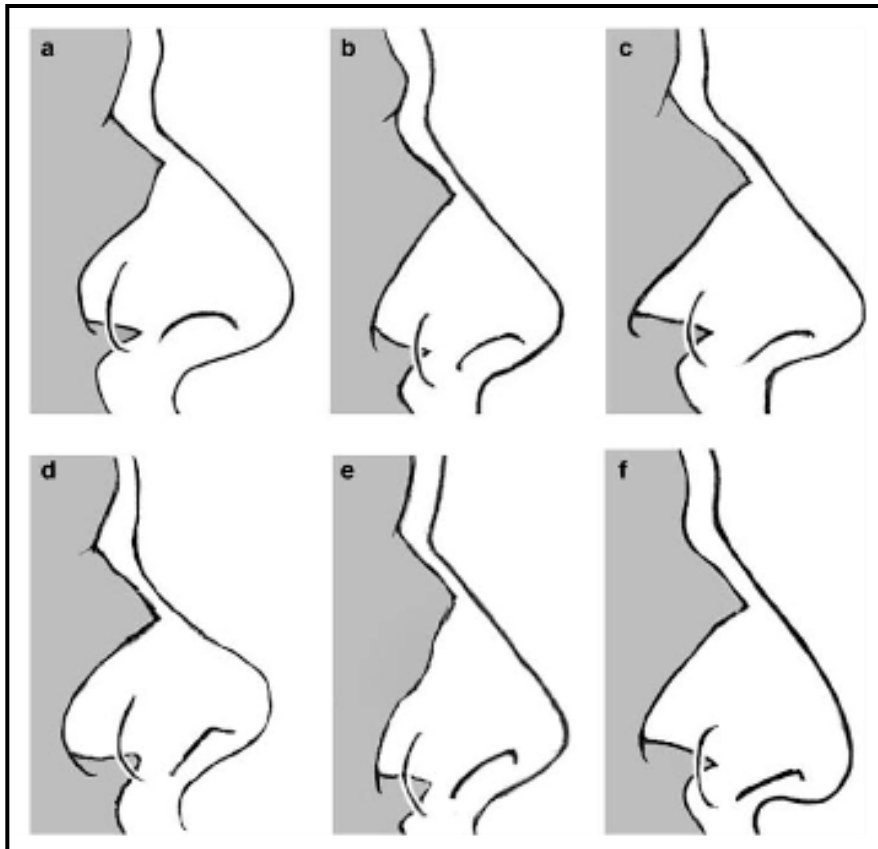


*Figure 2.5 Nasal tip shape variations and their relation to the underlying bony aperture structure* <sup>16</sup>

- a. Rounded nasal aperture and nasal tip
- b. Average aperture and nasal tip
- c. Sharply angled aperture and nasal tip
- d. Rounded aperture and nasal tip (upturned nose)
- e. Angled aperture and nasal tip (upturned nose)
- f. Angled aperture and nasal tip (down-turned nose)

### 2.2.3. The Lips

The lips are highly mobile musculo-fibrous folds surrounding the mouth. The shape of the mouth and the posture of the lips are controlled by the buccolabial muscle group. This muscle group is a complex three-dimensional assembly of muscular slips comprising the levator labii superioris alaeque nasi, levator labii superioris, zygomaticus major and minor, levator anguli oris, risorius, depressor labii inferioris, depressor anguli oris, mentalis, orbicularis oris and buccinator muscles. The lips function as the valves of the oral fissure and contain the sphincter

(orbicularis oris) that controls entry and exit from the mouth, as well as the superior and inferior labial muscles. The anatomy of the lips is illustrated in Figure 2.6. The lips extend from the nasolabial sulci and nares laterally and superiorly to the mentolabial crease inferiorly. The transitional zone of the lips, or vermilion<sup>58</sup>, is considered by itself to be the lip and is generally a darker colour, ranging from brown to red. The upper and lower lip meets laterally at the angle of the mouth or the commissure/cheilion. The skin-covered outer surface of the lips is continuous with the mucous membrane on the inside of the oral cavity and usually forms a defined border on the outside. In the midline, the upper lip's border forms an arch, commonly known as the cupid's bow. Extending upwards from the cupid's bow to the columella of the nose is a slight indentation, the philtrum, bordered by a philtral column on each side<sup>58</sup>. The literature suggests that there might be a correlation between the width of the philtrum and the distance between the midpoints of the upper central incisors<sup>25</sup>. This relationship between lips and teeth will also be explored in this study.

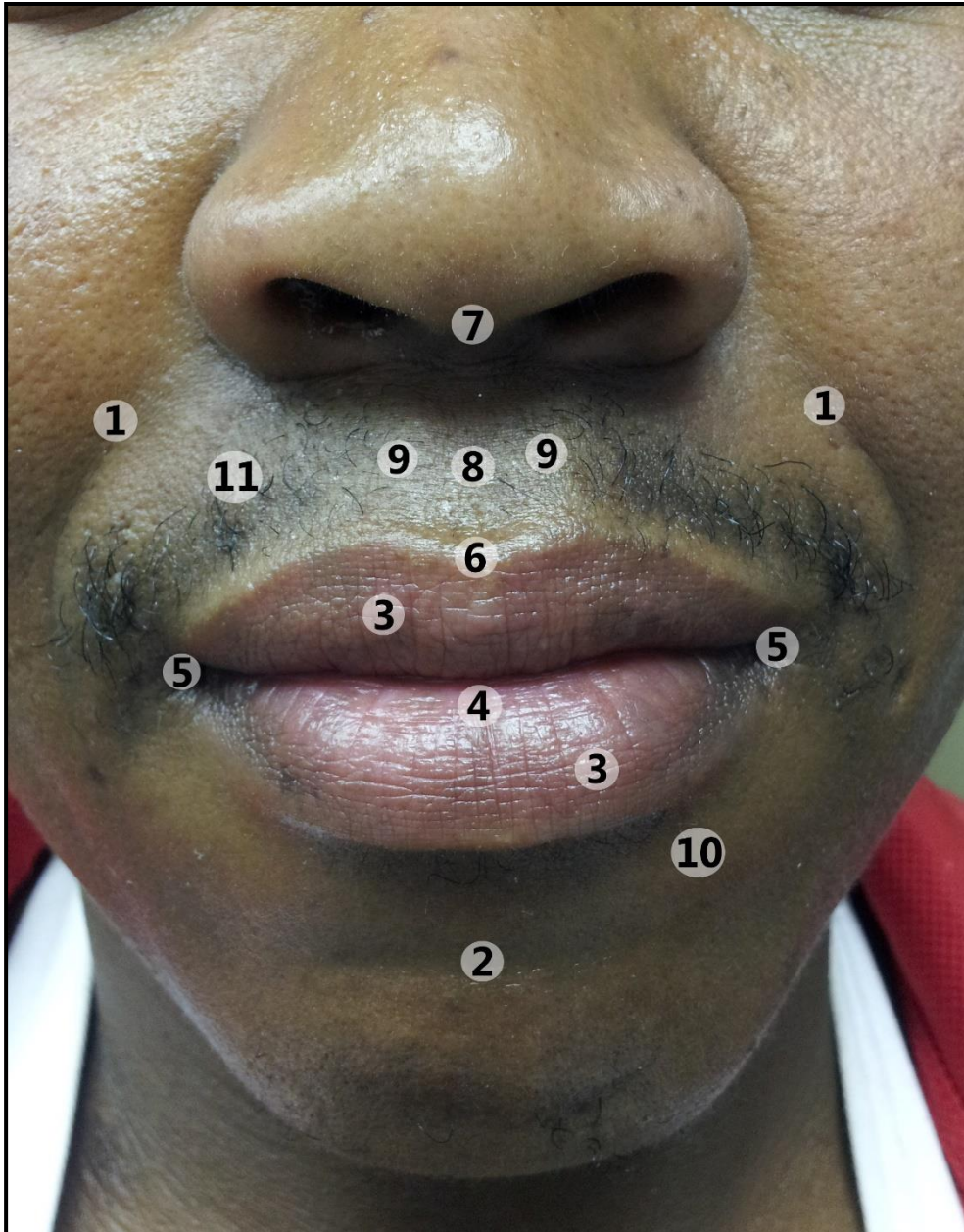


*Figure 2.6 The external anatomy of the lips*

- |   |                    |
|---|--------------------|
| 1. Nasolabial sulcus  | 7. Columella       |
| 2. Mentolabial sulcus   | 8. Philtrum        |
| 3. Dry vermilion  | 9. Philtral column |
| 4. Wet vermilion with stomion<br>(midpoint of labial fissure) | 10. Lower lip      |
| 5. Angle/commissure/cheilion                                  | 11. Upper lip      |
| 6. Cupid's bow  |                    |

#### 2.2.4. The External Ears

The external ear comprises the shell-like auricle, or pinna, and the external acoustic meatus. The functions of the pinnae are to collect and conduct sound waves along the external auditory canal to the tympanic membrane. The pinna projects from the side of the head and faces slightly forwards, as seen in Figure 2.7. The pinna is composed of an irregularly shaped plate of elastic cartilage covered by thin skin presenting externally as several eminences and depressions. The depressions on the lateral surface correspond to the elevations on the cranial surface of the auricle. The first obvious eminence is the outer margin, the helix. The antihelix is a curved eminence parallel and anterior to the posterior part of the helix. It divides into two crura, with the triangular fossa in between.

The antihelix encircles the deepest depression in the auricle, the concha, which is incompletely divided by the anterior end of the helix, or the crus. Between the helix and antihelix lies the curved depression named the scaphoid fossa. The tragus, a small curved flap below the crus of the helix, lies in front of the concha and projects posteriorly to partly overlap the opening of the external acoustic meatus. The antitragus lies opposite to the tragus and is separated from it by the intertragic notch. Below the antitragus lie the lobule, a soft non-cartilaginous flap consisting of fibrous and adipose tissue. The tragon is the notch on the upper margin of the tragus and can be used as reference point instead of the external acoustic meatus when aligning the head to FHP <sup>59</sup>.

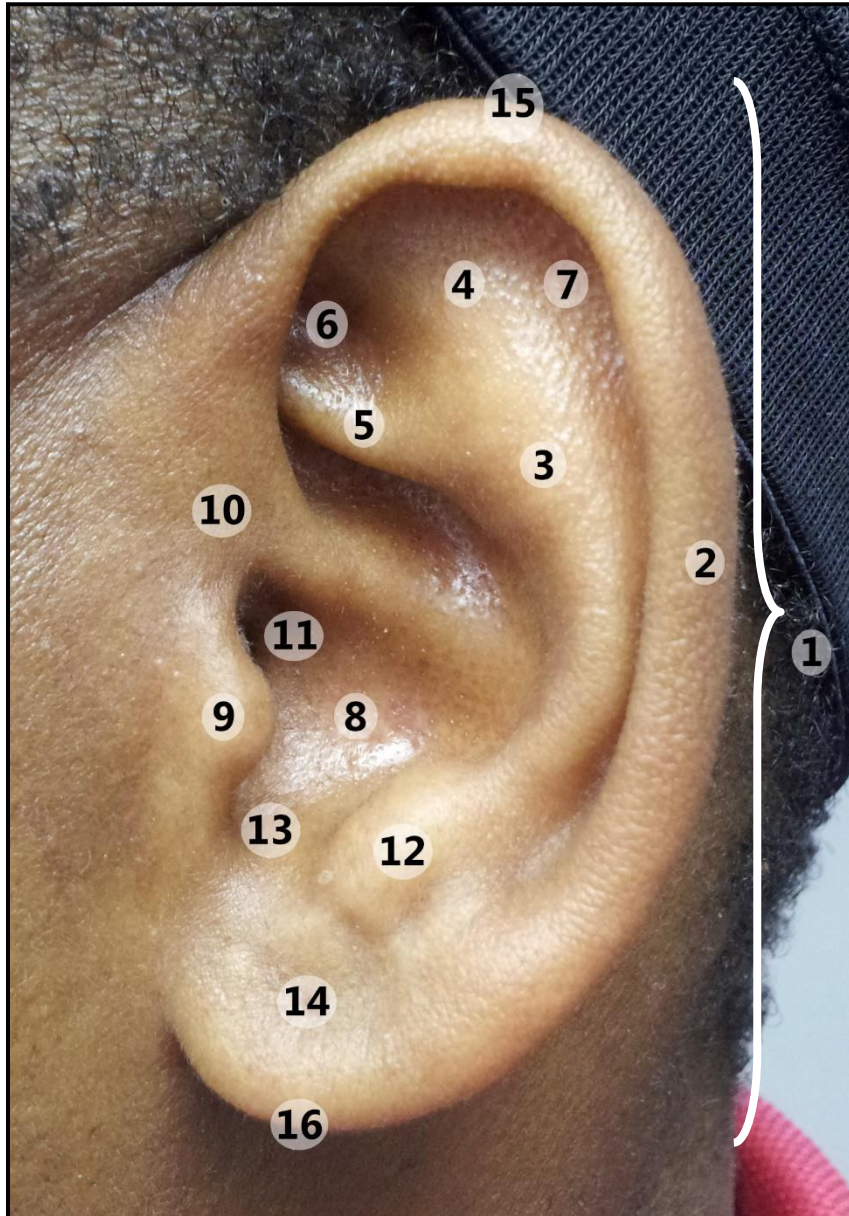


Figure 2.7 The external anatomy of the ear

- |                            |                              |
|----------------------------|------------------------------|
| 1. Pinna                   | 10. Crus of helix            |
| 2. Helix                   | 11. External acoustic meatus |
| 3. Antihelix               | 12. Antitragus               |
| 4. Upper crus of antihelix | 13. Intertragic notch        |
| 5. Lower crus of antihelix | 14. Lobule                   |
| 6. Triangular fossa        | 15. Superaurale              |
| 7. Scaphoid fossa          | 16. Subaurale                |
| 8. Concha                  | 17. Tragion                  |
| 9. Tragus                  |                              |

## 2.3. Known guidelines for reconstructing facial features in a forensic setting

Over the years, the approximation of faces has evolved from a purely artistic approach, where observational skills had resulted in loose “rules of thumb”<sup>9</sup>, into a more scientific approach, where careful research and data analysis were formulated into specific techniques and processes. In this section the evolved scientific approaches and processes will be discussed as specific to this study.

The focus of this study is to relate the skull to the soft facial features, specifically as relevant to FAs. Most of the information reviewed, however, is also applicable to other applications within a forensic context such as skull-photo superimpositions.

### 2.3.1. The Eyes

The FA process usually begins with the placement of the eyes. As facial recognition is very dependent of the morphology of the orbital area, it is very important to be precise and correct in placing the eyes<sup>19</sup>. Historically, the eye was placed in the center of the socket<sup>33, 39, 60</sup>, however, current practice take great care in positioning the eyeball supero-laterally according to expert studies<sup>10</sup>.

The location of the palpebral fissure is defined by a straight line connecting the malar tubercle with the base of the anterior lacrimal crest<sup>25</sup>. Variations in the exact position of the endocanthion and exocanthion are reported in the literature. In most research done previously, the endocanthion was reported to be situated lower than the exocanthion. According to Stephan and Davidson<sup>19</sup>, the endocanthion in an Australian population lies approximately 19.5 mm below the SOM reference plane and approximately 4.8 mm lateral to the MOM, while the exocanthion 18.5 mm below the SOM reference plane (or 8 mm below the frontomalar orbital point) and approximately 4.5 mm medial to the LOM and. The frontomalar orbital point is situated on the MOM near its flexure, located on the frontal process of the maxilla where the lower orbital wall sharply flattens<sup>26</sup>. Kim et al.<sup>61</sup> reported that in their sample of Korean individuals, the endocanthion lies on average 22.8 mm and the exocanthion 20.2 mm respectively below the SOM. Balueva et al.<sup>26</sup> found the endocanthion

to lie approximately 2 mm lateral to the MOM and the exocanthion to lie approximately 5 mm medial to the malar tubercle located on the LOM.

The mean antero-posterior diameter of the eyeball is approximately 23 - 24 mm <sup>15, 22, 62, 63</sup>. The medio-lateral diameter is approximately 24.3 mm <sup>22, 62</sup> while the supero-inferior diameter ranges from 23.3 – 24.6 mm <sup>22, 62</sup>. Several studies to determine the position of the eyeball in the orbit <sup>19, 29-31</sup> provide strong evidence of a more supero-lateral placement within the orbit (Fig. 2.8).

Specific distances measured by Stephan et al. <sup>29</sup> are consistent with measurements taken in other studies and are as follows: 4 mm from the SOM, 6.9 mm from the IOM, 8.0 mm from the MOM and 3.9 mm from the LOM.

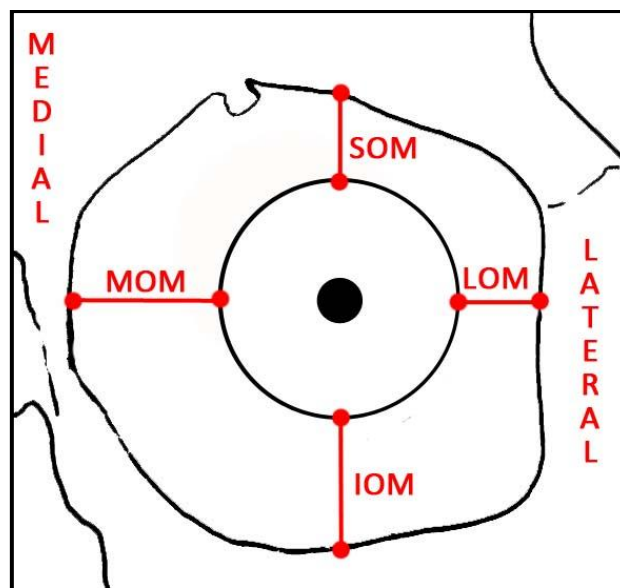


*Figure 2.8 Eyeball located supero-laterally within the orbit according to the literature*

The protrusion of the eyeball is based on the depth of the orbit, the vertical inclination of the orbit and the thickness and degree of overhang of the SOM <sup>25</sup>. Wilkinson and Mautner <sup>15</sup> suggest a practical standard by setting the eye in the horizontal plane when viewed in profile, (Fig. 2.9), so that the iris is on a level with a straight line (X) tangential to mid-SOM and mid-IOM. In this way the line touches the iris, with (a) showing eyeball protrusion approximately 3.8 mm past line X and (b) showing the depth of the orbit.

The upper eyelid shape traces the direction of the SOM. The fold of the eyelid is located centrally when the overhang of the rim is in the middle part of the SOM. If the outer rim at the side of the orbit is thickened, the fold is located more laterally. If the SOM is high with a low or medium height nasal bridge and a long lacrimal fossa, a medial epicanthic fold is present. <sup>10</sup>

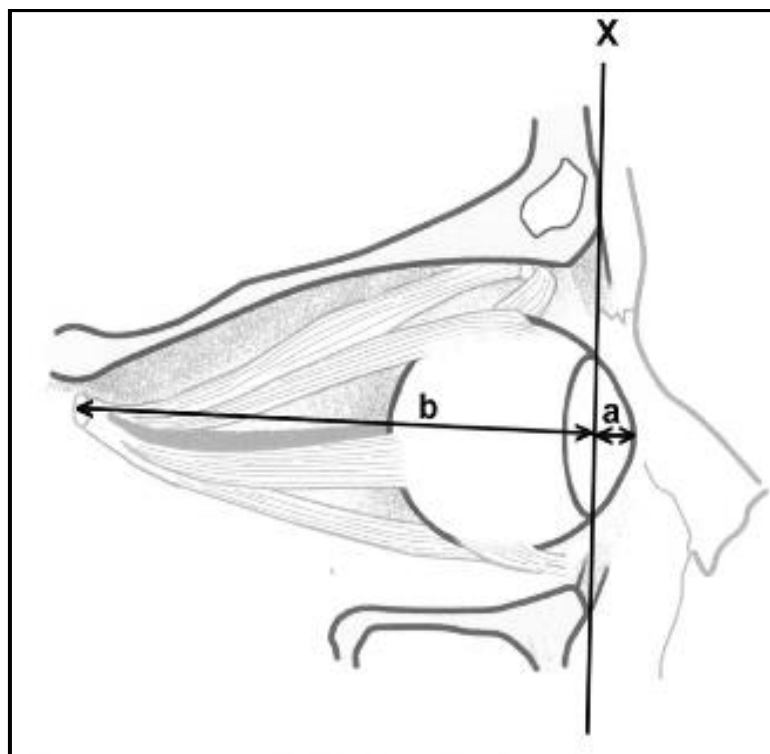


Figure 2.9 Eyeball protrusion <sup>15</sup>

X: Line tangential to mid-SOM and mid-IOM

- a) Eyeball protrusion
- b) Orbital depth

### 2.3.2. The Nose

Gerasimov utilised a two-tangent method for predicting the position of the nasal tip by projecting two lines from the bony nasal aperture<sup>35</sup>. The first line (Fig. 2.10 line A) follows the direction of the anterior nasal spine (ANS) and the second line (Fig. 2.10 line B) projects as a tangent to the distal third of the nasal bones. According to Gerasimov<sup>35</sup>, the intersection of these lines indicates the position of pronasale (most protruding point of the tip of the nose) (see Table 2.1). However, Rynn et al.,<sup>16</sup> states that it only predicts the position of the nasal tip and not necessarily pronasale, due to variation in the types of noses: e.g. pronasale being higher on the tip of more down-turned/hooked/aquiline noses and lower on tip of more upturned/snub noses. An adjustment to Gerasimov's method states that only the most distal portion of the nasal bones should be used to create the tangent (Fig. 2.10 line B) from which the position of the nasal tip will be derived<sup>7</sup>.

The "Threefold-ANS" method of estimating the anterior projection of the nose in profile<sup>34</sup> consists of "tripling the length of the ANS from the vomer-maxillary junction (VMJ) to the acanthion (the tip of the ANS), then adding the result to the mean tissue depth at the subnasale in the direction of a line projected from the ANS<sup>16</sup>. Rynn et al.,<sup>16</sup> published a study on the prediction of nasal morphology from the skull, which tested the Threefold-ANS and found it to be inaccurate as it often over-estimates the nasal projection. Furthermore, an accurate and comprehensive system of regression formulae to predict nasal profile dimensions in 3D (including maximum nasal width, position of the alae and nostrils as well as nasal asymmetry) were composed by utilising three linear distances between pairs of bony landmarks. The skull must be aligned in FHP and distances measured are visualised as shown in Fig. 2.11, with X as the distance from nasion to acanthion; Y as the distance between rhinion and subspinale; and Z as the distance between nasion and subspinale.

The literature researched also suggested that the shape of the ANS can give an indication of the shape of the nasal tip, where for example a spatulate nasal spine is associated with a wide or bulbous nasal tip, and a bifid nasal spine indicates a cleft nasal tip<sup>38</sup>. This suggested relationship is further explored in this study.

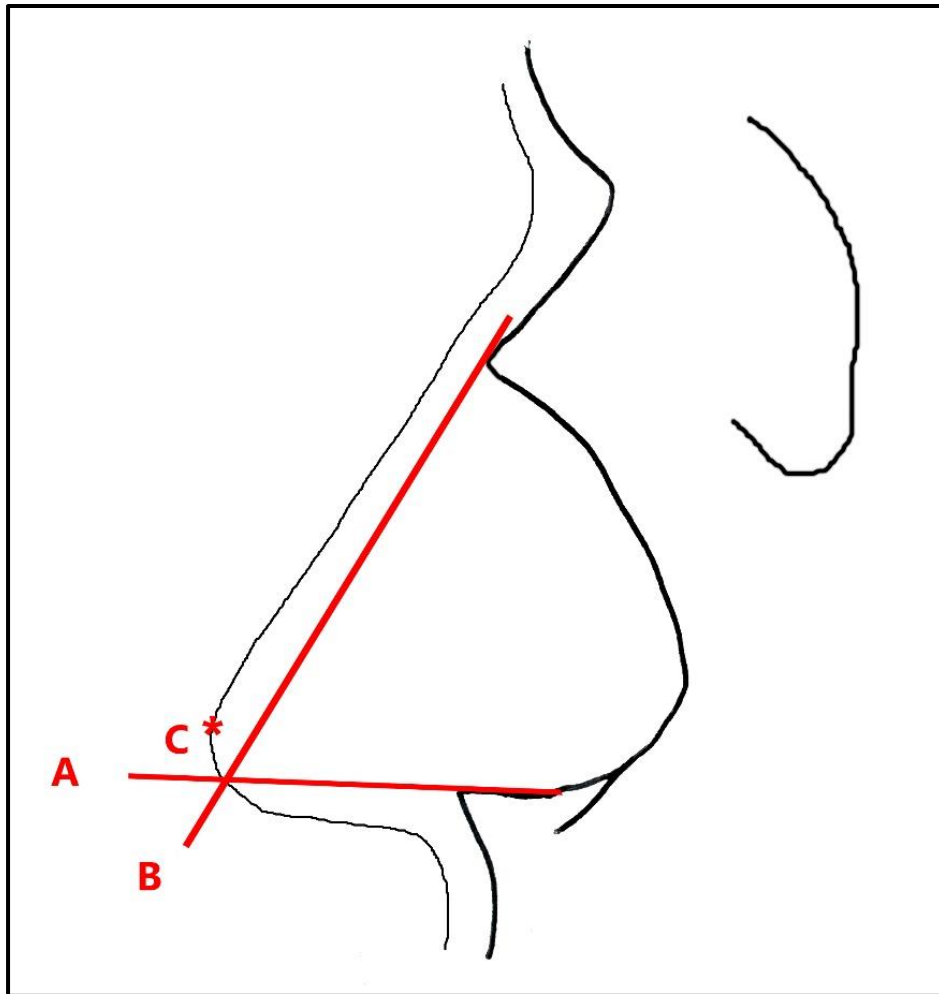


*Figure 2.10 Gerasimov's two-tangent method for predicting the position of the nasal tip where line A and B cross*

- A. Line following direction of ANS
- B. Tangential line to most distal part of nasal bones
- C. Pronasale (most protruding point of the tip of the nose)

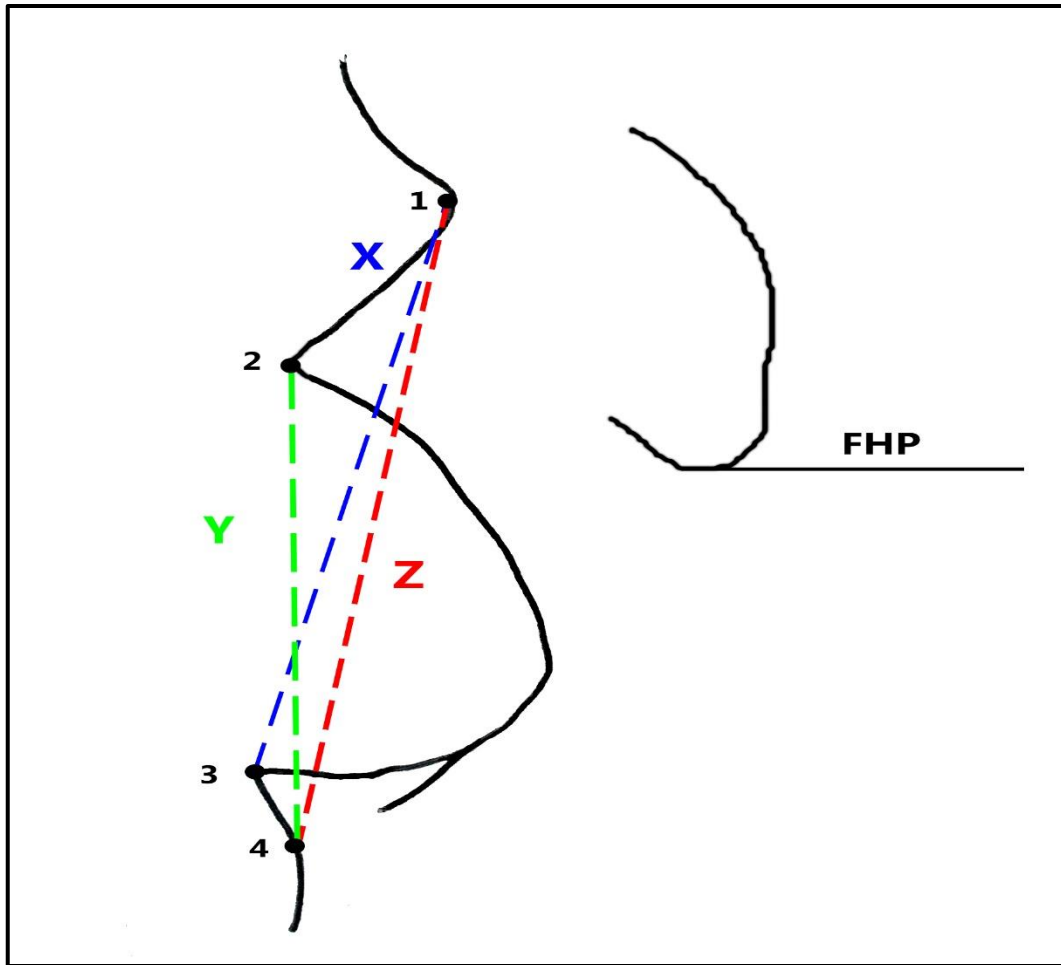


Figure 2.11 Measurements to be utilized in regression equations for prediction of the nasal morphology (redrawn from <sup>16</sup>)

1. Nasion
  2. Rhinion
  3. Acanthion
  4. Subspinale
- X: Distance between nasion and acanthion  
 Y: Distance between rhinion and subspinale  
 Z: Distance between nasion and subspinale

### 2.3.3. The Mouth

The skull does not provide many details for determining the position and shape of the mouth<sup>56</sup>. The first things to consider when attempting an approximation of the mouth should be the width of the mouth and the thickness of the lips <sup>25</sup>.

Various guidelines exist for estimating mouth width. The most reliable and accurate guide for mouth width has been considered to be the interlimbus distance<sup>20</sup>, or the width between the medial aspects of the irises<sup>56,64</sup>. However, these guidelines are limited, because it relies on the position of the eyes, and any error in eyeball positioning will result in inaccurate mouth width estimation<sup>17</sup>. Wilkinson<sup>38</sup> suggested a guideline based on Krogman's recommendations<sup>65</sup>, which only relies on known hard tissue landmarks. This guideline states that the position of the cheilia should be placed along reference lines radiating from the canines at angles perpendicular to the contour of the dental arcade. Stephan and Henneberg<sup>17</sup> proposed a 75% rule where the inter-canine width is equivalent to 75% of the width of the mouth, measured from cheilion to cheilion.

Wilkinson et al.<sup>20</sup> further stated that there is a correlation between lip thickness and maximum tooth (crown) height and provided formulae for calculating lip thickness for individuals of European and Asian ancestry.

#### 2.3.4. The Ears

Although the ears contribute less to facial recognition than other features such as the eyes or mouth<sup>66,67</sup>, it plays a role in the overall correct appearance of the face. Therefore, prediction guidelines (and its verification) for reconstructing the ear is important<sup>23</sup>. A few guidelines exist for the placement of the ears in FAs, although most of these seem to be artistic estimations rather than scientific principles. Currently, standard ear casts are used in approximations and vary only in relation to size and lobe pattern<sup>38,68</sup>.

Gerasimov<sup>35</sup> attempted to define the general relationship between the size of the ear and nose as the ear length roughly approximates the height of the nose, from subnasale to glabella. Porter and Olsen<sup>42</sup>, however, reported that the average African American woman has an ear length slightly greater than the nose length (nasion to subnasale) with a ratio of approximately 5:4. Relating the nose and the ear proportions in FAs still seems to be in use as Gibson<sup>9</sup> more recently states that a general guideline is to place the ear from a level through the top of the eye area to a level at the bottom of the nose so that the ear is more or less the same length as the nose. Various studies have measured the length of the ear from supraaurale to subaurale<sup>42,59,69-72</sup> and a common trend indicates that the male ear is larger than the female ear<sup>10</sup>.

Guyomarc'h and Stephan <sup>23</sup> formulated a total of 18 regression formulae for the prediction of various auricular dimensions. This was done by utilising a set of CT scan samples as well as verifying formulae from various previously published studies <sup>71, 73-75</sup> and unpublished work by TW Todd.

Russian scientists Fedosyutkin and Nainys <sup>25</sup> and Gerasimov <sup>35</sup> claim that the skull does provide some information on the shape and placement of the ears. Firstly, the external auditory meatus indicates the position of the ear, while the direction in which the mastoid processes are pointing, determines if the earlobes are free or attached. A downward directed mastoid process results in an attached earlobe, while a forward directed mastoid process results in a free lobe <sup>25, 35</sup>. These results have not been confirmed by other studies. The orientation of the ear, as it should be placed in FAs, may be estimated by the angle of the jaw as the long axis of the pinna seems to be parallel to the jawline (Fig. 2.11) <sup>38</sup>.

Ear protrusion can be total, or only in the upper or lower parts. If a strongly developed supramastoid crest is visible, the upper part will protrude, while a rough outer surface of the mastoid process results in protrusion of the lower part. If both characteristics are present, total ear protrusion occurs <sup>25</sup>.

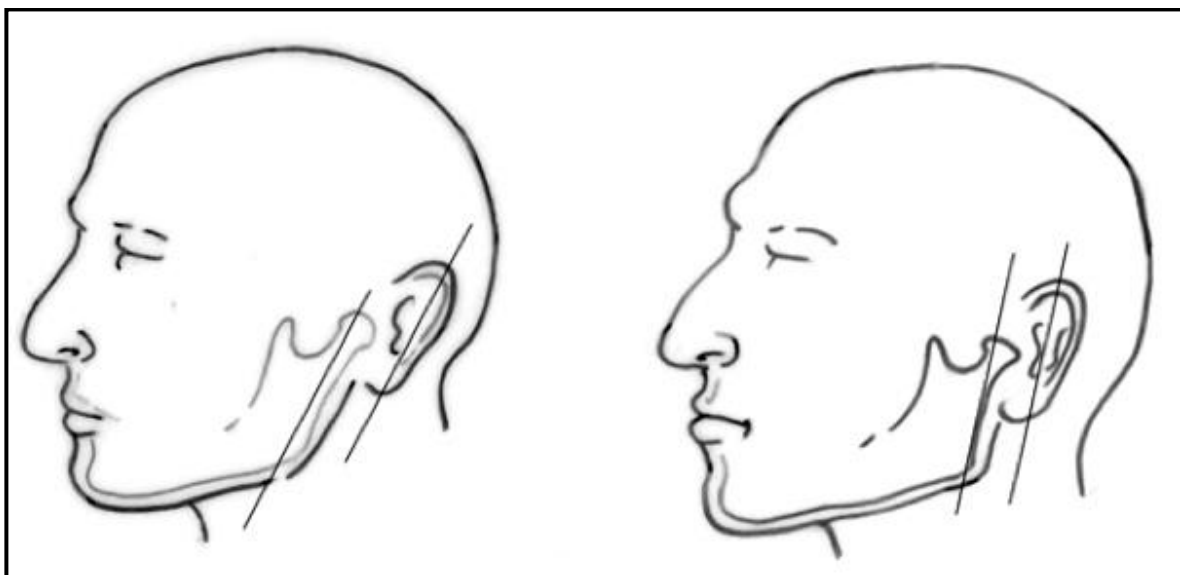


Figure 2.12 The relationship between the orientation of the ear and the angle of the jaw

## 2.4. Possible shortcomings of established guidelines

Guidelines used in FAs (and superimpositions) should be “constrained by real and verifiable anatomical relationships if they are to be employed under the umbrella of forensic science”<sup>76</sup>. In other words, if a method or guideline is not quantifiable, verified or repeatable, it should not be used for FAs. Some guidelines have been examined and verified and should be the preferred methods utilised in FAs.

Eyeball projection has been tested in various clinical studies <sup>77-80</sup>, however the method proposed by Wilkinson and Mautner <sup>15</sup> has not been verified to date. The position of the canthi have been substantiated <sup>53, 61, 81</sup>, although some discrepancies have been noted. Many studies agree on the position of the eyeball within the orbit <sup>19, 22, 28-32, 61</sup>, but it is unknown whether it will be relevant for South African populations.

Some approximation guidelines for the nose have been tested. Conflicting reports on for instance the accuracy of the Gerasimov’s two-tangent method <sup>35</sup> have been noted <sup>10, 13</sup>, but a clear consensus on the validity of the method has not been reached yet. On the other hand, the methods for predicting the nasal morphology from the skull, published by Rynn <sup>16</sup>, have not been verified in any other studies, but does not however form part of this study. The relationship between the anterior nasal spine and the nasal tip suggested by <sup>38</sup> have been partly confirmed by Rynn et al. <sup>16</sup>.

Guidelines on predicting the mouth width by means of interlimbus distance is not included in this study but have been reported to perform well <sup>18, 20</sup>. However other guidelines e.g. the 75% rule described by Stephan and Henneberg <sup>17</sup> as well as the statement by Fedosyutkin and Nainys’ <sup>25</sup> that the mouth corners correspond to the mandibular second molars or that the mouth corners correspond to radiating lines from the canine/first-premolar junction <sup>38</sup> remain untested. Of these untested guidelines, only the 75% rule will be assessed in this study.

Lastly, when considering approximation guidelines of the ear, very few have been verified. Some tested guidelines include the trend for male ears to be larger than female ears and the the position of the ear indicated by the external auditory meatus. Regression formulae by Guyomarc’h and Stephan <sup>23</sup> verified various formulae from previously published studies and will be tested in this study. Untested guidelines which are not included in this study are the relationship between the mastoid process and the ear lobe, the angle of the jaw reflecting

the orientation of the ear and the level of ear protrusion - all proposed by Fedosyutkin and Nainys <sup>25</sup>.

By utilising the information gained in this literature review, specific landmarks, structures and dimensions will be referred to throughout, in an attempt to relate the bony structures of the face to the soft tissues and so reflect and expand on the existing guidelines for FAs.

### 3. MATERIALS AND METHODS

The following dissections and measurements were performed on a sample of cadavers belonging to black South Africans. Cone beam computed tomography (CBCT) and computed tomography (CT) scans of patients were incorporated for verification of the cadaveric eye measurements.

#### 3.1. Sample

The South African people are broadly classified as Black, White, Coloured and Indian/Asian. Black South Africans form the majority of the population, and is thus also the most predominant when dealing with forensic cases.<sup>82</sup> This group was previously considered as broadly alike in genetic constitution with similar cranial size and shape<sup>83</sup>, but also significantly different from other African and American black ancestral groups<sup>83-86</sup>. For the purpose of this study, only black South Africans were assessed.

A total of 49 adult cadavers (38 males and 11 females, age range 22 – 73, mean age 47) from the dissection halls of two South African universities, namely Sefako Makgatho Health Sciences University (SMU) and the University of Pretoria (UP) were used in this study. Under the National Health Act no. 61 of 2003, cadavers for the purpose of medical teaching and research originate from either donations or unclaimed bodies from various hospitals. Unclaimed bodies forming part of the cadaver collection at UP generally come from local hospitals in Pretoria such as Mamelodi, Kalafong or Steve Biko<sup>1</sup>, while those at SMU may originate from a wider area in Gauteng and some areas in the North West Province of South Africa. Samples demonstrating damage, distortion or any effects of desiccation due to embalming were excluded.

A total of 30 CT scans (23 males, 7 females, age range 21 – 84, mean age 42) from Steve Biko Academic Hospital affiliated with UP and 30 CBCT scans (17 males and 13 females, age range 18 – 64, mean age 33) from the Oral and Dental Hospital, UP, were used for measurement and analyses. These hospitals service the greater Gauteng area, as well as parts of the Limpopo and North West provinces. Patient's heads were orientated in the standard natural

head position for scanning. Scans were excluded if not orientated in the desired plane, the implicated structures could not be clearly identified or injury to the orbital area was present.

### 3.2. Ethical considerations

Ethics approval for the MSc project was obtained from the Research Committee of the Faculty of Health Sciences of the University of Pretoria (Cadaver sample: 8/2016; Scan sample: 183/2016). The Faculty of Health Sciences Research Ethics Committee complies with the SA National Act no. 61 of 2003 as it pertains to health research.

### 3.3. Methodology

All measurements taken on the cadaver sample were obtained in the Frankfurt horizontal plane (FHP) (Fig. 3.3). The FHP is defined as the position when the orbitale is horizontally aligned with the porions of both sides. In certain situations, as for instance this study, it is more practical to use the tragion point than the porion<sup>25</sup>. Measurements were performed on each facial feature to verify existing guidelines.

Linear (quantitative) measurements on cadaver samples for the determination of the position and size of the facial features were done prior to dissection and included the position of the canthi, the size of the ears as well as distances measured on the mouth. The mouth was examined to determine the corresponding teeth at the corners of the mouth (Fig. 3.16). Measurements were taken to determine the correlation between the width of the mouth and the inter-canine width (Fig. 3.17) as well as the width of midpoints of the upper central incisors and the philtrum (Fig. 3.18 and 3.19). The orbital area was then dissected and measurements to determine the position and size of the eyeball were done (Fig. 3.4). Dissections were also done to determine the correlation between the shape of the anterior nasal spine (ANS) (Fig. 3.11) and the nasal tip as well as the applicability of Gerasimov's two-tangent method (Fig. 3.14). Dimensions were taken using a digital sliding calliper and rounded off to the nearest 0.01 mm, with reference to the landmarks identified and defined in Table 1.1 (Introduction/Literature review). All measurements were taken on the left side of the face

i.e. the left ear, the left eye, etc., except where specific landmarks to be measured involve the midline of the face e.g. the philtrum.

Regarding measurements on the scan sample, both the CT and CBCT scans were visualised using MevisLab ([www.mevislab.de](http://www.mevislab.de)), a medical visualisation program specifically designed for three-dimensional (3D) visualisation, analyses and measurements. MevisLab enables the user to identify landmarks and measure distances in 3D by ensuring that the points retain their respective positions regardless of scrolling through the slices.

Male and female samples were pooled in all three samples sets (cadaver, CT and CBCT) and statistical analyses performed on each feature, with distinct methodology for quantitative and qualitative parameters. In Figures 3.1 and 3.2 a summary of the work flow for analyses on both types of parameters is presented.

Intra-observer repeatability was tested for all quantitative parameters measured by obtaining three measurements and calculating the standard deviations. The parameters that were assessed using quantitative measurements were the position of the canthi, the position of the eyeball, the size of the eyeball (on cadaver dissections, CT and CBCT scans), the width of the philtrum and upper central incisors, the inter-canine and mouth widths, as well as the length of the ears. Qualitative nasal parameters and tooth position at the corners of the mouth were recorded once.

Inter-observer repeatability testing was conducted by obtaining measurements done by one other observer for cadavers, CT scans and CBCT scans.

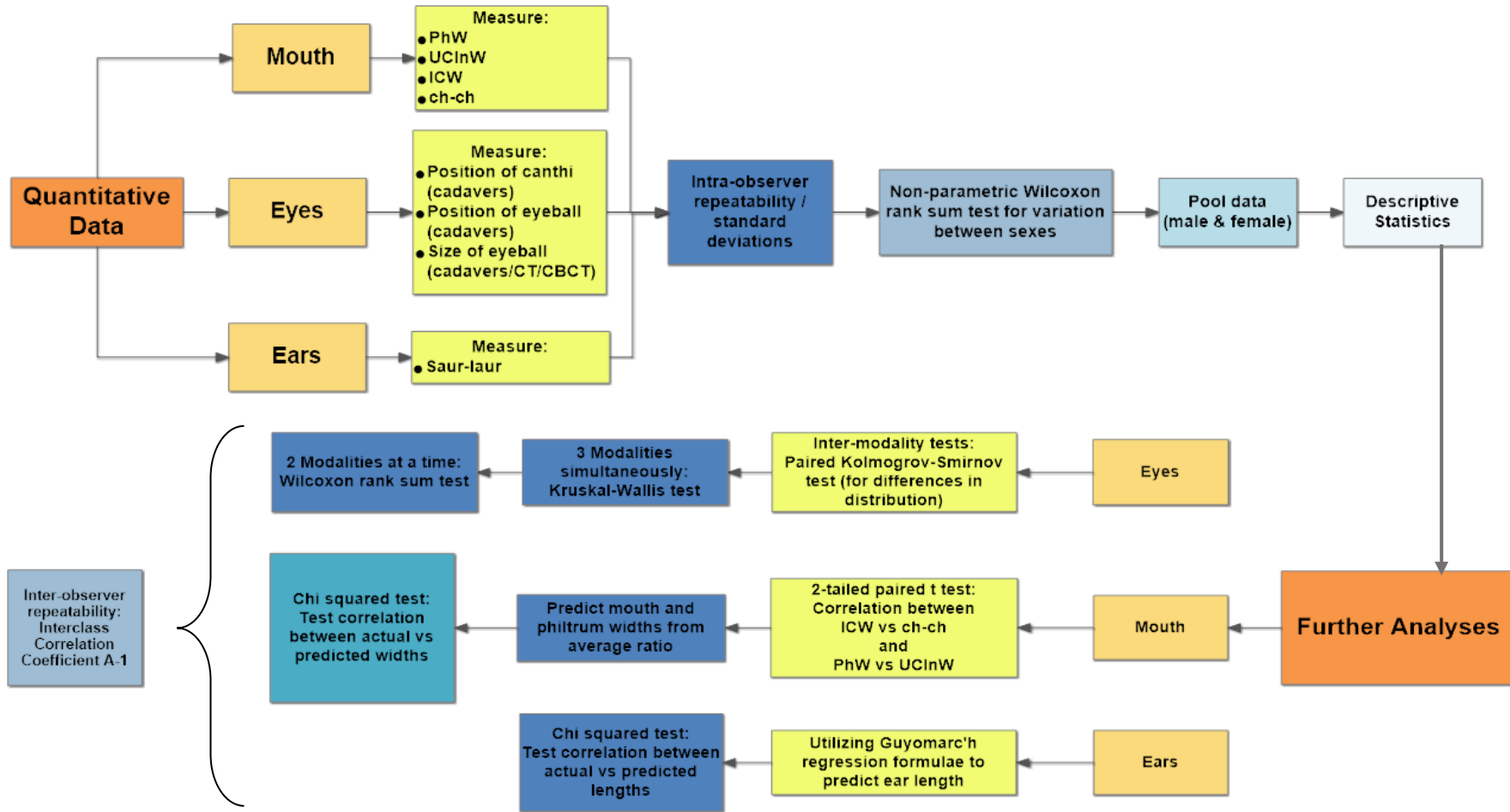


Figure 3.1. Statistical analyses work flow for quantitative data

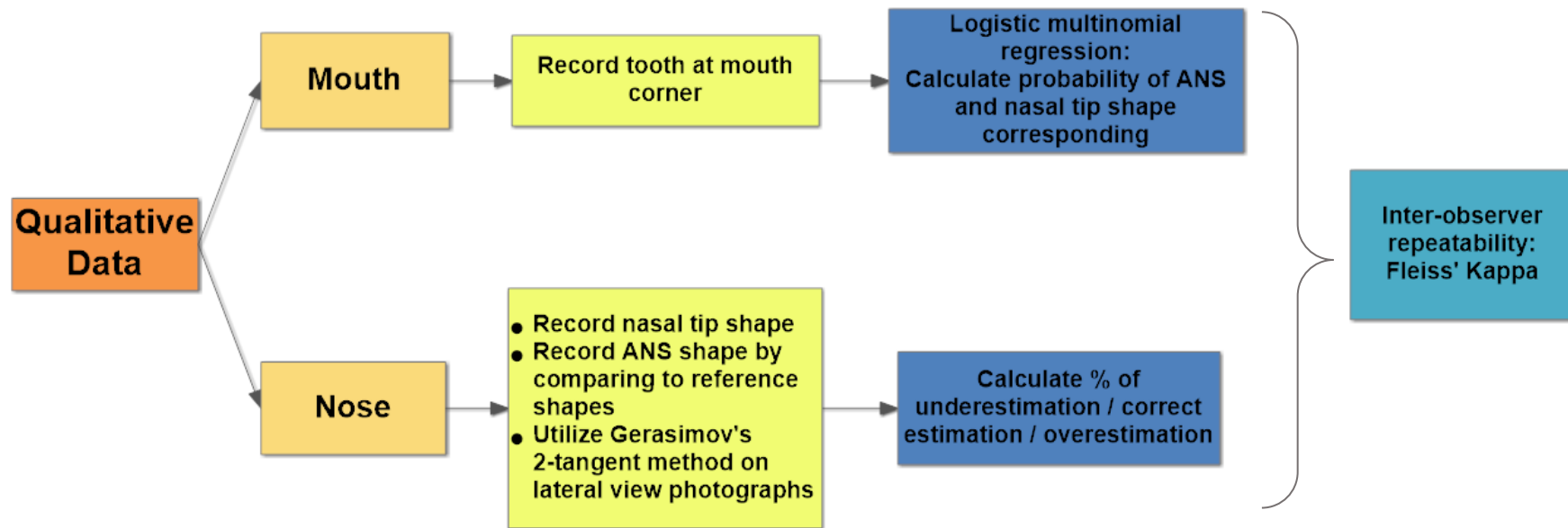
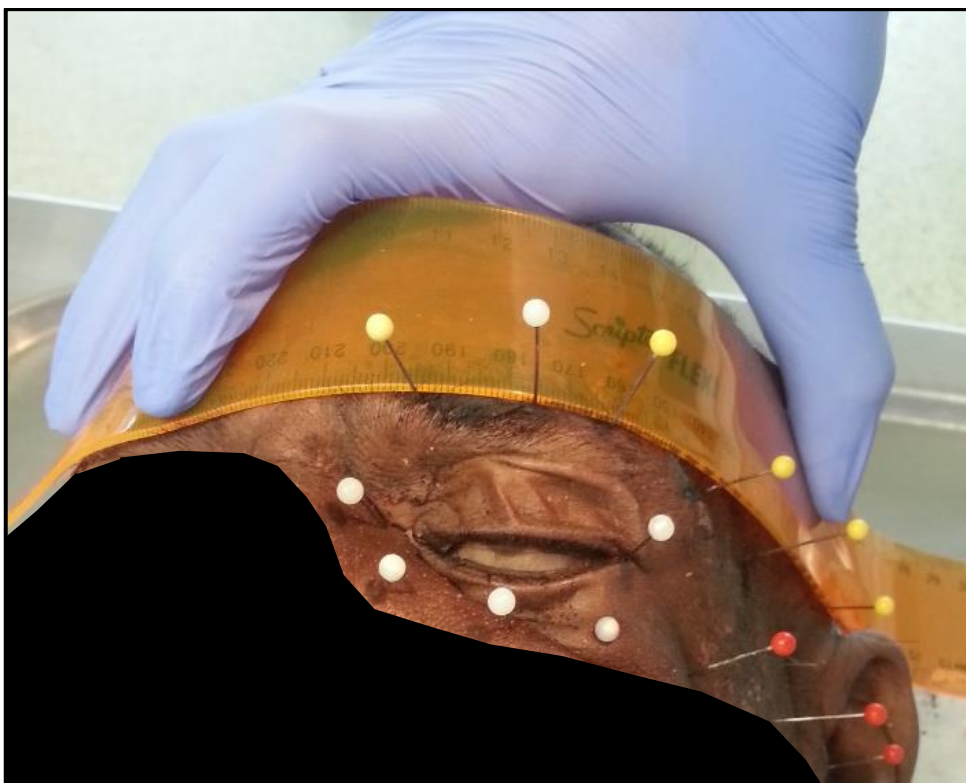


Figure 3.2. Statistical analyses work flow for qualitative data

### 3.3.1. Orbital and ocular measurements

To determine the position of the canthi, the orbital margin was firstly palpated and pinned. A flexible ruler was used to pin FHP from porion to orbitale and a reference plane was pinned parallel to the FHP and tangent to the most superior point on the SOM (Fig. 3.3). The endo - and exocanthions were identified and pinned and four distances were measured namely (1) between the endocanthion and MOM, (2) endocanthion and SOM, (3) the exocanthion and LOM and (4) exocanthion and SOM (Fig. 3.4a).



*Figure 3.3: FHP and parallel reference plane*

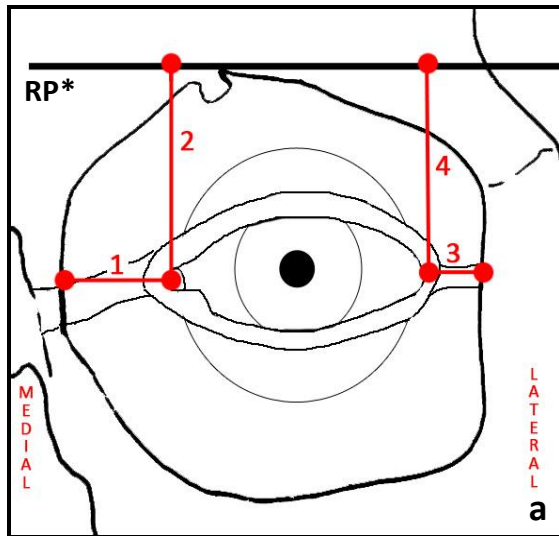
Red pins show the FHP, with yellow pins indicating the parallel reference plane. White pins were used to identify the orbital margin.

To determine the position of the eyeball in the orbit, a circular cut was made approximately 5 mm outside of the orbital margin. The skin and orbicularis oculi muscle were removed and the entire eyeball exposed by careful blunt dissection and removal of peri-orbital fat and tissue. Pins were placed perpendicular to the surface of the bone at the most extreme points on the LOM, MOM, IOM and SOM as previously defined. Another set of four pins were placed

at the shortest distances respectively from the LOM, MOM, IOM and SOM on the equator of the eyeball (an imaginary line encircling the globe of the eye equidistant from the anterior and posterior poles) <sup>87</sup>. Four distances were measured between the pins, namely (1) inferior equator to IOM, (2) superior equator to SOM, (3) lateral equator to LOM and (4) medial equator to MOM (Fig. 3.4b).

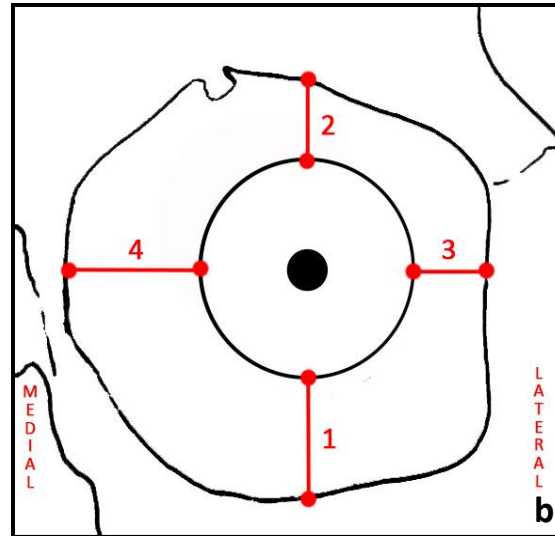
Two measurements were taken to determine the size of the eyeball, namely (1) medio-lateral diameter (distance between pins at medial and lateral equators) and (2) supero-inferior diameter (distance between pins at superior and inferior equators) (Fig. 3.4c).

The medial equator of the eye to the MOM (Fig. 3.4b (4)), the medio-lateral diameter of the eye (Fig. 3.4c (1)) and the distance between the lateral equator of the eye and the LOM (Fig. 3.4b (3)) were used to obtain the horizontal diameter (width) of the orbit. To obtain the vertical diameter (height) of the orbit, the distances added were: the distance between the superior equator of the eye and the SOM (Fig. 3.4b (2)); the supero-inferior diameter of the eye (Fig. 3.4c (2)); and the distance between the inferior equator of the eye and the IOM (Fig. 3.4b (1)).



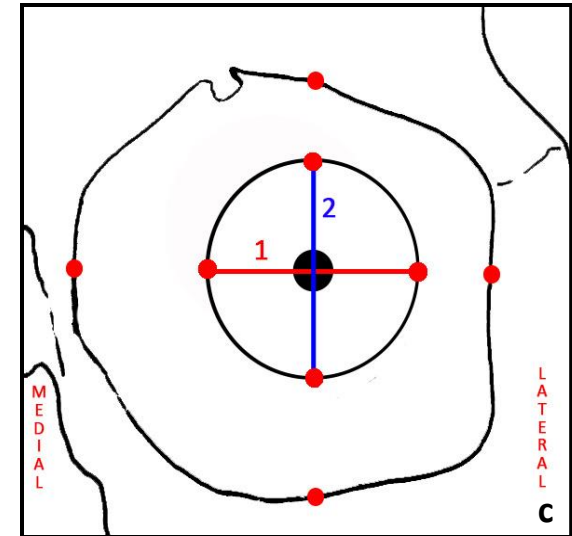
a) Position of the canthi:

- 1: distance between the medial canthus and MOM
- 2: distance between the medial canthus and SOM reference plane
- 3: distance between the lateral canthus and LOM
- 4: distance between the lateral canthus and the SOM reference plane.



b) Position of the eyeball in the orbit

- 1: distance between the inferior equator and the IOM
- 2: distance between the superior equator and SOM
- 3: distance between the lateral equator and LOM
- 4: distance between the medial equator and MOM.



c) Size of the eyeball

- 1: medio-lateral diameter (the distance from the medial equator to the lateral equator)
- 2: supero-inferior diameter (distance from the superior to inferior equator)

Figure 3.4: Orbital and optic measurements

\*RP: Reference plane parallel to FHP

CBCT and CT scans were imported into MevisLab as DICOM (.dcm) files from the source folder and the image loaded.

ExaminerViewer was used to visualise the 3D reconstruction of the files to ensure the correct voxel size and reconstruction. ROI Select was used to select a specific region of interest, enlarging the relevant areas, in this case the orbital area (Fig. 3.5). OrthoView2D was then used to visualise the region of interest and identify two points corresponding in all three planes (coronal, sagittal and transverse). The relevant points to determine the diameter of the eyeball were the most inferior, superior, medial, lateral, anterior and posterior points on the equator of the eyeball. The points identified to measure the orbital depth were the most anterior point on the equator of the eyeball (the cornea) and the anterior opening of the optic canal. Lastly XMarkerListMaxDistance was used to measure the distance between the identified points. Scans were orientated, points identified and measurements taken on a multiplanar level as the relevant dimensions were not necessarily visible on a single plane simultaneously. The points, however, retained their respective positions in all three dimensions regardless of scrolling through the slices.

Dimensions measured to determine the size of the eyeball were the antero-posterior diameter, between the anterior equator (the cornea) and the posterior equator (where the optic nerve exits the eyeball) (Fig. 3.6), medio-lateral diameter, between the medial and lateral equators of the eyeball (Fig. 3.7), supero-inferior diameter, between the superior and inferior equators (Fig. 3.8) and the orbital depth, from the cornea (anterior equator) to orbital canal (Fig. 3.9).

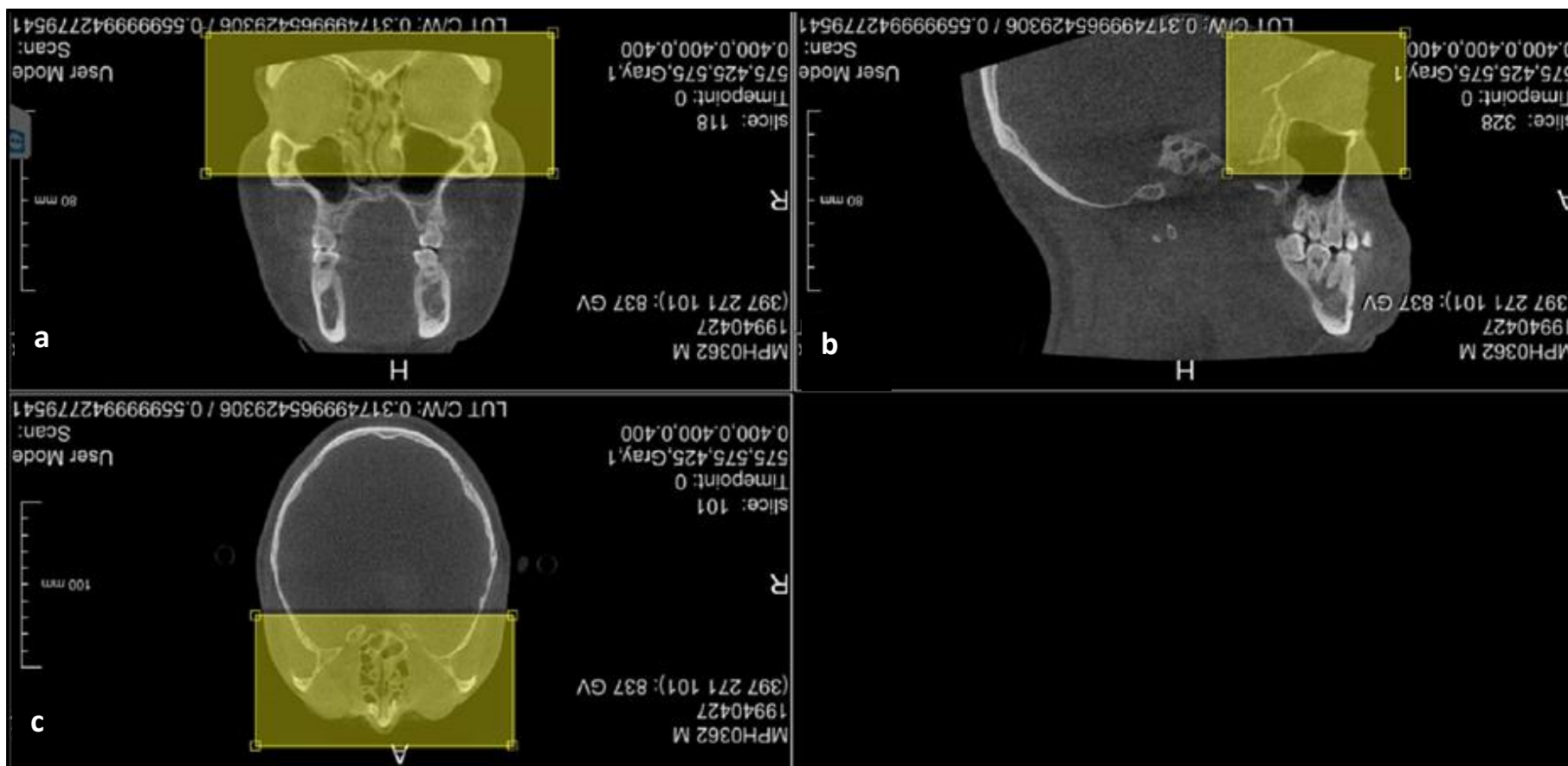


Figure 3.5: Selecting the region of interest on MevisLab

a) Coronal plane, b) Sagittal plane, c) Transverse plane

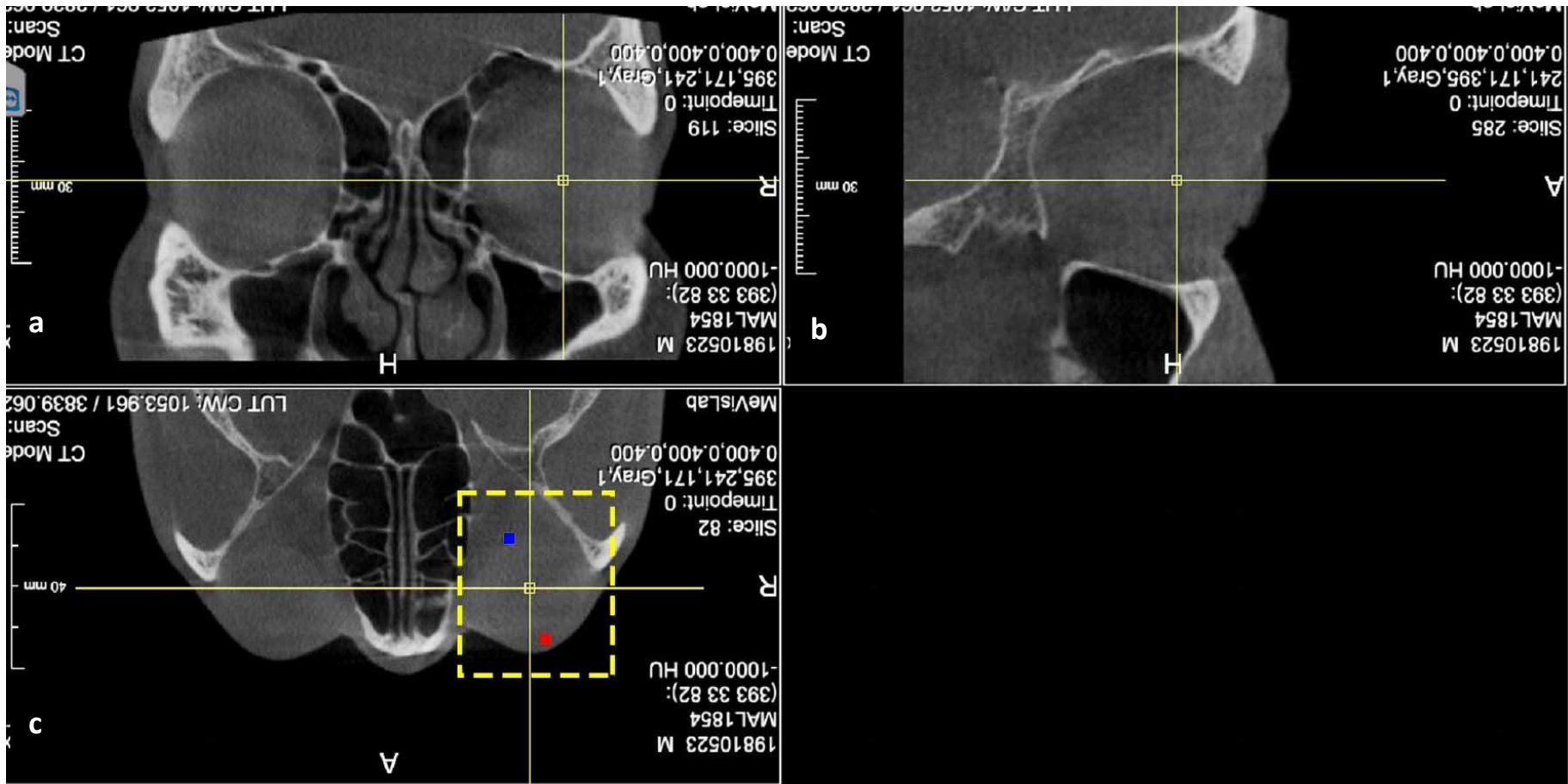


Figure 3.6: Antero-posterior diameter of the eyeball

a and b) Scan orientation in coronal and sagittal planes respectively

c) Transverse plane demonstrating antero-posterior diameter measured between blue mark (posterior equator of the eyeball) and red mark (anterior equator of the eyeball)

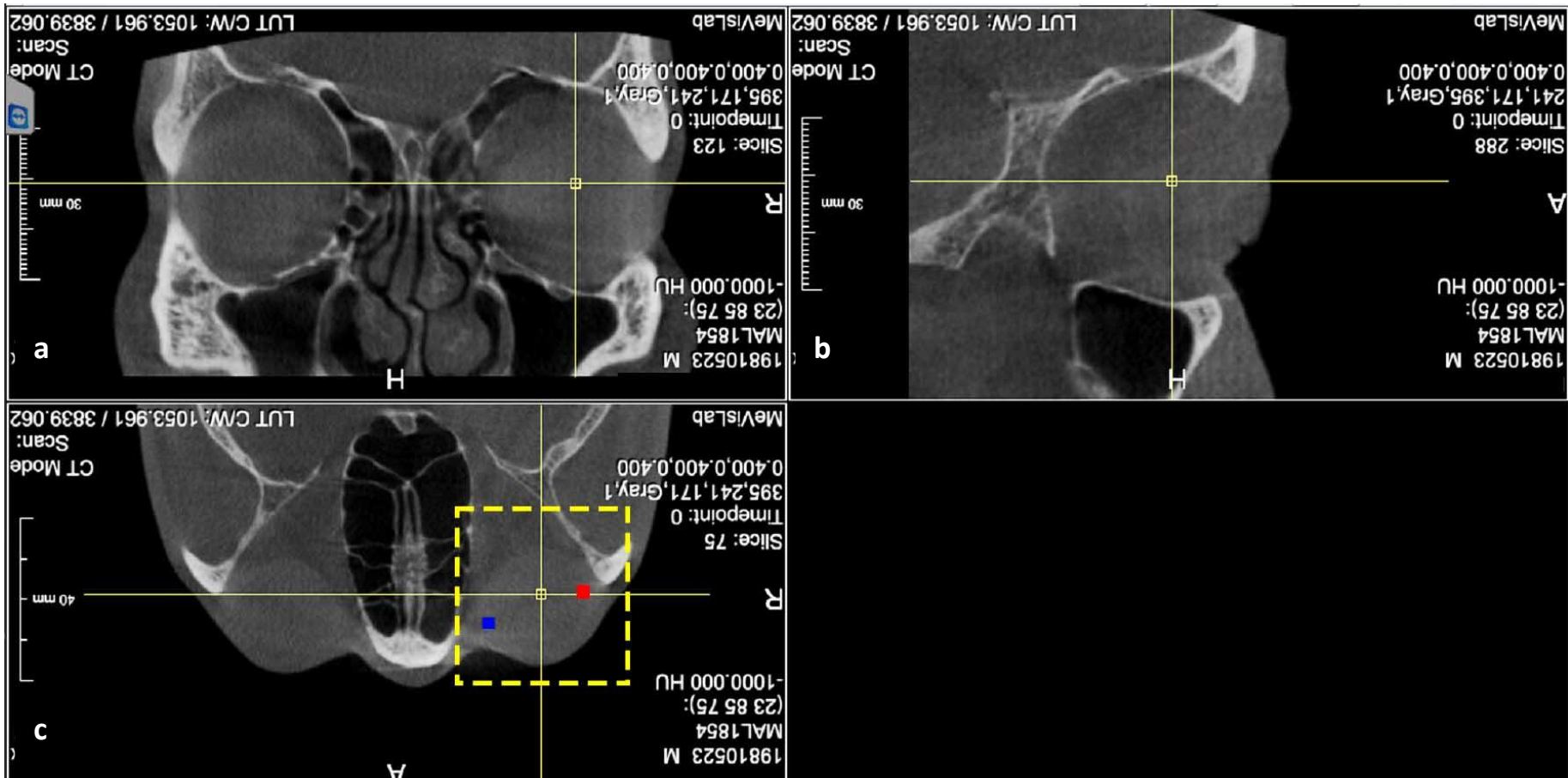


Figure 3.7: Medio-lateral diameter of the eyeball

a and b) Scan orientation in coronal and sagittal planes respectively

c) Transverse plane demonstrating medio-lateral diameter measured between medial equator (blue mark) and lateral equators of the eyeball (red mark)

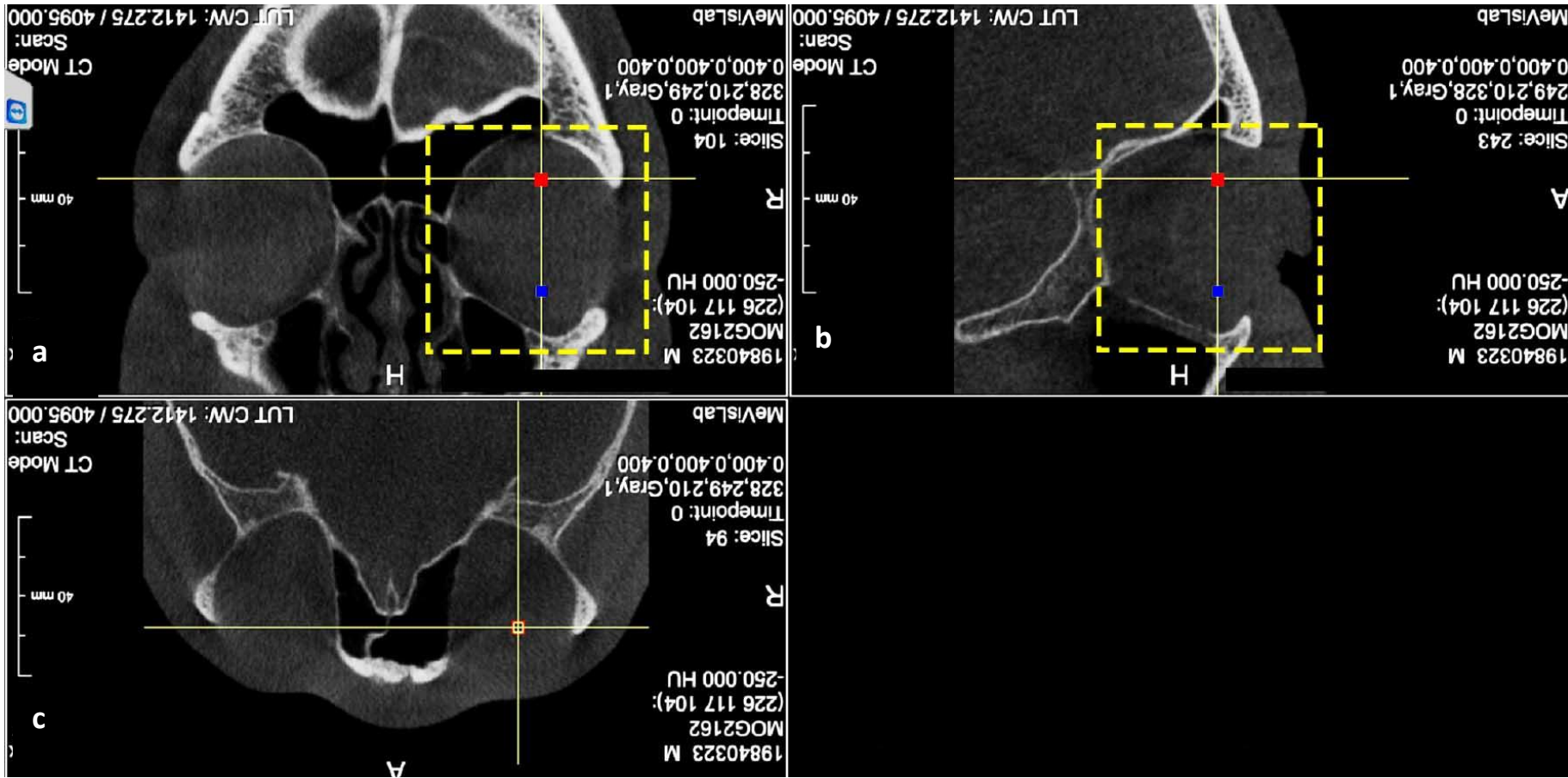


Figure 3.8: Supero-inferior diameter of the eyeball

a and b) Supero-inferior diameter of the eyeball measured between the superior equator (red mark) and inferior equators of the eyeball (blue mark)

c) Scan orientation in the transverse plane

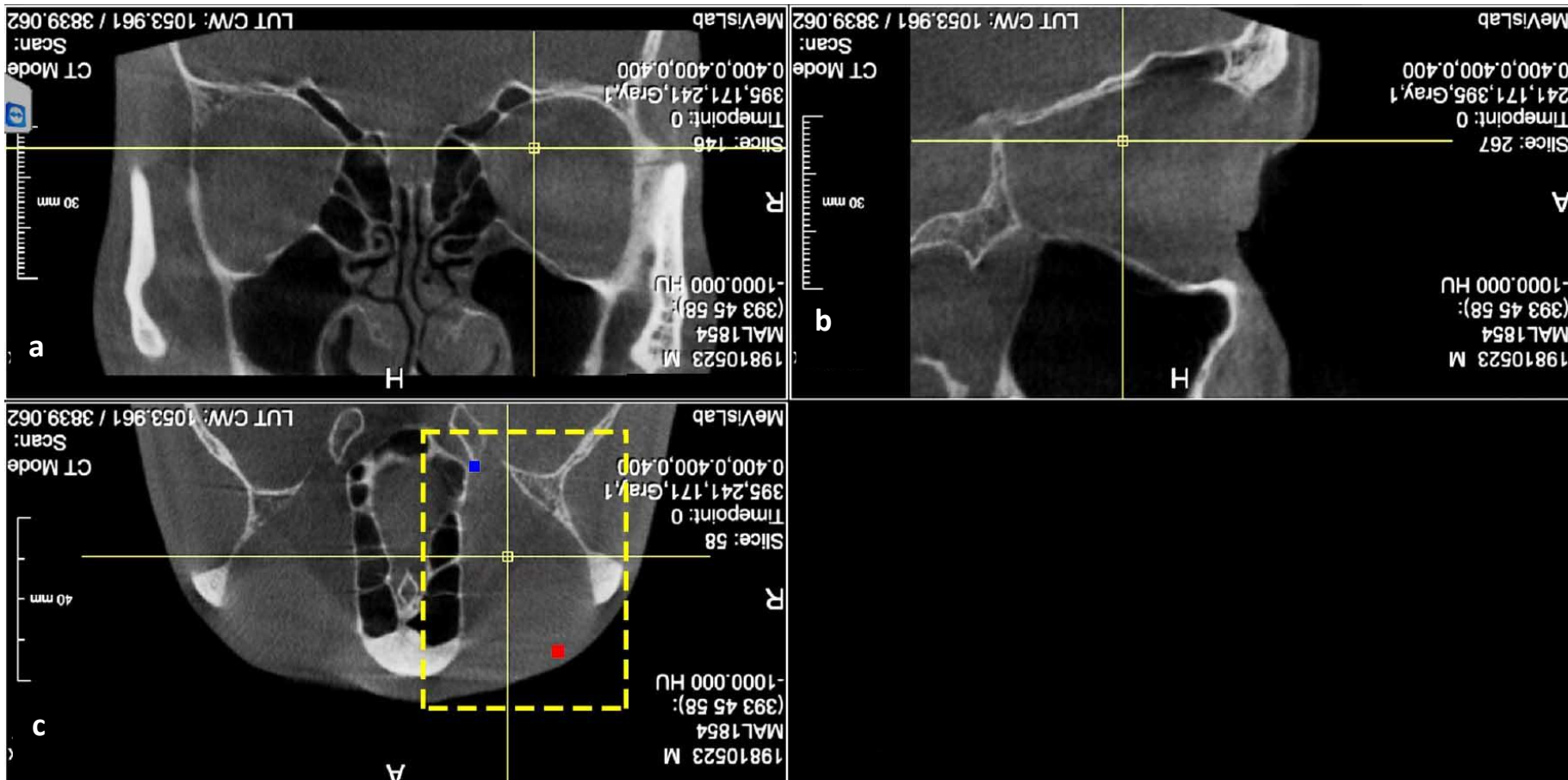


Figure 3.9: Orbital depth

- a) Scan orientation in coronal plane
- b) Scan orientation in the sagittal plane
- c) Orbital depth as the distance measured from the cornea (red mark) to the anterior opening of the optic canal (blue mark)

### *(i) Statistical analysis on orbital and ocular measurements*

Descriptive statistics were calculated on the average of all orbital and ocular measurements (minimum, maximum, mean, median, skewness, first and third quartiles, standard deviation as well as confidence intervals).

### ***Testing between modalities***

Simultaneous comparisons were made between all 3 measurement methods namely cadaver dissections, CT and CBCT scans, utilising the Kruskal-Wallis test. The Kruskal-Wallis test is a non-parametric version of the classical one-way ANOVA, and an extension of the Wilcoxon Rank Sum test to more than two groups. One-way ANOVA cannot be used in this case because the assumptions are not met, namely that the distributions of the residuals are not normal, and the variances are not homogeneous.

Firstly, the Paired Kolmogorov-Smirnov test was used to test for differences in distributions between the different measurement methods. Due to the asymmetrical distribution of most of the measurements, the Wilcoxon Rank Sum test (2-sided) was used for further comparisons between 2 the measurement methods.

Comparisons between the medio-lateral and supero-inferior diameters were made between two modalities at a time by utilising the Wilcoxon Rank Sum test. These comparisons were CT vs CBCT; CT vs dissection and dissections vs CBCT respectively.

## **3.3.2. Nasal measurements**

The relationships between the shape and features of the anterior nasal spine (ANS) and the shape of the nasal tip, as suggested by Angel <sup>55</sup> and Wilkinson <sup>38</sup>, were determined by dissections and measurements. The nasal tip shape was identified as round, bifid, sharp or bulbous. An incision in the midline of the nose (from nasion to supradentale) was made, followed by a small transverse incision of approximately 15 mm superiorly at the nasion, and another of approximately 25 mm inferiorly at the supradentale. A circular incision around the left nostril was made and the skin of the nose bluntly dissected to flap open the left side of the nose (Fig. 3.10). The nose was then bisected by gently separating the nasal cartilage in the midline (indicated by the blue pins in Figure 3.9) and the nasal septum from the ANS. Lastly,

the surrounding area was dissected to expose the entire ANS and photographed from above (Fig. 3.11). Lateral view photographs of the bisected nose were also taken (Fig. 3.12).

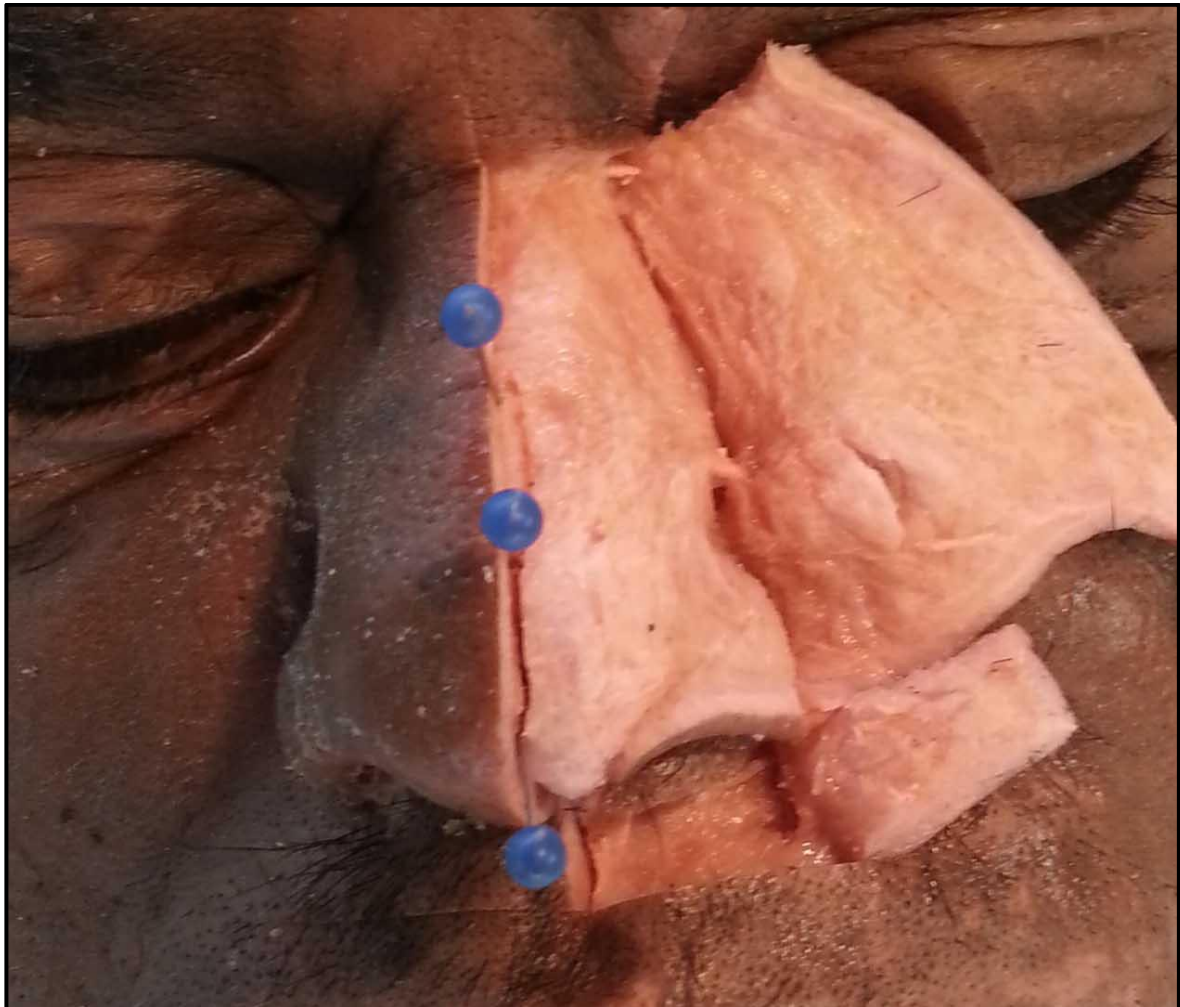


*Figure 3.10: Separating the skin from the nose*

The blue pins follow the nasal cartilage in the midline where the nose was bisected.



*Figure 3.11: Visualising the ANS in an antero-superior view*

1) Rhinion 2) Nasal cartilage pulled laterally 3) ANS visible as spatulate-shaped bone (within red circle)

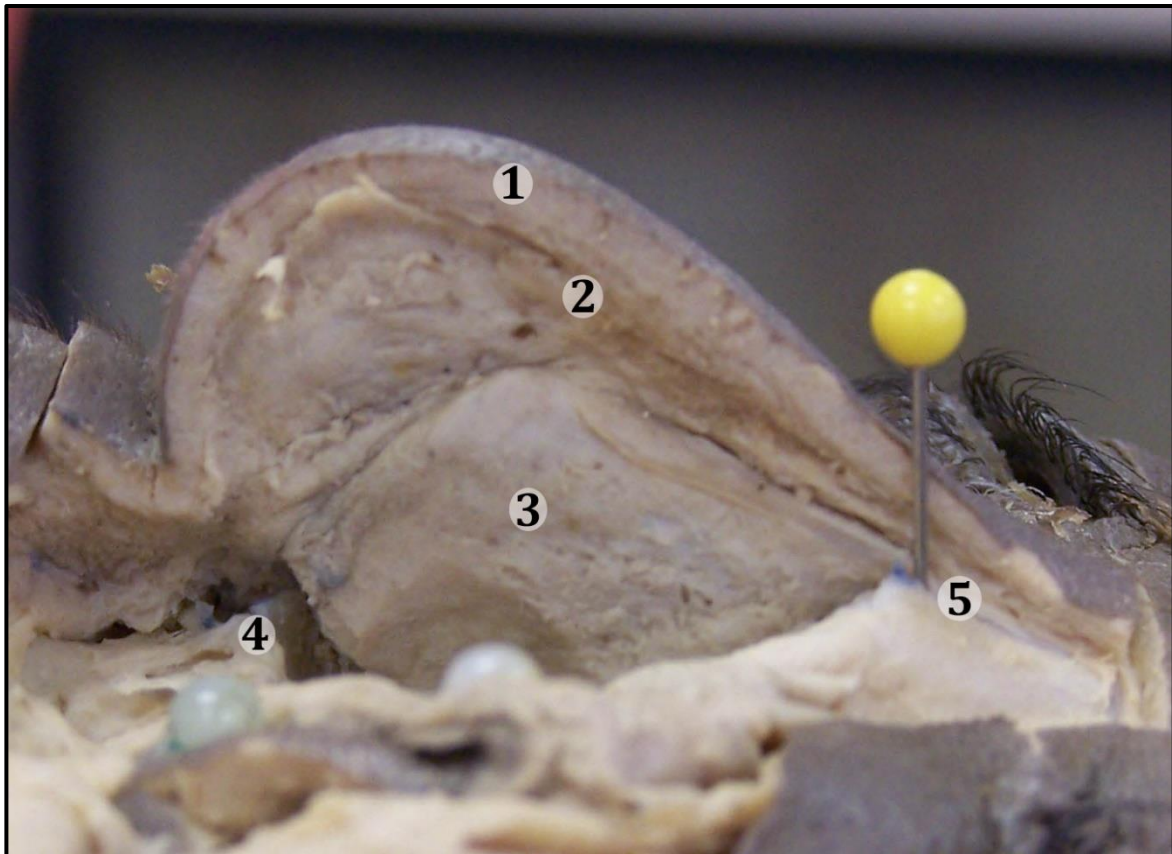


*Figure 3.12: Lateral view photograph of bisected nose*

A slightly supero-lateral view of the bisected nose ensures optimal visualization of both the ANS and the nasal bones for utilizing Gerasimov's two-tangent method of determining the position of the nasal tip. The yellow pin marks the end of the nasal bones (rhinion).  
 1) Skin of the nose 2) Nasal cartilage 3) Nasal septum 4) ANS 5) Nasal bones

The photographs were visualised using Adobe Photoshop. The ANS were classified as sharp, spatulate, round (full or half) or bifid by comparing it to predetermined reference shapes (Fig. 3.13) as defined by Angel<sup>55</sup> and Wilkinson<sup>38</sup>. Figure 3.14 demonstrates examples of various dissected ANS from the cadaver sample classified as the assorted shapes.

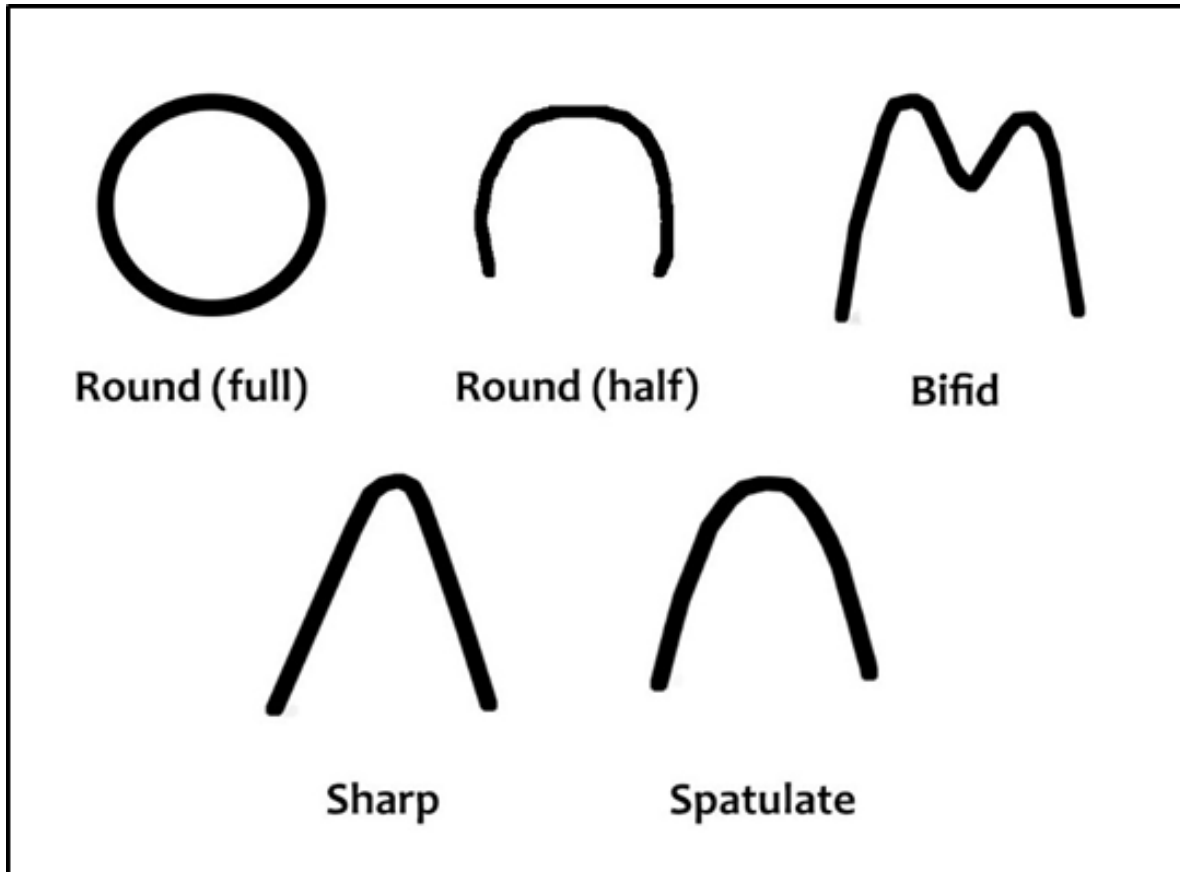


*Figure 3.13: Reference shapes for ANS*

Gerasimov's two-tangent method<sup>35</sup> for determining the position of the nasal tip was also performed by utilizing the lateral view photographs of the nose. A line tangent to the nasal bones (from rhinion) was drawn, with another line inserted following the direction of the ANS. Gerasimov postulated that the intersection of the two lines will correlate with the position of the nasal tip. The intersection of the two lines was recorded as (1) underestimation, (2) correct estimation or (3) overestimation of the nasal tip (Fig. 3.15).

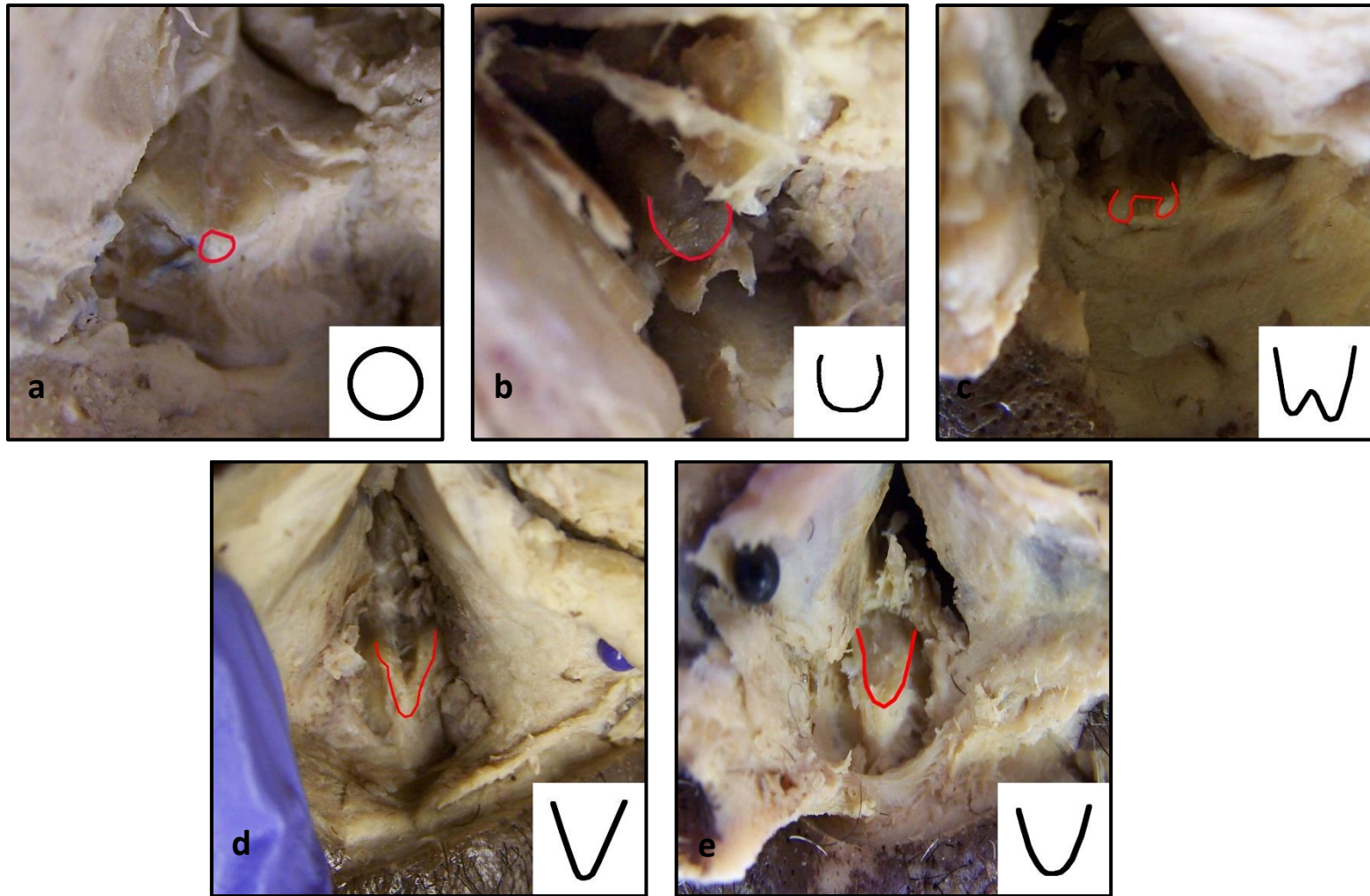


*Figure 3.14 Visualising the anterior nasals spine from antero-superiorly*

a) Round (full) ANS b) Round (half) ANS c) Bifid ANS d) Sharp ANS e) Spatulate ANS

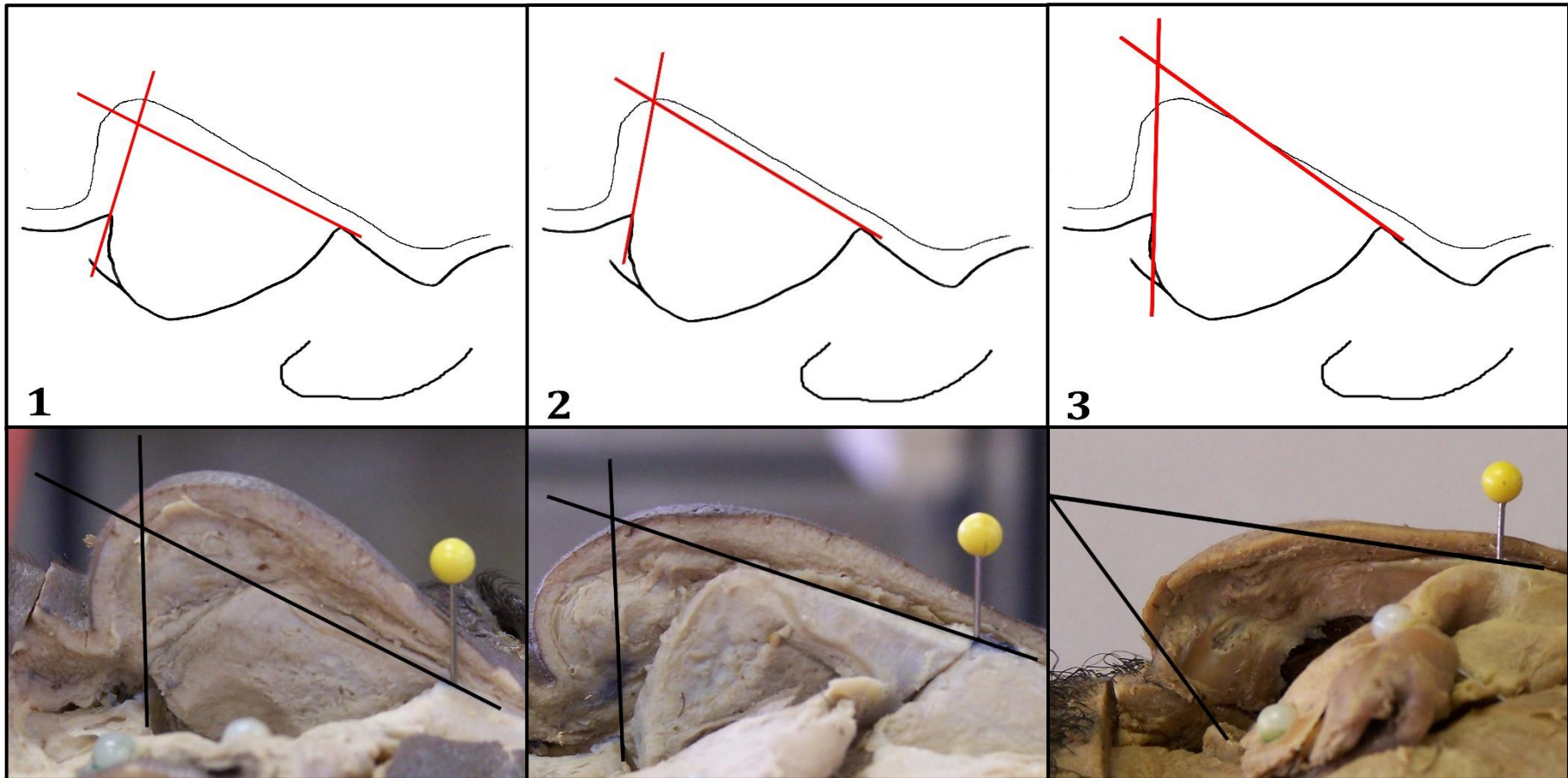


*Figure 3.15: Gerasimov's two tangent method*

A line tangent to the rhinion (yellow pin) was drawn, with second line following direction of the ANS.

1) Underestimation of the position of the nasal tip. 2) Correct estimation of the position of the nasal tip 3) Overestimation of the position of the nasal tip

### *(i) Statistical analysis of nasal measurements*

Qualitative data analysis was conducted by calculating the number of times each nasal tip shape and ANS shape was recorded. The probability of each nasal tip shape occurring for a given ANS shape was calculated by multinomial logistic regression. Since both variables are categorical, discriminant analysis could not be used. The number of times each nasal tip shape correlated to its corresponding ANS shape was also calculated. Lastly, Gerasimov's two-tangent method for determining the position of the nasal tip was calculated as the percentage of times the nasal tip was underestimated, correctly estimated or overestimated.

### **3.3.3. Oral measurements**

Oral measurements were taken only in relation to the maxillary teeth. Samples with missing teeth, specifically the upper central incisors or canines, were excluded from this part of the study, however samples with any missing mandibular teeth were still included in the measurements. All dimensions described here were taken with a digital sliding calliper.

Predictions regarding the width of the mouth as described by Angel <sup>55</sup> were tested by inserting a probe into the mouth at the cheilia and perpendicular to the teeth (Fig 3.16). The corresponding maxillary tooth/tooth-junction was noted as: C for canine; C/PM1 for canine – first premolar junction; PM1 for first premolar; PM1/PM2 for first premolar – second premolar junction; and PM2 for premolar 2. Stephan and Henneberg <sup>17</sup> found a correlation between the width of the mouth and the inter-canine width, as described by the 75% rule, where the inter-canine width was found to be three-quarters of the width of the mouth. The width of the mouth was measured from cheilion to cheilion and the inter-canine width was also measured between the most lateral edges of the maxillary canines to determine if a similar population-specific rule exists in this sample (Fig. 3.17).



*Figure 3.16: Correlating a specific tooth/tooth-junction to the cheilia*

A probe (red arrows) was inserted into the mouth perpendicular to the teeth at the corner of the mouth. The corresponding tooth/tooth-junction was recorded as C, C/PM1, PM1, PM1/PM2 or PM2.

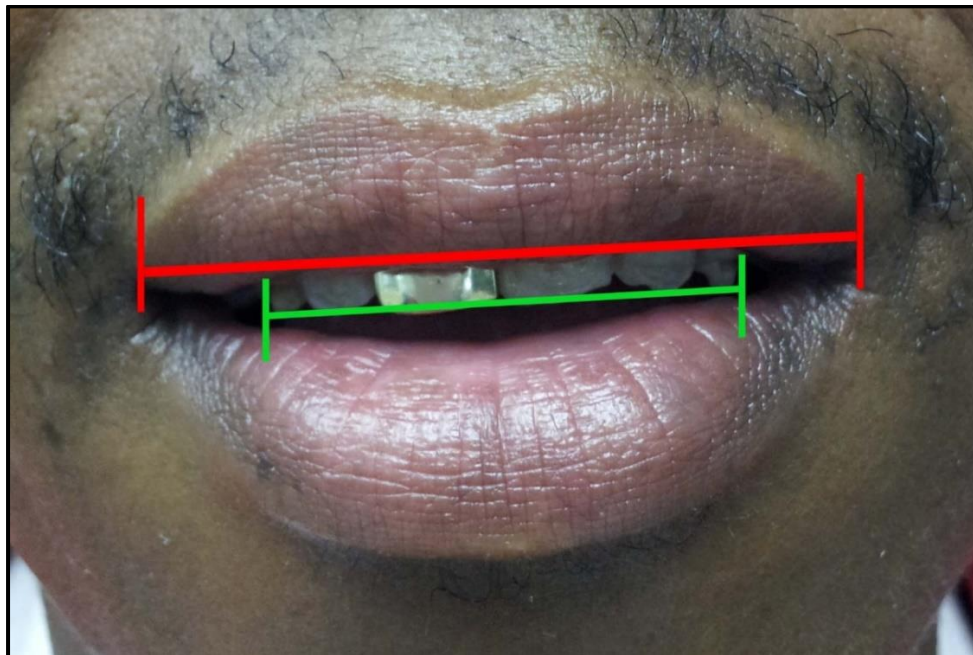


*Figure 3. 17: Width of the mouth and inter-canine width*

The red bracket visualises the width of the mouth as measured between the cheilia. The green bracket shows the inter-canine width as measured between the most lateral edges of the maxillary canines.

The reported correlation between the width of the philtrum and the width of the midpoints of the upper central incisors <sup>25,88</sup> was also investigated. The philtral columns were identified as originating from the highest points on the arch of the upper lip's vermilion and forming a slight thickening that extends to the columella of the nose. The philtral columns were pinned and the width of the philtrum measured between the pins placed on the border of the upper lip's vermilion (Fig. 3.18). The midpoint of each upper central incisor was identified by measuring the width of each tooth and dividing the distance by two. The width of the midpoints of the upper central incisors was then measured as the distance between these mid-points (Fig. 3.19).



*Figure 3.18 The philtrum width*

The philtral columns were identified and pinned (red pins) and the distance measured between the pins along the vermilion of the upper lip represents the philtrum width (red bracket).

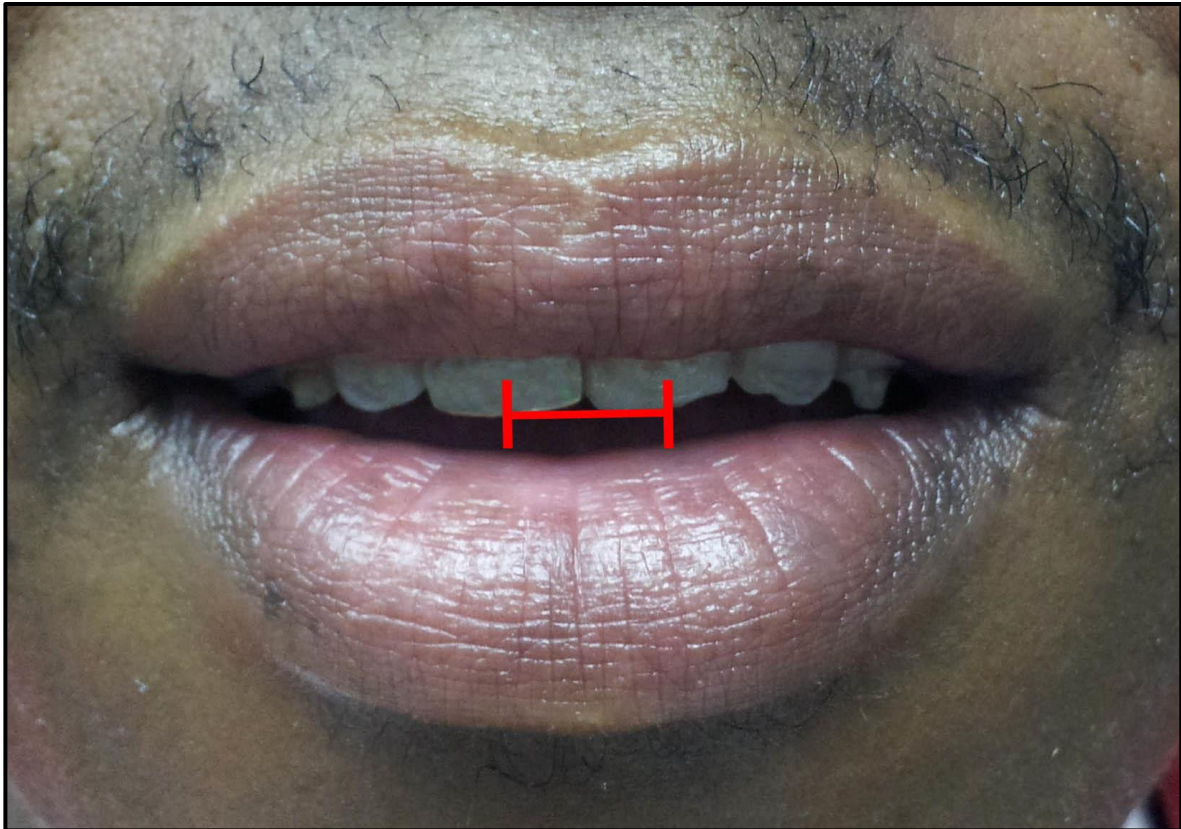


*Figure 3.19: The width of the upper central incisors*

The red bracket indicates the distance measured between the midpoints of the upper central incisors.

*(i) Statistical analysis of oral measurements*

Basic descriptive statistics were calculated on the average of the mouth width, inter-canine width, upper central incisor width and the philtrum width (minimum, maximum, mean, median, skewness, first and third quartiles, standard deviation as well as confidence intervals).

The percentage was calculated for each tooth/tooth-junction corresponding to the mouth corners, as well as whether the teeth corresponding to the mouth was symmetrical (i.e. the same tooth/tooth-junction occurring at the left and the right cheilia).

The correlation between the mouth width and the inter-canine width was determined by firstly calculating the average ratio of the two i.e. inter-canine width divided by mouth width. The average ratio was then used to predict the mouth width from the inter-canine width by dividing the inter-canine width with the average ratio.

The formulae used are:

$$\begin{aligned} \text{Average ratio (k)} &= \text{ICW}/\text{ch-ch} \\ \text{Predicted ch-ch} &= \text{ICW}/k \end{aligned}$$

Where k = average ratio; ICW = inter-canine width; ch-ch = mouth width (from cheilion to cheilion)

A comparison was made between the predicted widths and measured widths and tested with a Chi-squared test.

The descriptive statistics (minimum, maximum, mean, median, skewness, first and third quartiles, standard deviation as well as confidence intervals) for the philtrum width and upper central incisor width were calculated. The same process for determining the correlation between the mouth width and inter-canine width was followed to determine the correlation between the philtrum and upper central incisor widths. The formulae used are:

$$\begin{aligned} \text{Average ratio (k)} &= \text{UCInW}/\text{PhW} \\ \text{Predicted PhW} &= \text{UCInW}/k \end{aligned}$$

Where k = average ratio; UCInW = width between the midpoints of the upper central incisors; PhW = philtrum width

The average ratio was calculated as 0.96 by dividing the upper central incisor width by the philtrum width and comparisons were done by means of a Chi-squared test.

### 3.3.4. Auricular measurements

The length of the ear was measured between the supraurale and subaurale (Fig. 3.20). Supraurale and subaurale are defined as the highest and lowest points on the free margin of the auricle, respectively <sup>56</sup>.

Guyomarc'h and Stephan<sup>23</sup> formulated a range of regression formulae for the prediction of various auricular dimensions. A total of 18 formulae were presented of which 14 can be used to estimate the length of the ear. Seven of these formulae were used to predict the length of the ear given the age and sex of cadaver samples in this study. Results were then compared to measurements obtained from these samples.

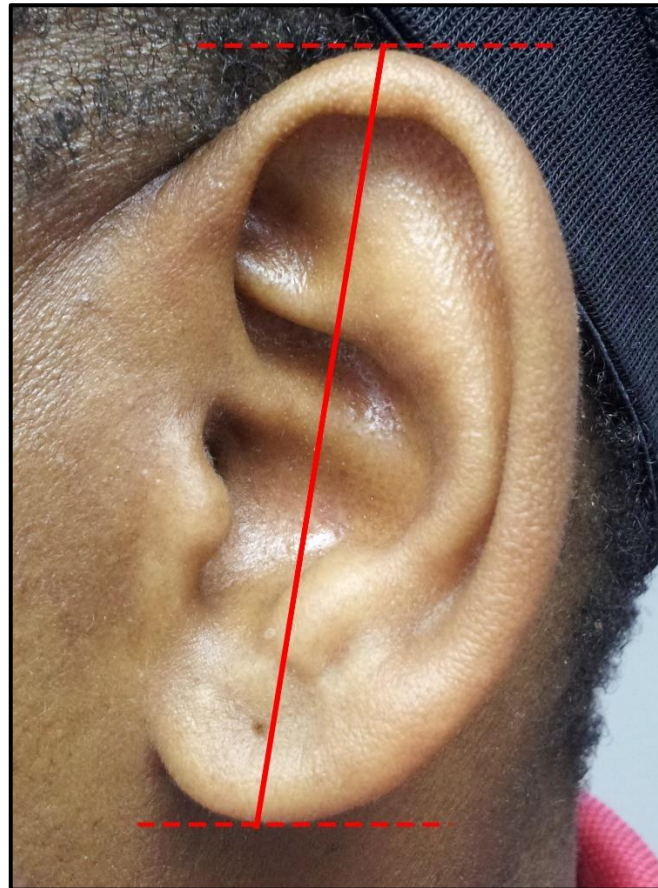


*Figure 3.20: The length of the ear*

The length of the ear was measured as the distance between subaurale and supraurale.

*(i) Statistical analysis on auricular measurements*

Descriptive statistics were calculated for the auricular measurements (minimum, maximum, mean, median, skewness, first and third quartiles, standard deviation as well as confidence intervals). The regression formulae provided by Guyomarc'h and Stephan<sup>23</sup> were used to predict ear lengths of the cadaver sample. Predicted lengths were then compared to actual lengths by utilizing a Chi-squared test.

### 3.4. Statistical analyses: Intra - and inter-observer repeatability testing

As mentioned previously, intra-observer repeatability was tested for all quantitative parameters by obtaining three measurements and calculating the standard deviations. Qualitative parameters were only recorded once. The data was cleaned of outliers (if any) before descriptive statistics were calculated on the averages of all measurements. The non-parametric Wilcoxon Rank Sum tests (2-sided) were used to assess differences between sexes for the different parameters.

Inter-observer repeatability testing was conducted by comparing measurements to one other observer. Basic training on the use of a sliding digital calliper was given as well as descriptions of each measurement to be taken. A total of 38 cadaver samples were re-measured for all parameters, excluding Gerasimov's two tangent method, where evaluation was not dependant on measurement. A total of 28 CBCT scans and 30 CT scans were re-measured for all parameters. The intra-class correlation coefficient (ICC) was calculated for each quantitative parameter to compare measurements obtained by different observers, and is expressed as a kappa value. The variation of the ICC used assumed a 2-way mixed effects model with the mean of  $k$  raters who are in absolute agreement <sup>89</sup>. This measures the agreement between observers showing if correlation exists. For the ICC, the following scale (Table 3.1) can be used as a general guideline:

Table 3.1 Interpretation of the ICC test <sup>89</sup>

<i>Value of ICC</i>	<b><i>Interpretation</i></b>
<i>Less than 0.5</i>	Poor reliability
<i>Between 0.5 and 0.75</i>	Moderate reliability
<i>Between 0.75 and 0.9</i>	Good reliability
<i>Greater than 0.9</i>	Excellent reliability

Also note that because the ICC calculated is an expected value of the actual underlying ICC, it is better practice to use the 95% confidence interval of the estimated ICC to interpret the reliability <sup>89</sup>.

Fleiss' kappa was calculated for qualitative data (nasal parameters and tooth position at the mouth corners) to determine the extent to which the observed amount of agreement among observers exceeds what would be expected if all observers made their ratings completely randomly<sup>90</sup>. Agreement can be thought of as follows: if a fixed number of people assign numerical ratings to a number of items then the kappa rating will give a measure for how consistent the ratings are. The scoring range is between 0 and 1. The closer to 1, the higher the level of agreement. Agreement should however not be due to chance. The statistical significance (p-values) of Fleiss' kappa determines whether the estimated value of kappa is due to chance or not.

## 4. RESULTS

Dimensions obtained on certain aspects of facial features in a South African sample are reported in this section. The following features are considered under subheadings: orbital and ocular measurements, nasal measurements, oral measurements and auricular measurements. The initial step in the statistical analysis comprised an evaluation of the intra-observer repeatability involving the determination of the standard deviation on individual measurements. Following on this, the extent of variation between sexes was determined in order to consider the possibility of pooling the samples. Lastly, inter-observer repeatability testing was conducted to test the level of agreement between observers.

### 4.1. Intra-observer repeatability testing and standard deviations on individual measurements

As stated in the Materials and Methods section 3.4, three separate measurements were obtained for all linear (quantitative) parameters. Standard deviations were calculated for the three individual measurements performed by the investigator on each of the following parameters to test for intra-observer repeatability: (1) the position of the canthi; (2) the position of the eyeball; (3) the size of the eyeball (on cadaver dissections, CT and CBCT scans); (4) the width of the philtrum; (5) the width of the upper central incisors; (6) the inter-canine width; (7) the mouth width and (8) the length of the ears.

The results for all standard deviations calculated are summarized in Tables 4.1 and 4.2. All average standard deviations were below 0.30, with some as low as 0.01. The accuracy of the measurements, when repeated by the same researcher, was considered higher the closer the standard deviation average was to zero. Therefore, due to such small standard deviations, the average measurement for each parameter was used for all further statistical analyses.

## 4.2. Inter-observer repeatability testing

The intra-class correlation coefficient (ICC) was calculated for each quantitative parameter to compare measurements obtained by different observers. Qualitative parameters were tested by means of Fleiss' Kappa. Table 4.3 reports the results for inter-observer reliability on both qualitative and quantitative parameters. Qualitative parameters all showed low levels of agreement between observers. The quantitative parameters on cadaver measurements performed much more consistently, with excellent agreement (above 0.90; not considered due to chance) between observers for ex-SOM, Meq-MOM, Leq-LOM, leq-IOM, Leq-Meq and Saur-laur. Good agreement that was not considered due to chance was found between observers for en-SOM, Seq-SOM, Seq-leq and ICW. However, at a 10% level of significance, good agreement between observers was considered due to chance for UCInW and ch-ch. The ex-LOM showed moderate agreement due to chance while the en-MOM and PhW performed poorly, with any agreement between observers occurring accidentally. The quantitative parameters on scan measurements performed poorly, with all measurements scoring kappa values less than 0.25. The average differences though, were mostly less than 2 mm, apart from the orbital depth exhibiting a greater difference. A comparison of absolute values on CBCT measurements showed that the average difference between observers for the medio-lateral, supero-inferior, antero-posterior and orbital depth parameters were 0.88 mm, 1.14 mm, 2.29 mm and 4.60 mm respectively. For measurements on CT scans, the average difference between observers for the same parameters were 0.81 mm, 1.21 mm, 1.06 mm and 4.14 mm respectively.

Table 4.1 Standard deviations calculated for all orbital and ocular measurements.

SD	Position of the Canthi (Cadavers)				Position of the Eyeball diameters (Cadavers)				Eyeball and orbit diameters (CBCT)				Eyeball and orbit diameters (CT)					
	<i>en-MOM</i>	<i>en-SOM</i>	<i>ex-LOM</i>	<i>ex-SOM</i>	<i>Meq-MOM</i>	<i>Leq-LOM</i>	<i>Seq-SOM</i>	<i>Ieq-IOM</i>	<i>Meq-Leq</i>	<i>Seq-leq</i>	<i>Meq-Leq</i>	<i>Seq-leq</i>	<i>Aeq-Peq</i>	<i>Cornea - Optic canal</i>	<i>Meq-Leq</i>	<i>Seq-leq</i>	<i>Aeq-Peq</i>	<i>Cornea - Optic canal</i>
<b>MAX</b>	0.58	0.06	0.05	0.09	0.05	0.05	0.06	0.05	0.05	0.06	0.36	0.33	0.44	0.46	0.46	0.39	0.34	1.26
<b>MIN</b>	0.00	0.00	0.01	0.01	0.00	0.00	0.01	0.00	0.00	0.00	0.03	0.00	0.01	0.05	0.00	0.00	0.00	0.02
<b>AVE</b>	0.03	0.02	0.02	0.02	0.01	0.01	0.01	0.01	0.02	0.02	0.17	0.15	0.15	0.22	0.14	0.11	0.13	0.18

*en-MOM* = endocanthion to medial orbital margin

*en-SOM* = endocanthion to superior orbital margin reference plane

*ex-LOM* = exocanthion to lateral orbital margin

*ex-SOM* = exocanthion to superior orbital margin reference plane

*Meq-MOM* = medial equator of the eyeball to the medial orbital margin

*Leq-LOM* = lateral equator of the eyeball to the lateral orbital margin

*Seq-SOM* = superior equator of the eyeball to the superior orbital margin

*Ieq-IOM* = inferior equator of the eyeball to the inferior orbital margin

*Meq-Leq* = medial equator to the lateral equator of the eyeball (medio-lateral diameter)

*Seq-leq* = superior equator to the inferior equator of the eyeball (supero-inferior diameter)

*Aeq-Peq* = anterior equator to the posterior equator of the eyeball (antero-posterior diameter)

Table 4.2 Standard deviations calculated for all oral and auricular measurements on cadaver samples.

SD	Oral measurements				Auricular measurement
	<i>PhW</i>	<i>UCInW</i>	<i>ICW</i>	<i>Ch-Ch</i>	<i>Saur-laur</i>
<b>MIN</b>	0.23	0.30	0.07	0.14	0.36
<b>MAX</b>	0.01	0.02	0.00	0.00	0.01
<b>AVE</b>	0.06	0.10	0.01	0.03	0.10

*PhW* = philtrum width, measured between philtral columns at vermilion border

*UCInW* = width measured between the midpoints of the upper central incisors

*ICW* = inter-canine width, measured between most lateral points of upper canines

*Ch-Ch* = mouth width, measured from cheilion to cheilion

*Saur-laur* = Ear length, measured from supraaurale to subaurale

Table 4.3 Inter-observer repeatability testing by means of ICC or Fleiss's Kappa (level of agreement between observers).

	Parameter	Test	ICC or Kappa	p-value	Interpretation - 5% level of significance unless otherwise stated
<b>Position of Canthi</b>	en-MOM	ICC Case A-k	0.0429*	0.1217	Poor reliability – any agreement is accidental
	en-SOM	ICC Case A-k	0.8745	0.0030	Good reliability – agreement is not accidental
	ex-LOM	ICC Case A-k	0.6875	0.1133	Moderate reliability – any agreement due to chance
	ex-SOM	ICC Case A-k	0.9339	0.0078	Excellent reliability – agreement is not accidental
<b>Position of Eyeball</b>	Meq-MOM	ICC Case A-k	0.9482	0.0143	Excellent reliability – agreement is not accidental
	Leq-LOM	ICC Case A-k	0.9339	0.0005	Excellent reliability – agreement is not accidental
	Seq-SOM	ICC Case A-k	0.8734	0.0473	Good reliability – agreement is not accidental
<b>Diameters of Eyeball</b>	leq-IOM	ICC Case A-k	0.9602	0.0036	Excellent reliability – agreement is not accidental
	Leq-Meq	ICC Case A-k	0.9094	0.0263	Excellent reliability – agreement is not accidental
	Seq-leq	ICC Case A-k	0.8825	0.0056	Good reliability – agreement is not accidental
<b>Oral measurements</b>	L Tch	Fleiss's kappa	0.0024*	0.8528	Low level of agreement - agreement is accidental
	R Tch	Fleiss's kappa	0.0303*	0.0202	Low level of agreement - agreement is not accidental
	PhW	ICC Case A-k	0.2294*	0.2031	Poor reliability – any agreement is accidental
	UClnW	ICC Case A-k	0.7807	0.0869	Good reliability – 10% level of significance: agreement is accidental
	ICW	ICC Case A-k	0.8646	0.0000	Good reliability – agreement is not accidental
<b>Size of Ears</b>	Ch-Ch	ICC Case A-k	0.8993	0.0503	Good reliability – 10% level of significance: agreement is accidental
	Saur-laur	ICC Case A-k	0.9551	0.0033	Excellent reliability – agreement is not accidental
<b>Nasal tip shape</b>	Round/bulbous/bifid/sharp	Fleiss's kappa	0.1066*	0.0000	Low level of agreement - agreement is not accidental
<b>ANS shape</b>	Round/spatulate/bifid/sharp	Fleiss's kappa	0.0311*	0.0241	Low level of agreement - agreement is not accidental
	Meq-Leq	ICC Case A-k	0.2176	0.1179	Poor reliability – any agreement is accidental
<b>CBCT measurements</b>	Scan Seq-leq	ICC Case A-k	-0.1603	0.7871	Poor reliability – any agreement is accidental
	Aeq-Peq	ICC Case A-k	0.0179	0.3782	Poor reliability – any agreement is accidental
	Orbital depth	ICC Case A-k	-0.2031	0.8571	Poor reliability – any agreement is accidental
<b>CT Scan measurements</b>	Meq-Leq	ICC Case A-k	0.1952	0.1486	Poor reliability – any agreement is accidental
	Seq-leq	ICC Case A-k	0.0023	0.4934	Poor reliability – any agreement is accidental
	Aeq-Peq	ICC Case A-k	-0.0980	0.7308	Poor reliability – any agreement is accidental
	Orbital depth	ICC Case A-k	0.0847	0.3164	Poor reliability – any agreement is accidental

\* Red: Poor reliability/low level of agreement

### 4.3. Variation between the sexes

Non-parametric Wilcoxon Rank Sum tests (Tables 4.4 and 4.5), were performed to determine the variance between sexes so as to decide whether the data may be pooled. No statistically significant variations were found between sexes on cadaver measurements. All measurements had p-values much greater than 0.05, except Saur-laur which had a p-value of 0.0845.

Variation between the sexes on CT and CBCT scans were also evaluated by means of non-parametric Wilcoxon Rank Sum tests. No statistically significant variations were reported on CT scans, apart from the dimensions: Meq-Leq and the depth of the optic canal where the variation between sexes were statistically significant with p-values of 0.0466 and 0.0107 respectively. Due to the predominantly non-significant variation between sexes, the samples were pooled for further statistical analyses.

### 4.4. Dimensions obtained on facial features

#### 4.4.1. Orbital and ocular measurements

Description statistics for the orbital and ocular measurements are depicted in Figure 4.1. The data show that distances between ex-SOM were greater than the en-SOM, indicating a lower position of the exocanthion relative to the endocanthion when using the SOM reference plane. The mean distance between ex-LOM was also greater than the mean distance from en-MOM, showing that the endocanthion is located closer to the orbital margin than the exocanthion.

Table 4.4 Variation between male and female parameters Investigated by means of non-parametric Wilcoxon Rank Sum Test (2-sided)  
(p-values where <0.05 indicates significance)

	Body dissections	CT scans	CBCT scans
en-MOM	0.5734	-	-
en-SOM	0.6926	-	-
ex-LOM	0.8762	-	-
ex-SOM	0.2601	-	-
Meq-MOM	0.2898	-	-
Leq-LOM	0.5480	-	-
Seq-SOM	0.1980	-	-
leq-IOM	0.3752	-	-
Meq-Leq	0.1653	0.0606	0.0466
Seq-leq	0.4834	0.2077	0.0567
Aeq-Peq	-	0.8446	0.1604
Orbital depth	-	0.8887	0.0107
Orbit width	0.9202	-	-
Orbit height	0.1881	-	-
PhW	0.9129	-	-
UCInW	0.5398	-	-
ICW	0.2750	-	-
Ch-ch	0.5495	-	-
Saur-laur	0.0845	-	-

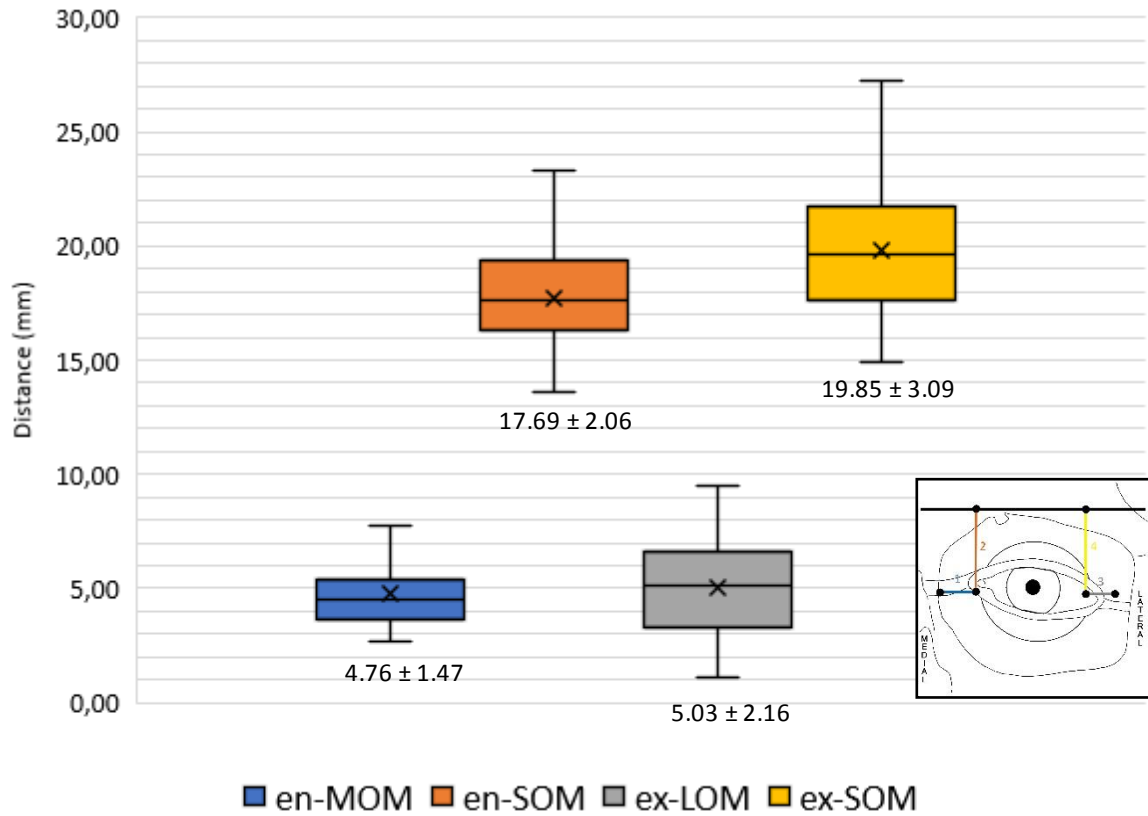


Figure 4.1 Basic descriptive statistics for the measurements pertaining to the position of the canthi

Measurements to determine the position of the eyeball in the orbit were performed on 42 dissected cadavers. The distances measured were between the (1) inferior equator and IOM, (2) superior equator and SOM, (3) lateral equator and LOM and (4) medial equator to MOM and are depicted in Figure 4.2. The data show that average distances between Seq-SOM and Leq-LOM were smaller than the distances between leq-IOM and Meq-MOM, indicating a supero-lateral position of the eyeball within the orbit.

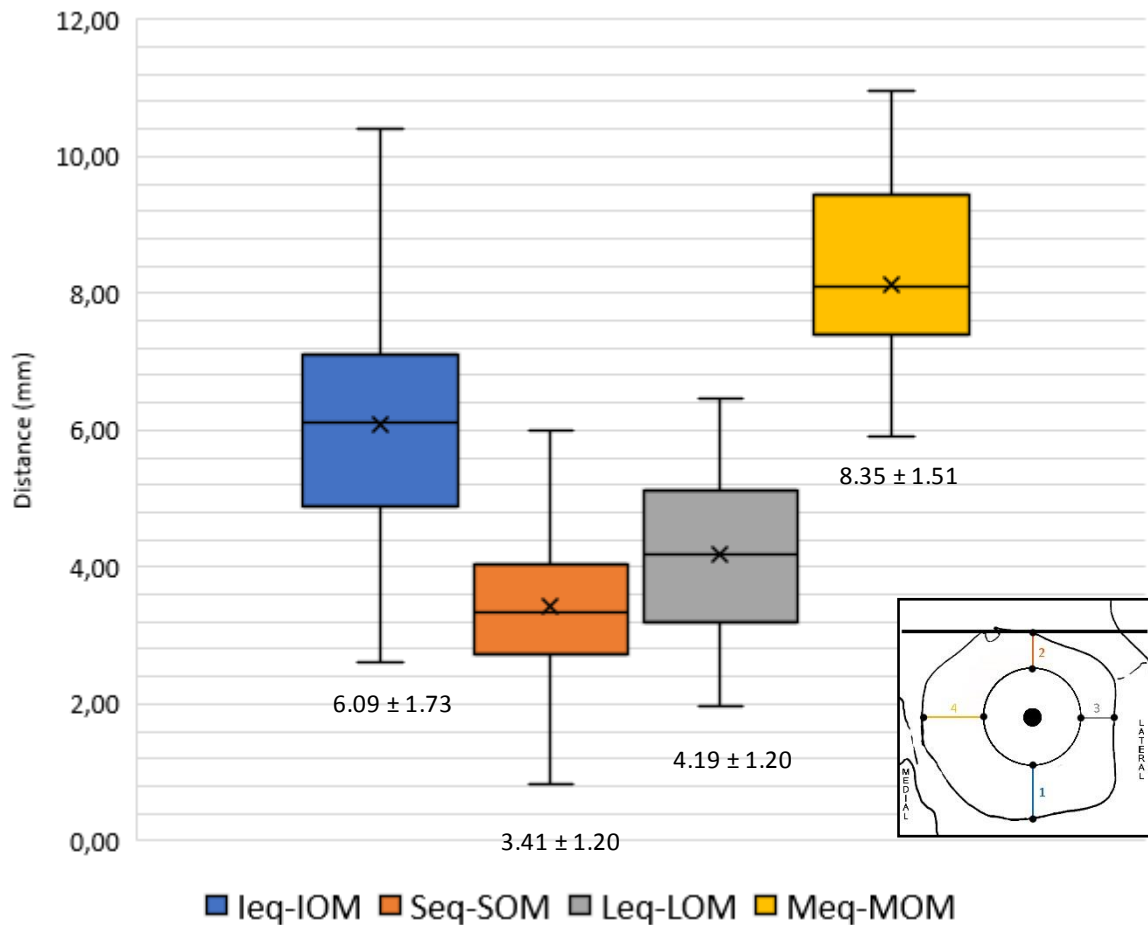


Figure 4.2 Basic descriptive statistics for measurements pertaining to the position of the eyeball in the orbit in dissections

The size of the eyeball was determined by measuring the medio-lateral and supero-inferior diameters on all three modalities (Figs. 3.4c, 3.7 and 3.8) while the antero-posterior diameter was only possible on CBCT and CT scans (Fig. 3.6). Figure 4.3 summarises results obtained on the diameters of the eyeball. Results from dissections indicated that the mean medio-lateral diameter (purple) was greater than the supero-inferior diameter (light blue). Similar results are portrayed by CT (orange and red, respectively) and CBCT scans (yellow and dark blue, respectively). These findings indicate that the eyeball is transversely elongated.

The width and height of the orbits were derived from individual measurements. The width of the orbit was consistently greater than the height of the orbit, indicating a more rectangular shaped orbit (Fig 4.4).

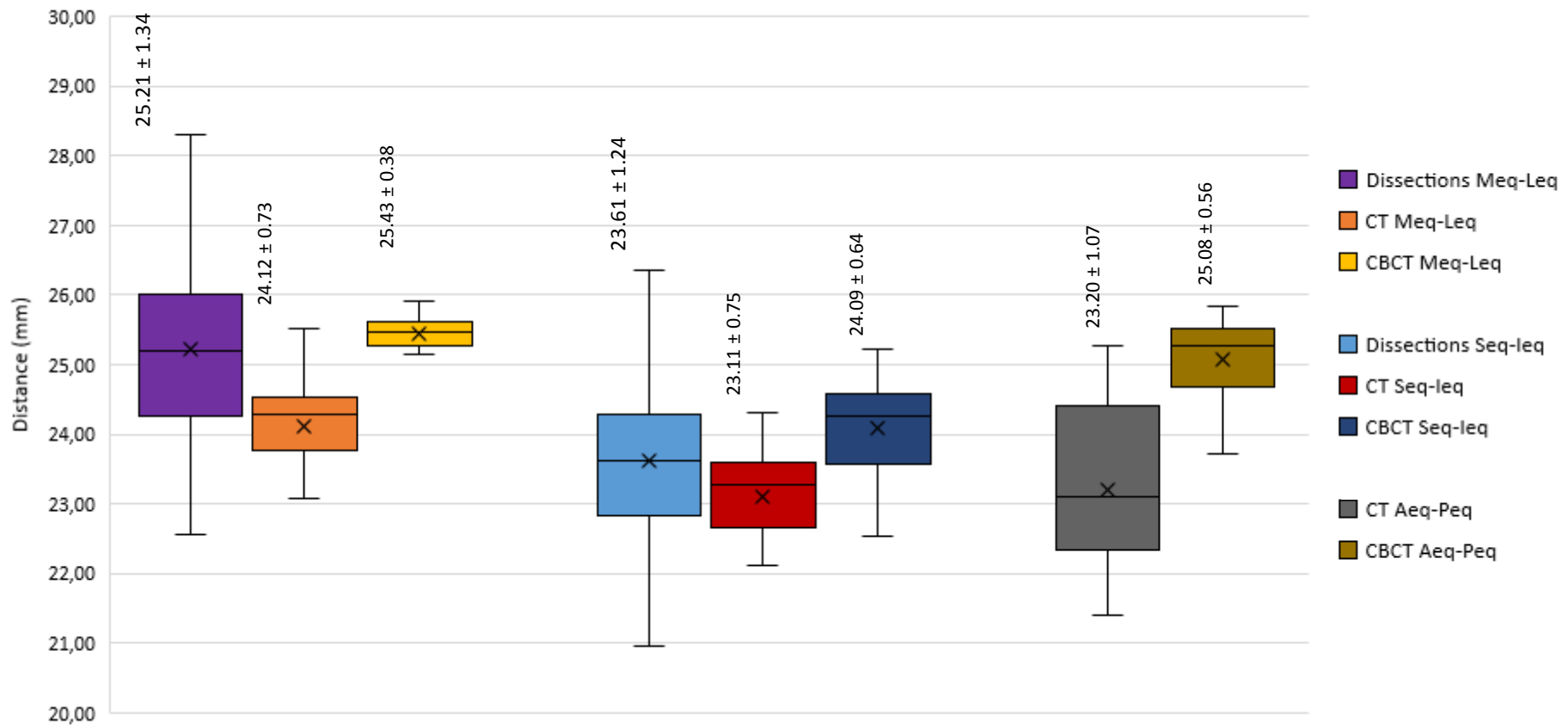
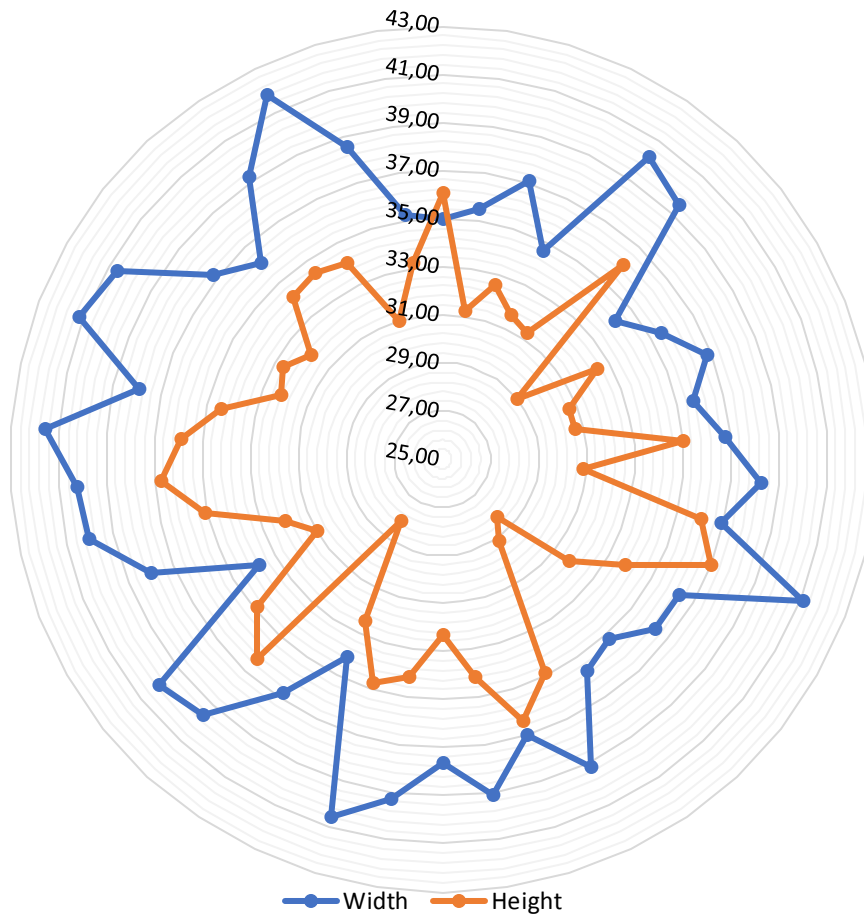


Figure 4.3 Basic descriptive statistics for measurements pertaining to the size of the eyeball in all three modalities

Medio-lateral diameter for dissections vs CT vs CBCT (Kruskal-Wallis test p-value < 0.0000)

Supero-inferior diameter for dissections vs CT vs CBCT (Kruskal-Wallis test p-value < 0.0000)

Antero-posterior diameter for CT vs CBCT (Wilcoxon Rank Sum test p-value p < 0.0001)



*Figure 4.4 Radar plot of the orbital width and height*

The width of the orbit (blue line) is consistently greater than the height of the orbit (orange line) indicating a more rectangular shaped orbit.

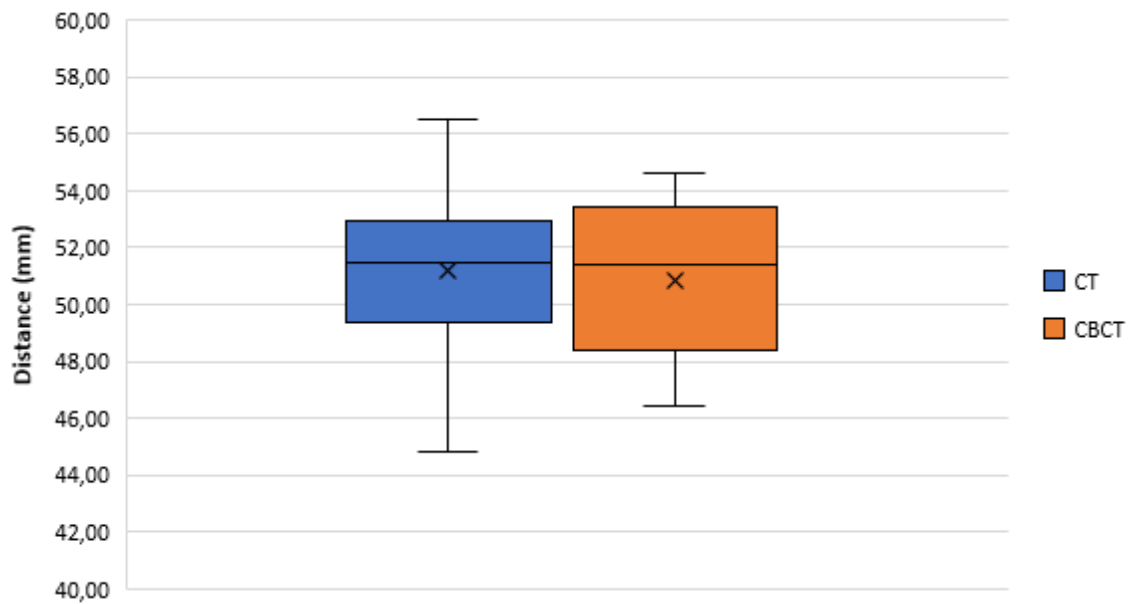


Figure 4.5 Orbital depth as measured from the cornea to the optic canal on CT and CBCT scans

*(i) Statistical analyses between different modalities for eyeball measurements*

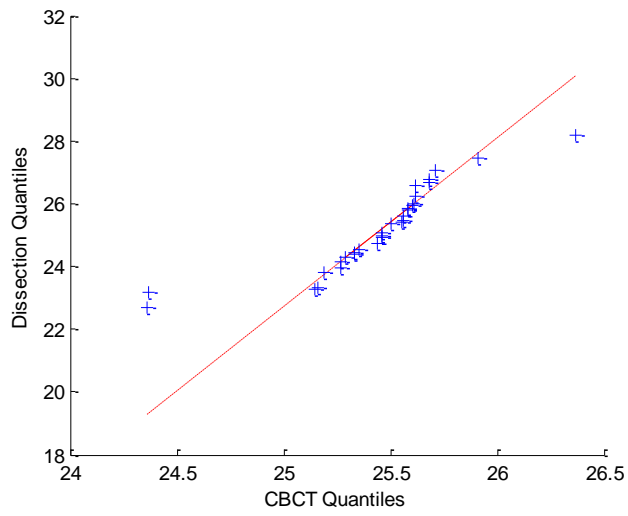
The Kruskal-Wallis Test for simultaneous comparison between all three modalities (cadaver dissections, CT and CBCT scans) on the medio-lateral diameter and supero-inferior diameter indicated statistically significant differences ( $p < 0.0001$  for both diameters).

Further comparisons on the three diameters (medio-lateral, supero-inferior and antero-posterior) were done between two modalities at a time by utilising the Wilcoxon Rank Sum test. Box-and-whisker plots (Fig. 4.3) were employed to illustrate the variations in measurements obtained by using the various modalities.

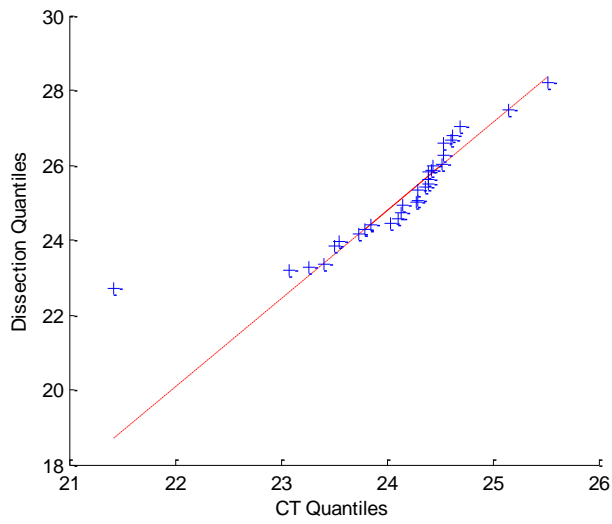
When comparing variations between modalities on the medio-lateral diameter, cadaver measurements had the greatest range, followed by the CT data and lastly the CBCT. The variation between CBCT vs CT measurements concerning the medio-lateral diameter was statistically significant ( $p < 0.0001$ ) as was CT vs dissection ( $p = 0.0003$ ), while no statistical significant differences could be demonstrated in the CBCT vs dissection derived means ( $p = 0.3916$ ) (Fig. 4.6).

Similarly, when comparing the variation between modalities on the supero-inferior diameter, cadaver measurements had the greatest range, followed by CT data and lastly CBCT. However, when considering the mean values, CBCT data had the highest mean, followed by dissection data and then CT data. A statistically significant difference existed in the supero-inferior diameter (Fig. 4.7) when comparing CBCT and CT ( $p < 0.0001$ ), and to a lesser extent when comparing CBCT to cadaveric measurements ( $p = 0.0192$ ). The variation in the supero-inferior diameters when comparing CT to cadaveric measurements was not statistically significant ( $p = 0.0522$ ).

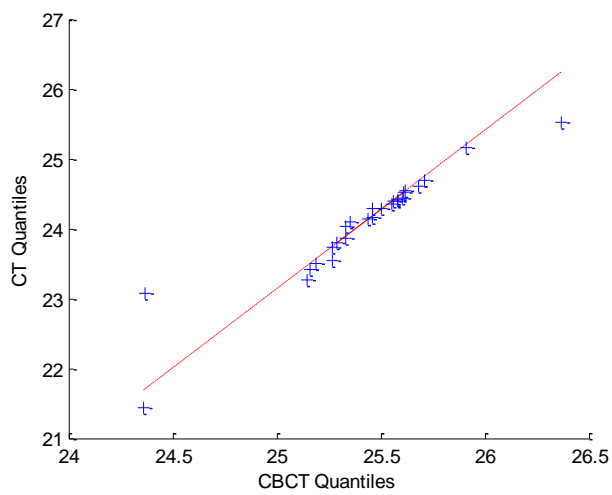
When comparing CBCT to CT measurements for the antero-posterior diameter, a statistically significant difference was observed ( $p < 0.0001$ ).



$p = 0.3916$

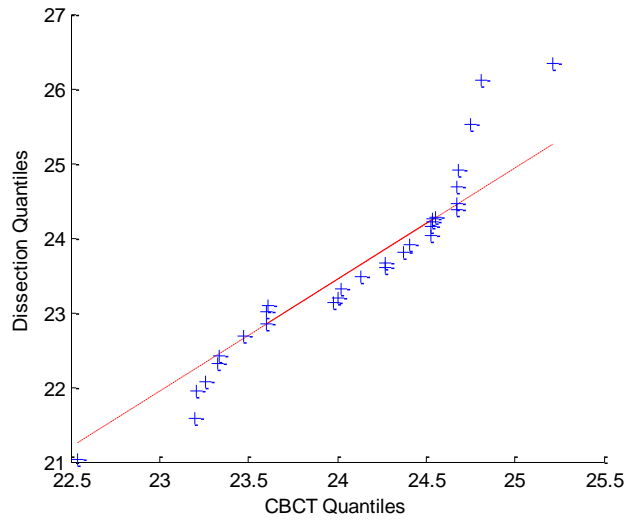


$p = 0.0003$

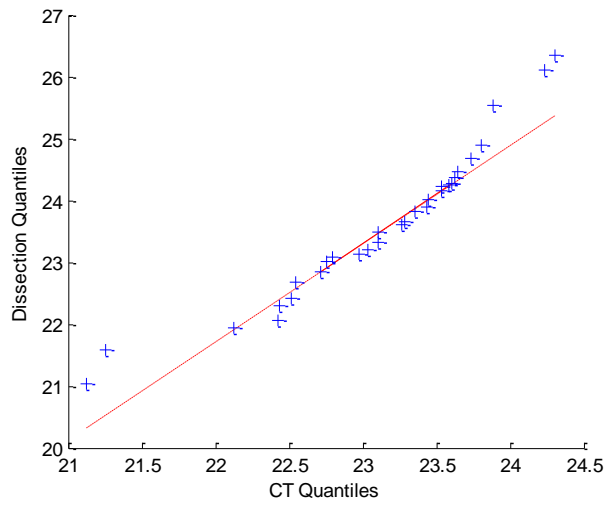


$p < 0.0001$

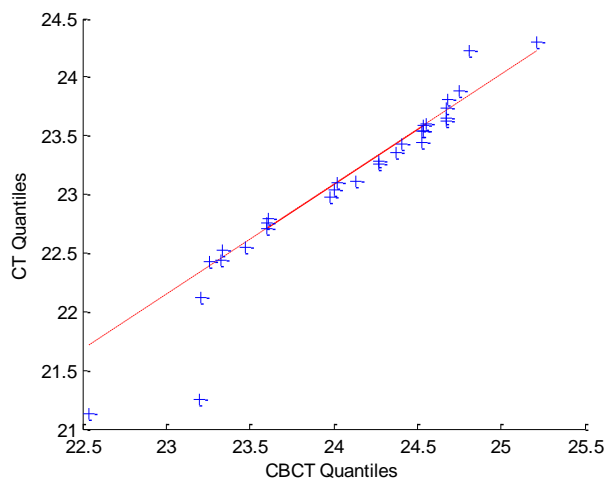
Figure 4.6 Comparisons on the medio-lateral diameter of the eyeball between modalities by means of the Wilcoxon Rank Sum test (2-sided)



$p = 0.0192$



$p = 0.0522$



$p < 0.0001$

Figure 4.7 Comparisons on the supero-inferior diameter of the eyeball between modalities by means of the Wilcoxon Rank Sum test (2-sided)

#### 4.4.2. Nasal Measurements

The relationship between the shape of the ANS and the shape of the nasal tip was determined by recording the shapes of both these features, and correlating its occurrence. The ANS was classified according to predetermined reference shapes, adapted from Angel<sup>55</sup>, and assigned numbers 1 (round), 2 (spatulate), 3 (bifid) and 4 (sharp). The nasal tip shape was also recorded and assigned numbers 1 (round), 2 (bulbous), 3 (bifid) and 4 (sharp).

The most prevalent shapes were the spatulate shaped ANS (17 out of 34) and the bulbous nasal tip shape (26 out of 34), followed by the round shaped ANS (10 out of 34) and round shaped nasal tip (7 out of 34) (Table 4.5).

Table 4.5 Occurrence of ANS shapes.

ANS shape		Number of ANS classified as specific shape
1. Round		10
2. Spatulate		17
3. Bifid		3
4. Sharp		4
<b>Total</b>		<b>34</b>

Table 4.6 Occurrence of nasal tip shapes.

Nasal tip shape	Number of nasal tips classified as specific shape
1. Round	7
2. Bulbous	26
3. Bifid	1
4. Sharp	0
<b>Total</b>	<b>34</b>

Table 4.7 summarises the probability of each ANS shape corresponding to its associated nasal tip shape. Probability was derived using multinomial logistic regression as both variables are categorical. The probability that the nasal tip would be bulbous, given any ANS shape was greater than 70%. Table 4.6 illustrates that although each ANS shape has a corresponding nasal tip shape, it is not exclusively related to each other. The spatulate shaped ANS is the most common and it yields the highest probability for corresponding to any tip shape. Irrespective of the ANS shape, no sharp nasal tips were observed in the sample.

Table 4.7 Probability of nasal tip shape predicted by ANS shape.

ANS	Tip			
	1. Round	2. Bulbous	3. Bifid	4. Sharp
1. Round	21%	78%	1%	0%
2. Spatulate	21%	77%	2%	0%
3. Bifid	20%	75%	5%	0%
4. Sharp	19%	70%	11%	0%

Overall, the ANS predicted the nasal tip shape correctly 21 out of 34 times (62%). The number of correct and incorrect predictions for each individual shape is visualised in Figure 4.8.

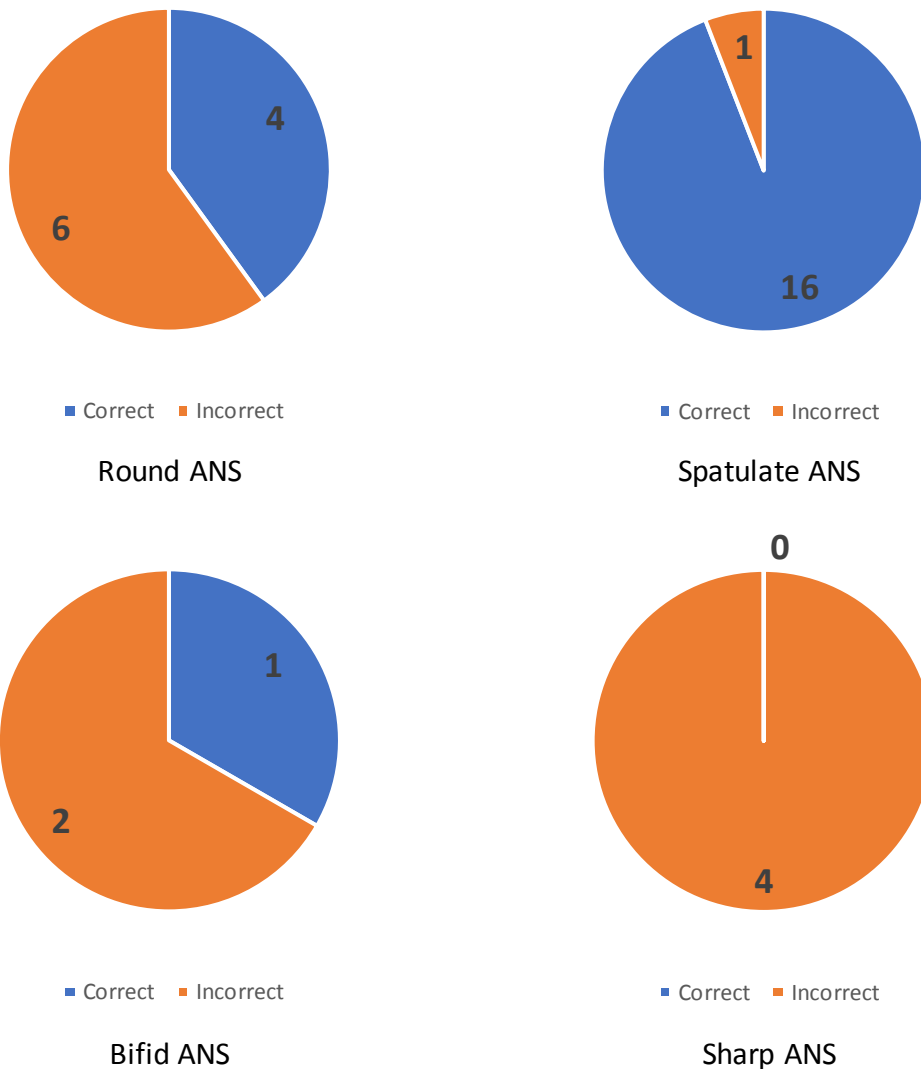


Figure 4.8 Correctly or incorrectly predicted nasal tip from ANS shape

The efficacy of Gerasimov’s two-tangent method to predict the position of the nasal tip was tested by calculating the percentage of times the position of the nasal tip was 1) underestimated, 2) correctly estimated or 3) overestimated. The results show that the position of the nasal tip was less likely to be underestimated (12%) than correctly estimated (44%) or overestimated (44%).

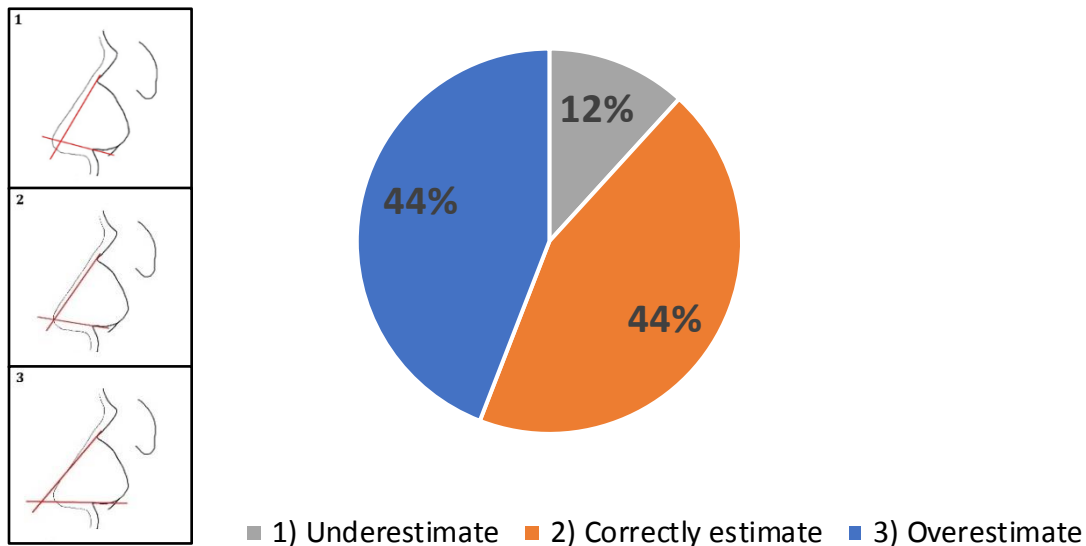


Figure 4.9 Gerasimov’s two-tangent method predictions

The position of the nasal tip shape was underestimated 12 out of 34 times, and correctly estimated or overestimated 15 out of 30 times.

#### 4.4.3. Oral measurements

Descriptive statistics for oral measurements are summarized in Figure 4.10. The occurrence of the observed tooth/tooth-junction corresponding to each mouth corner (cheilion) was calculated as a percentage. The cheilia occurred the most often at the canine/first-premolar junction (58% left, 56% right), followed by the middle of the first premolar (21% left, 28% right), the middle of the canine (16% left, 12% right) and lastly the first-premolar/second-premolar junction and the second premolar (2% each left and right) (Fig. 4.11 and Fig. 4.12 respectively). The percentage of times that the mouth corners were placed symmetrical to a tooth/tooth-junction, i.e. the same tooth/tooth-junction occurring at left and right cheilia, was 63%.

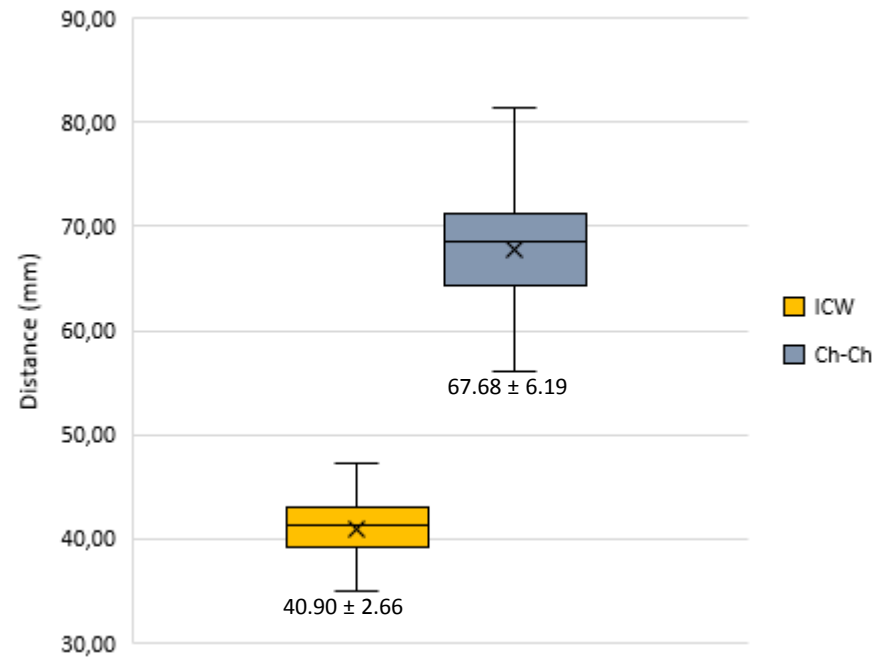
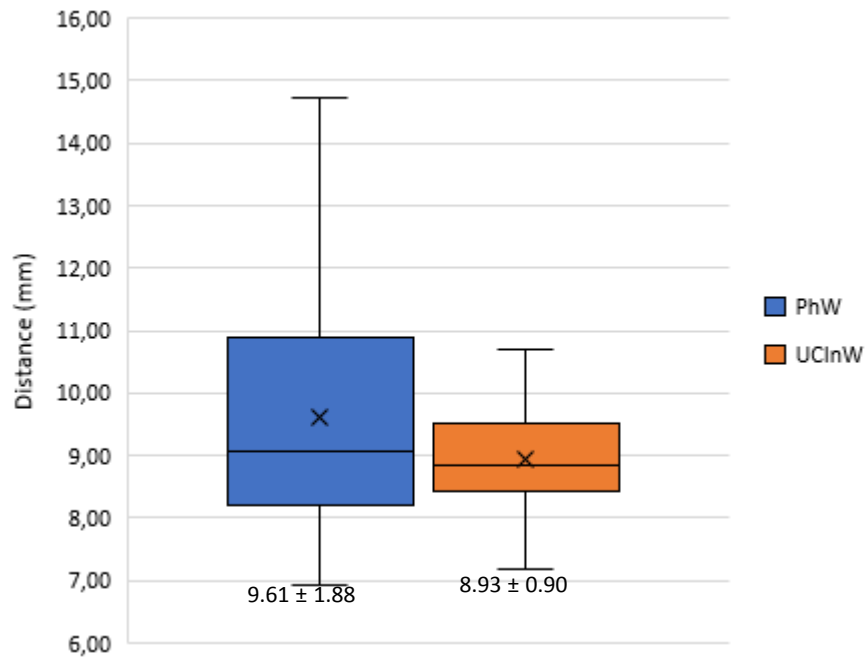
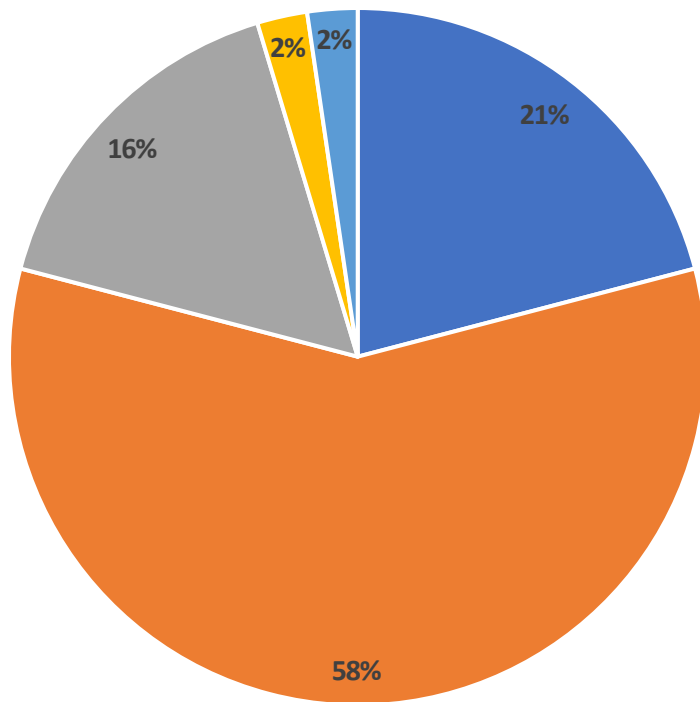


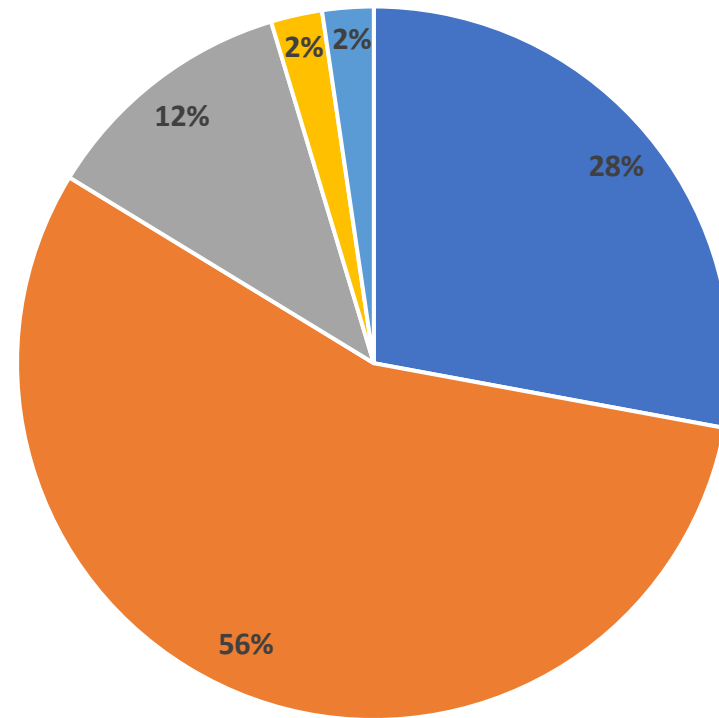
Figure 4.10 Basic descriptive statistics for measurements pertaining to the mouth



■ PM1 ■ C/PM1 ■ C ■ PM1/PM2 ■ PM2

*Figure 4.11 Tooth position at left cheilio.*

The left cheilion occurs most often at the canine/first premolar tooth junction (orange) and the least often at the first premolar/second premolar tooth junction (yellow) and the second premolar tooth (light blue).



■ PM1 ■ C/PM1 ■ C ■ PM1/PM2 ■ PM2

*Figure 4.12 Tooth position at right cheilion*

The right cheilion occurs most often at the canine/first premolar tooth junction (orange) and the least often at the first premolar/second premolar tooth junction (yellow) and the second premolar tooth (light blue).

Correlation between the mouth width and the inter-canine width was determined by calculating the average ratio of the two i.e. inter-canine width divided by mouth width. The average ratio was 0.61. The inter-canine width was then divided by 0.61 to estimate the mouth width. The residual was calculated between the actual and estimated mouth widths (estimated width minus actual width). A comparison was made between the estimated widths and measured widths and yielded a p-value of 0.711 for a two-tailed paired t-test, indicating that there was no statistically significant difference between the actual and predicted widths. Further analysis by means of Chi-squared test showed that a mild to moderate correlation existed that was statistically significant. The correlation coefficient ( $R^2$ ) was calculated as 0.13 with a p-value of 0.0249. Table 4.8 summarises the results and the correlation between actual and predicted mouth widths is visualised in Figure 4.13.

The graph comparing the residuals versus actual widths (Fig. 4.14) shows that the residuals are not random and fairly widely distributed around zero. These results indicate that although the inter-canine width and mouth width do show a mild to moderate correlation, it is not adequate in predicting an accurate mouth width.

Table 4.8 Correlation between mouth width and inter-canine width.

n	Mean ICW	Mean ch-ch	Average ratio	Average residual	SD for residual	Mean predicted ch-ch	$R^2$	p-value for correlation
36	40.90	67.29	0.61	-0.37	5.88	66.92	0.1393	0.0249

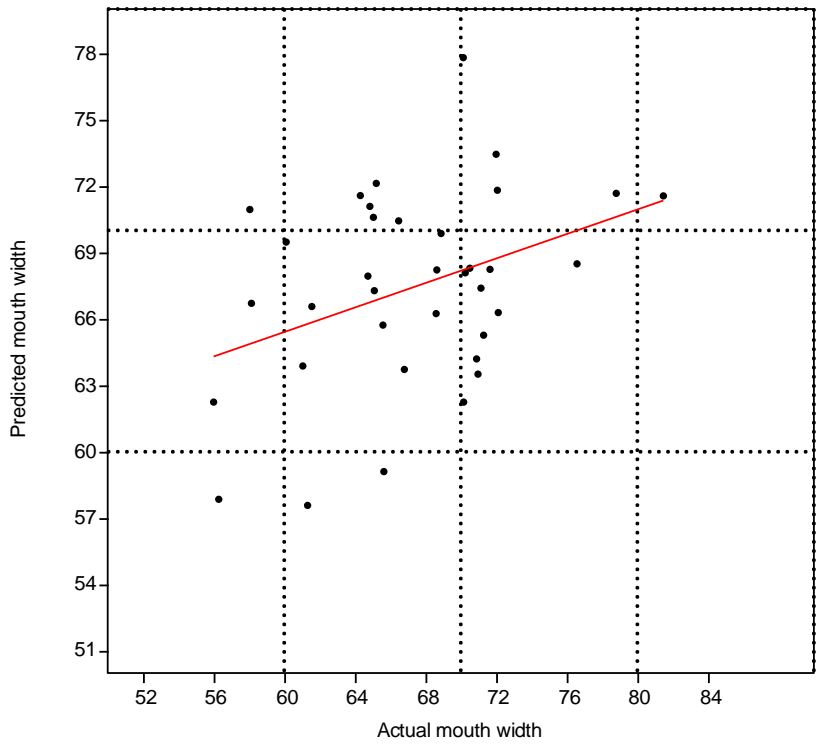


Figure 4.13 Correlation between actual and predicted mouth widths

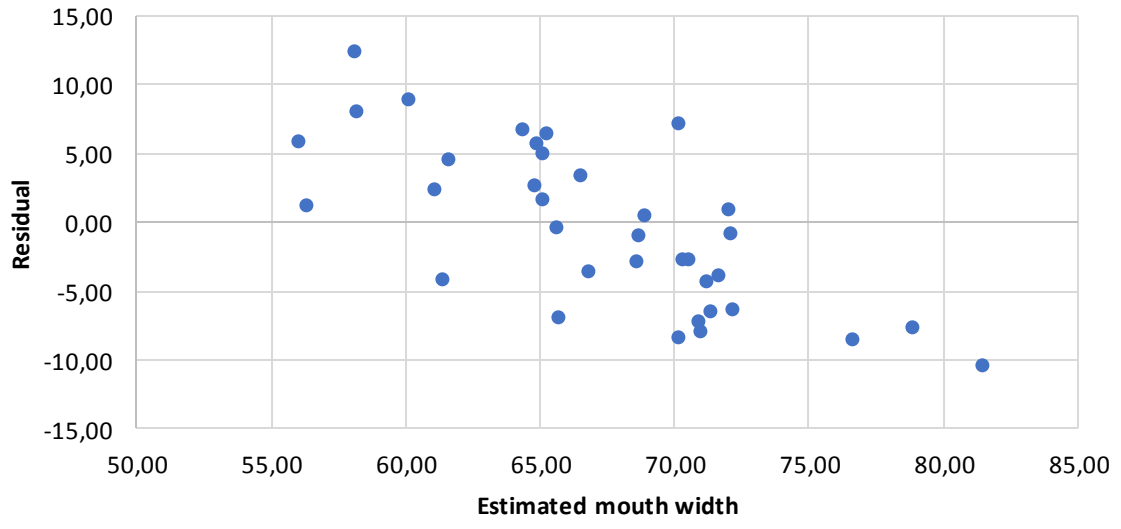


Figure 4.14 Accuracy of estimated mouth width as indicated by residuals versus actual mouth width

The philtrum width and the upper central incisor width were also tested for correlation by firstly calculating the average ratio of the two, i.e. upper central incisor width divided by philtrum width. The average ratio was 0.96. The upper central incisor width was then divided by 0.96 to estimate the philtrum width. The residual was calculated between the actual and estimated philtrum widths (estimated width minus actual width). A p-value of 0.5995 was calculated by means of a two-tailed paired t-test when comparing the actual and predicted philtrum widths, indicating that there was no statistically significant difference between these widths. Further testing by means of Chi-squared regression showed that a mild correlation ( $R^2 = 0.04$ ) existed but that it was not statistically significant ( $p = 0.3011$ ). Table 4.9 summarises the results and the correlation between actual and predicted philtrum widths is visualised in Figure 4.15. The accuracy of the estimated philtrum width is visualised in Figure 4.16 by comparing residuals versus actual philtrum width. The residuals are fairly widely distributed around zero in a non-random spread, once again indicating that although a mild correlation exists between the upper central incisor width and the philtrum width, it is not nearly adequate in predicting the philtrum width accurately.

Table 4.9 Correlation between philtrum width and upper central incisor width.

n	Mean UCInW	Mean PhW	Average ratio	Average residual	SD for residual	Mean predicted PhW	$R^2$	p-value for correlation
24	8.90	67.29	0.61	-0.37	5.88	66.92	0.0484	0.3011

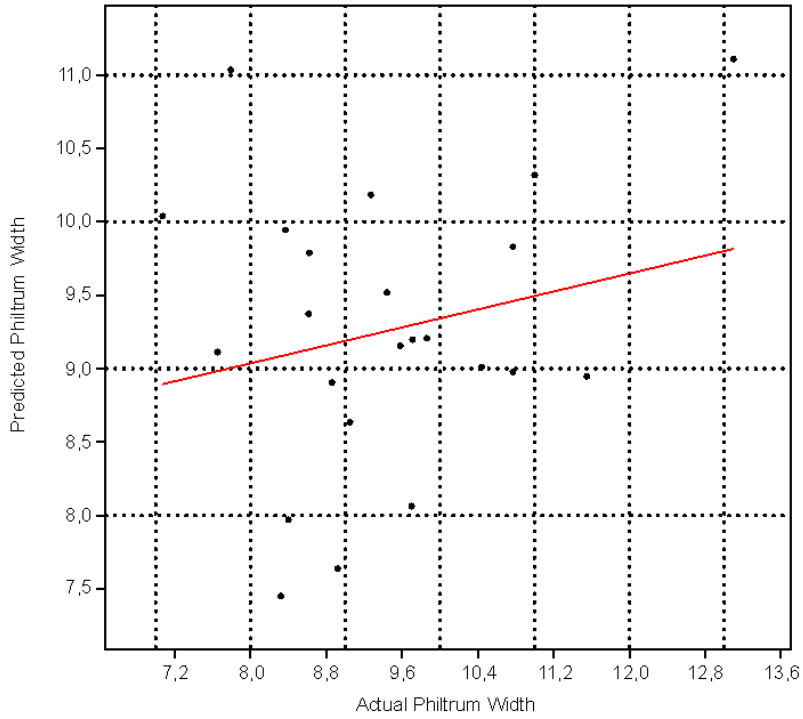


Figure 4.15 Correlation between actual and predicted philtrum widths

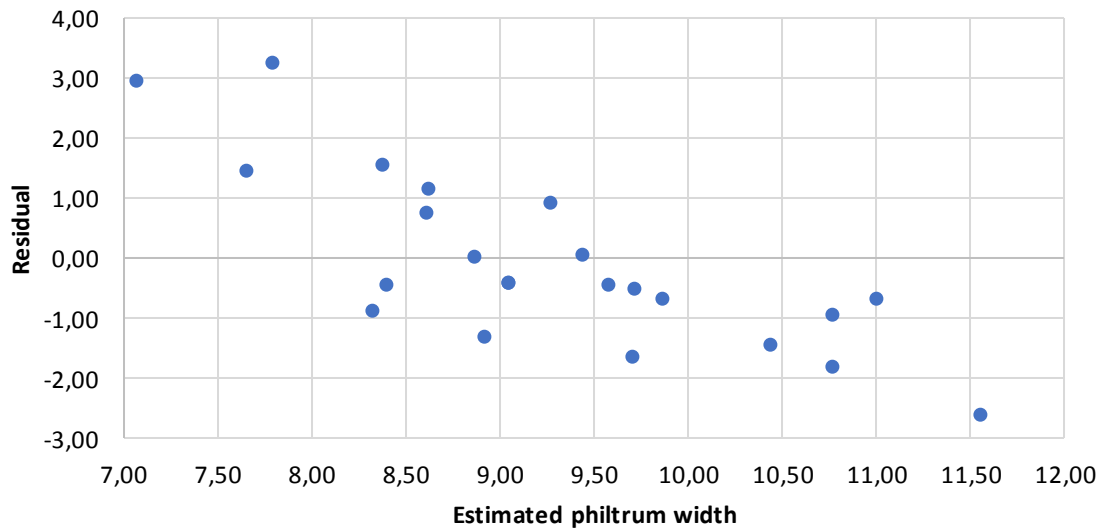


Figure 4.16 Accuracy of estimated philtrum width as indicated by residuals versus actual philtrum width

#### 4.4.4. Auricular measurements

The size of the ear was measured between the supraaurale and subaurale. Basic descriptive statistics are visualised in Figure 4.17 as calculated for male and female samples separately, as well as pooled. Multivariate regression was used to suggest two regression models for predicting the length of the ear. Only samples where both the sex and age is known was included in this part of the study. The first model has two variables, namely sex and age; while the second model only incorporated age. The regression models suggested are:

$$1) L = 0.1307 * \text{Age} + 0.4243 * \text{Sex} + 53.3008$$
$$2) L = 0.1336 * \text{Age} + 53.4728$$

Where L = estimated ear length; Age = chronological age in years; and Sex = a dummy variable (female = 0 and male = 1)

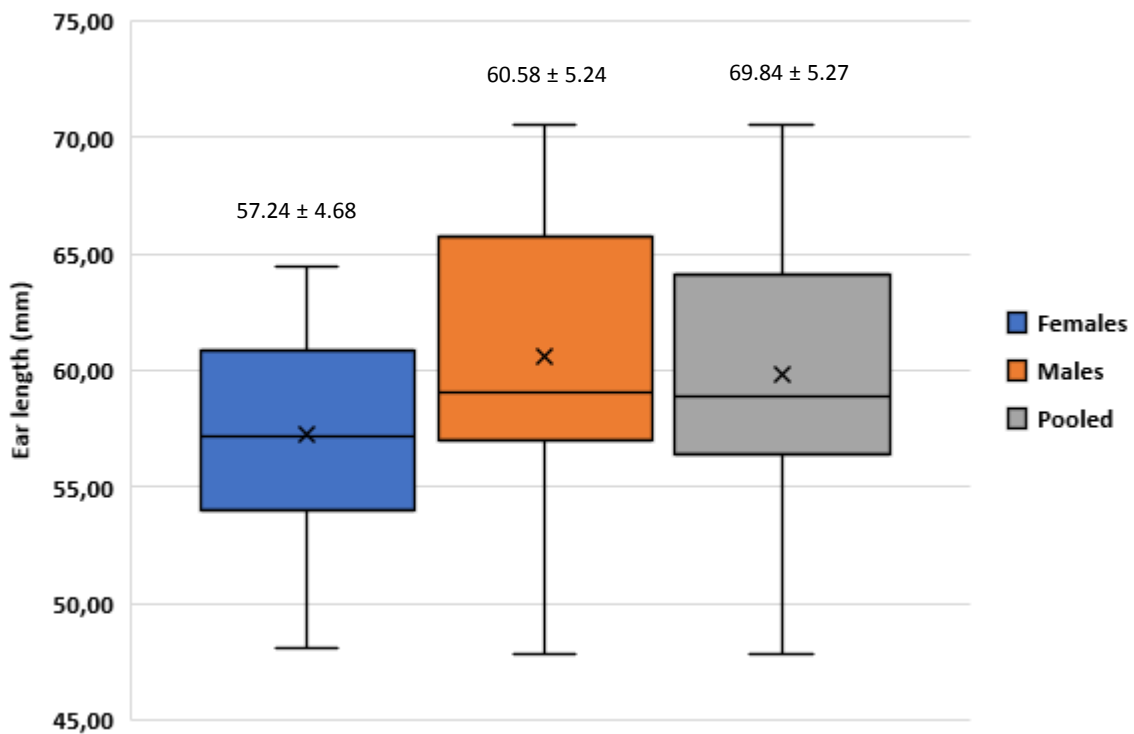


Figure 4.17 Basic descriptive statistics on auricular measurements (n for M = 38 and F = 11)

Both regression models were used to calculate the predicted length of the ear and compared to the actual measurements. The correlation between estimated and actual lengths when utilising regression formula no. 1 is visualised in Figure 4.18. This formula takes both sex and age into account and shows that a mild correlation exists ( $R^2 = 0.1444$ ). The F test and Prob(F) statistics test the overall significance of the regression model. The F value was calculated as 2.5432, however, the correlation is not statistically significant ( $p = 0.0816$ ). Furthermore, although the residuals are distributed in a random manner, it is spread relatively widely around zero (Fig. 4.19), indicating that although a mild correlation does exist, it is not adequate in predicting the ear length accurately.

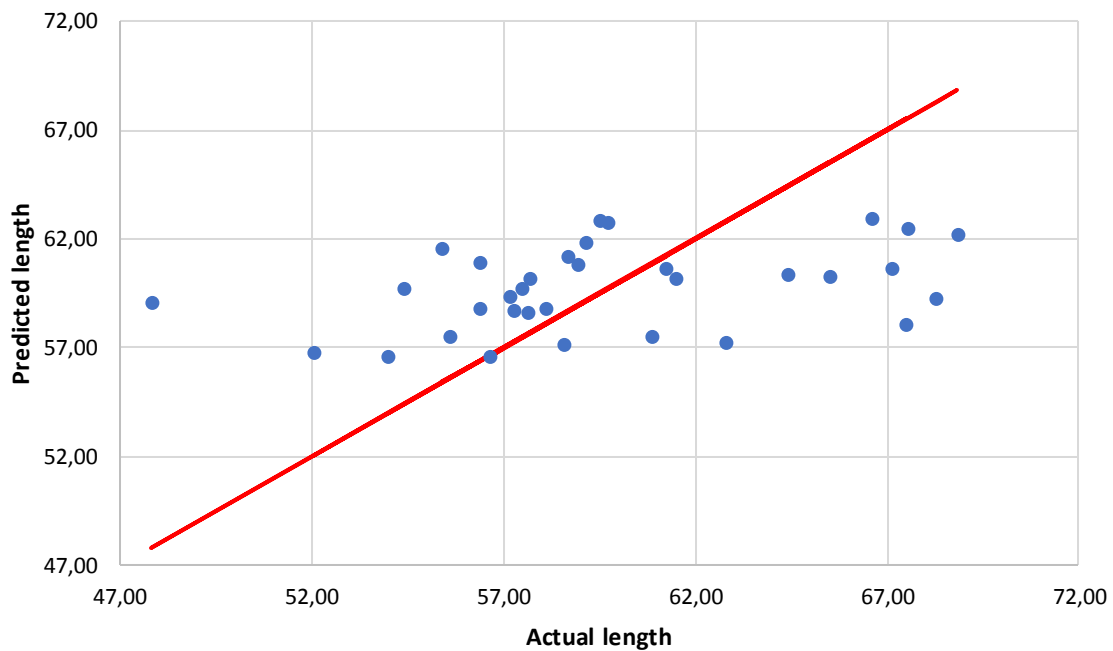
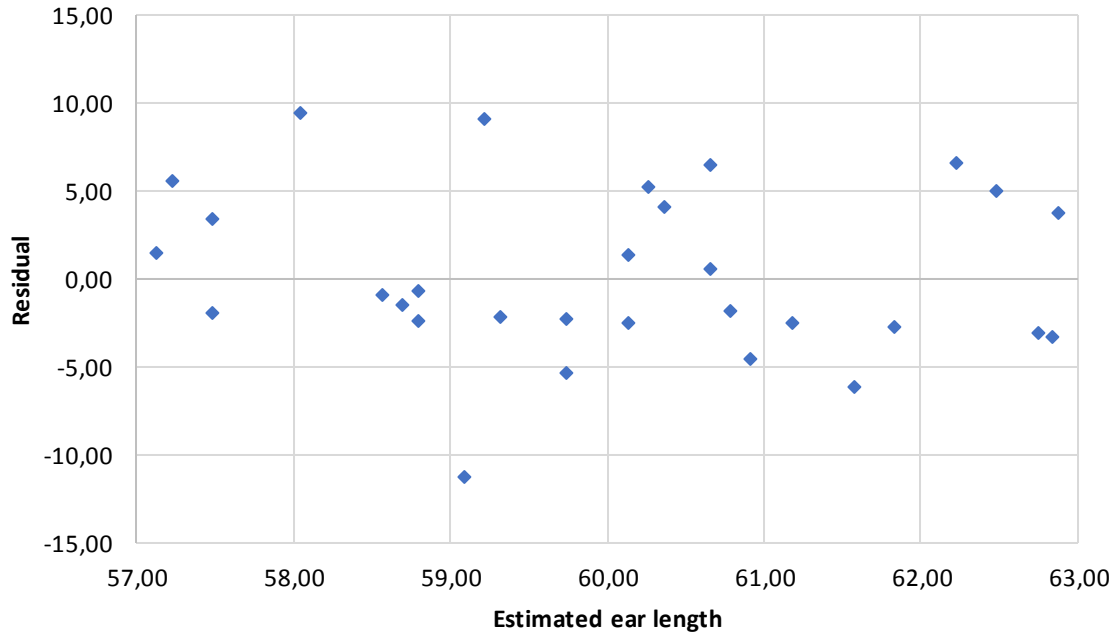


Figure 4.18 Non-statistically significant correlation between actual and estimated ear length utilising regression formula no. 1 ( $R^2 = 0.1444$  and  $p = 0.0816$ )



*Figure 4.19 Accuracy of estimated ear length utilising regression formula 1 as indicated by residuals versus actual ear length*

Regression formula no.2 only incorporates the effect of age into its calculation. The F value was calculated as 5.1734, indicating that mild correlation ( $R^2 = 0.1430$ ) that is statistically significant ( $p = 0.0300$ ) exists and is visualised by Figure 4.20. Although the residual plot is randomly distributed around zero, the upper and lower bounds are further from zero than is optimal (Fig. 4.21).

From these results, it can be concluded that in this sample, age is a linear predictor of ear length indicating that the ear length increases with age. Figure 4.22 visualises the relationship between age and actual ear length.

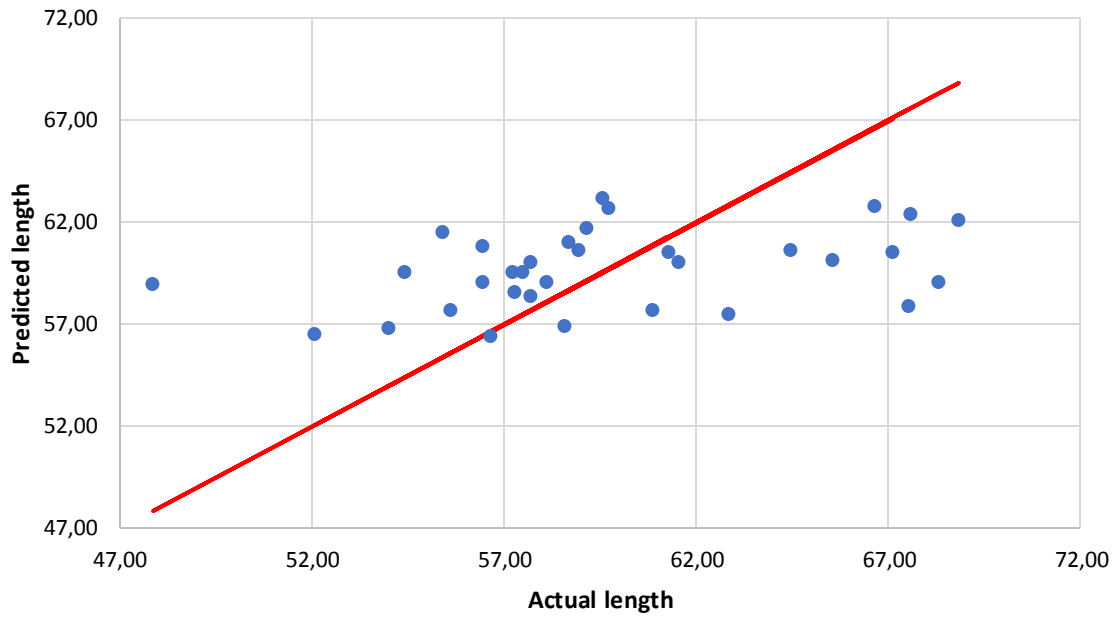


Figure 4.20 Mild statistically significant correlation between actual and estimated ear length utilising regression formula no. 2 ( $R^2 = 0.1430$  and  $p = 0.0300$ )

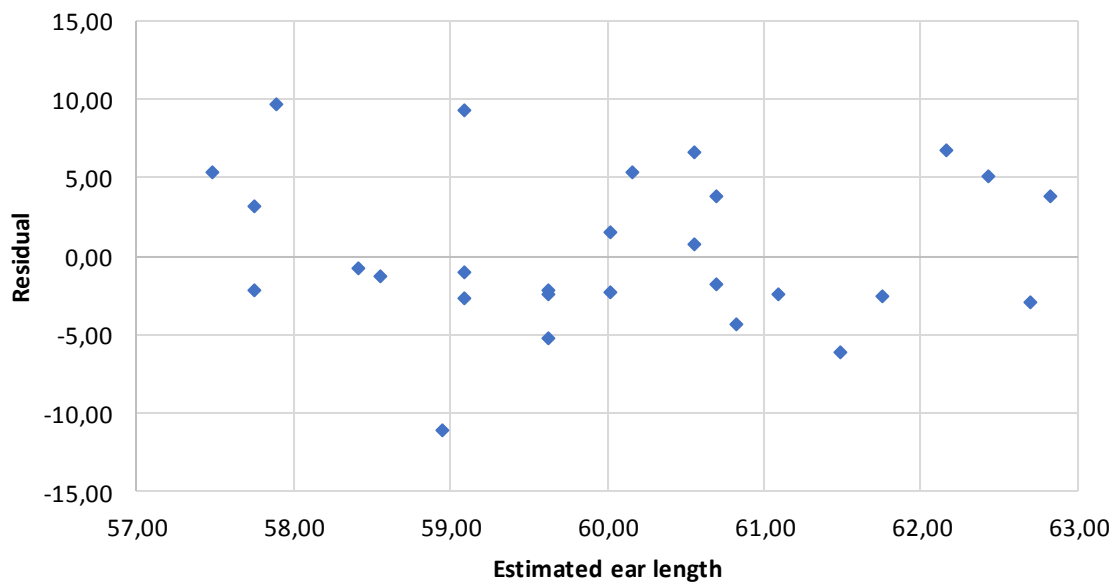


Figure 4.21 Accuracy of estimated ear length utilising regression formula 2 as indicated by residuals versus actual ear length

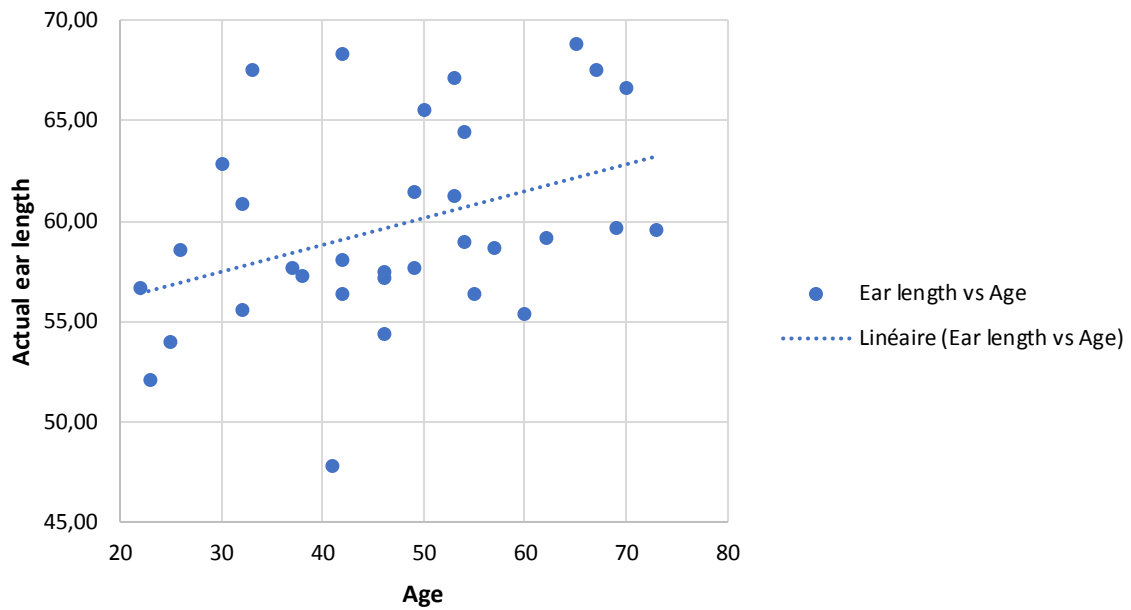


Figure 4.22 Linear relationship between age and ear length

Seven of the regression formulae (RF) presented by Guyomarc'h and Stephan <sup>23</sup> were utilised to predict the length of the ear and the relationship tested by means of Chi-squared regression (Table 4.10). Residual plots for each formula visualise the accuracy of each estimation (Fig. 4.23 to Fig. 4.29). All of these plots are relatively widely spread around zero. The  $R^2$  value of RF10 (0.3669) indicates that this formula is the most applicable for this population group, although not as applicable as the formula (no. 2) specifically designed for this sample.

Table 4.10 Regression formulae utilised in this study (where age is chronological age in years and sex is a dummy variable (female = 0 and male = 1)).

	Formulae	R <sup>2</sup>	Statistical significance (p value)
No. 1	$L = 0.1307 * \text{Age} + 0.4243 * \text{Sex} + 53.3008$	0.1444	0.0816
No. 2	$L = 0.1336 * \text{Age} + 53.4728$	0.1430	0.0300
RF1†	$L = (0,22 * \text{age}) + 55,9$	0.1430	0.0300
RF2†	$L = (0,13 * \text{age}) + 61,8$	0.1430	0.0300
RF7†	$L = (5,89 * \text{sex}) + (0,21 * \text{age}) + 52,36$	0.1073	0.0626
RF8†	$L = (5,06 * \text{sex}) + (0,15 * \text{age}) + 55,90$	0.0692	0.1393
RF10†	$L = (2,13 * \text{sex}) + (0,16 * \text{age}) + 54,20$	0.3669	0.0356
RF12†	$L = (4,85 * \text{sex}) + (0,10 * \text{age}) + 54,95$	0.0778	0.1159
RF18†	$L = (4,95 * \text{sex}) + (0,19 * \text{age}) + 53,05$	0.1110	0.0581

† Regression formulae designed by Guyomarc'h and Stephan <sup>23</sup>

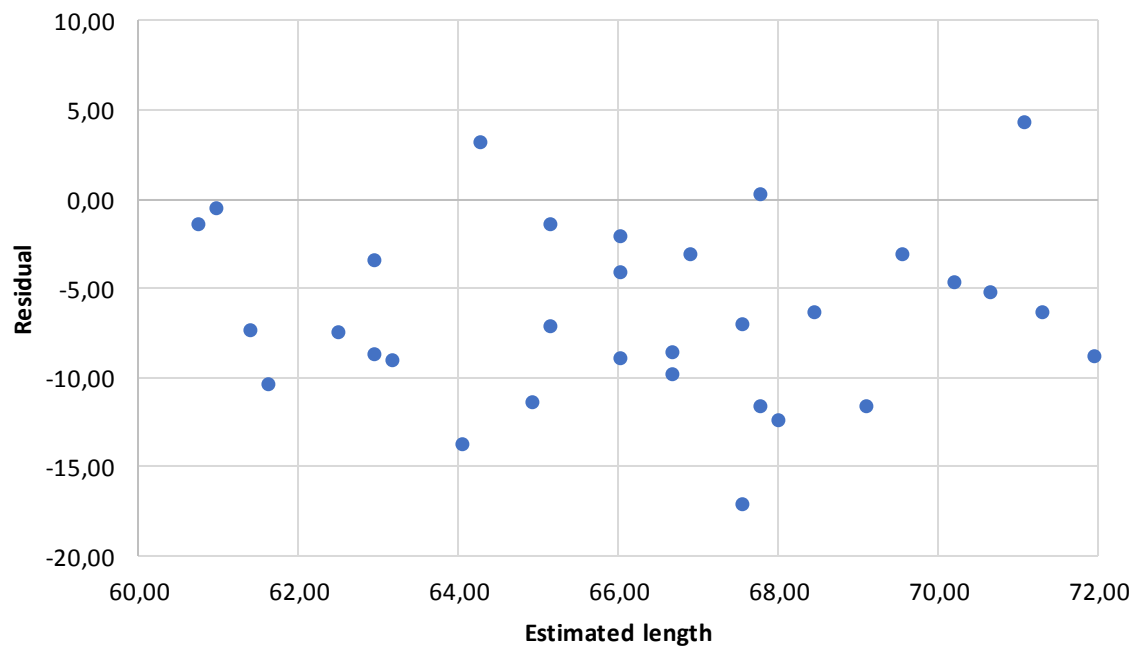


Figure 4.23 Accuracy of estimated ear length utilising Guyomarc'h & Stephan RF1 as indicated by residuals versus actual ear length

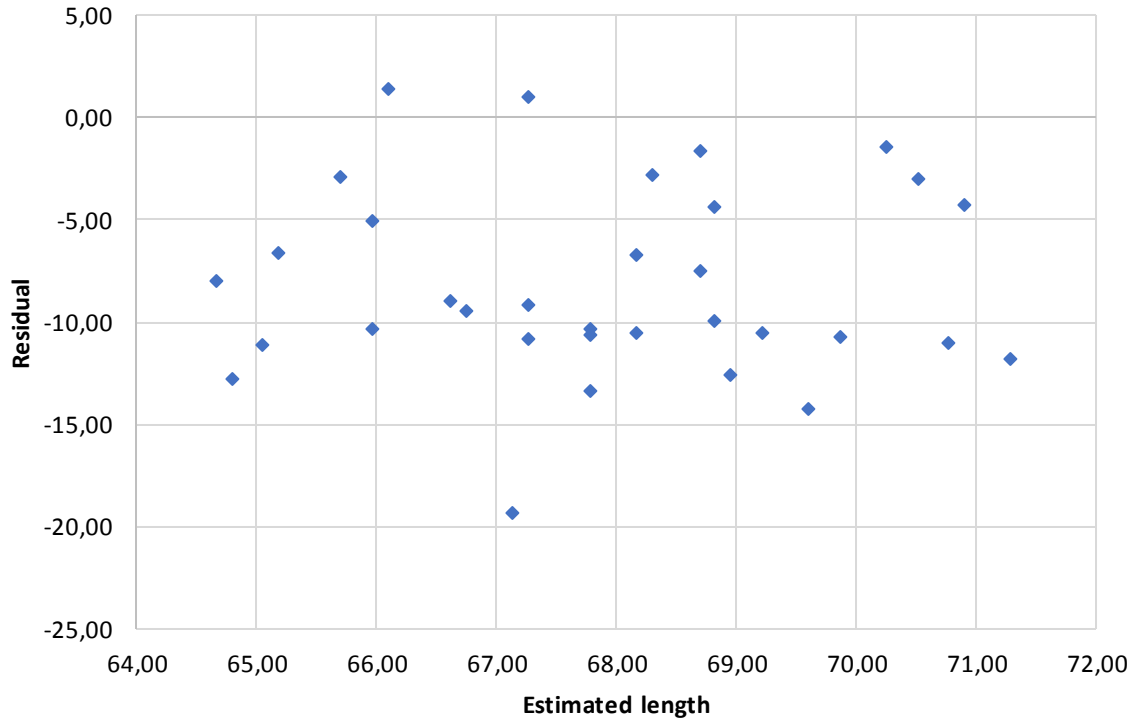


Figure 4.24 Accuracy of estimated ear length utilising Guyomarc'h & Stephan RF2 as indicated by residuals versus actual ear length

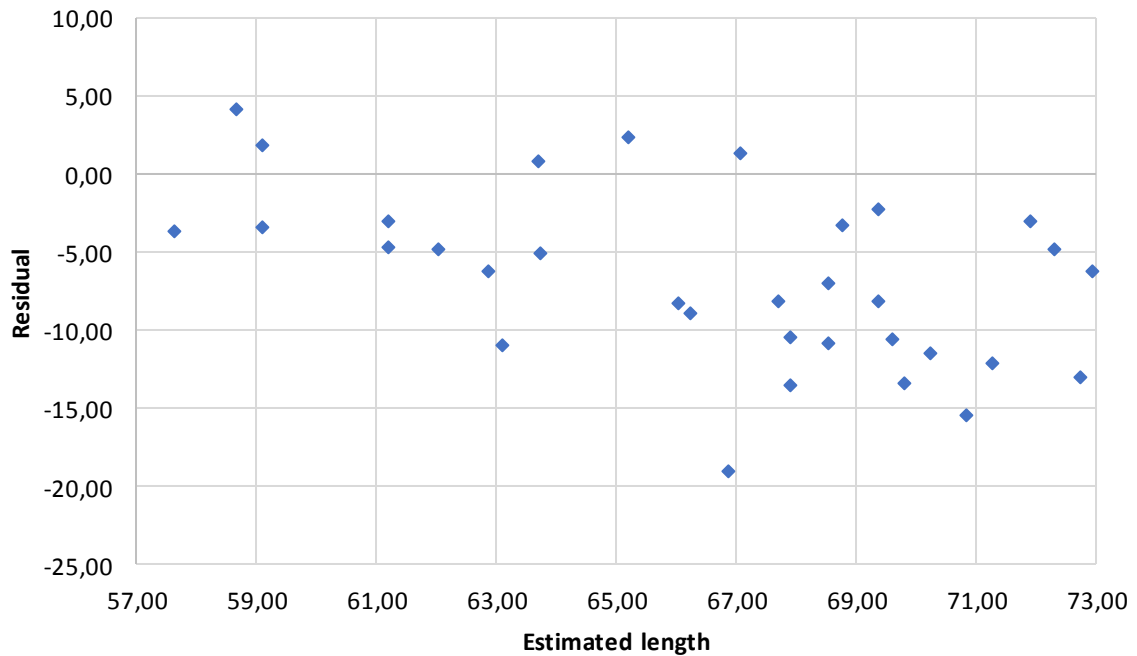


Figure 4.25 Accuracy of estimated ear length utilising Guyomarc'h & Stephan RF7 as indicated by residuals versus actual ear length

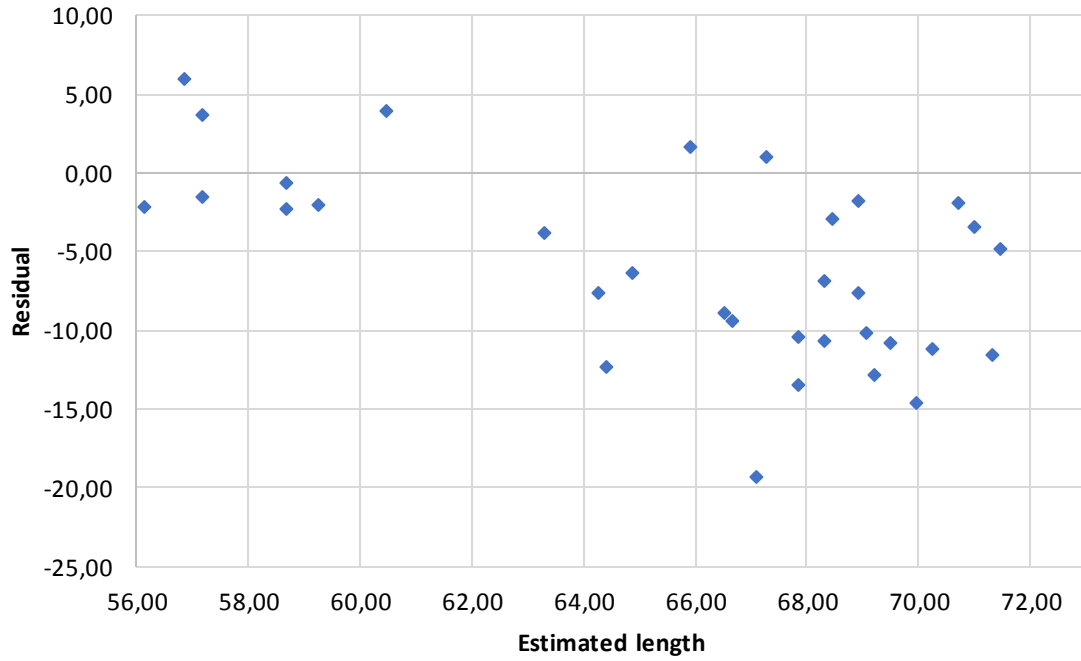


Figure 4.26 Accuracy of estimated ear length utilising Guyomarc'h & Stephan RF8 as indicated by residuals versus actual ear length

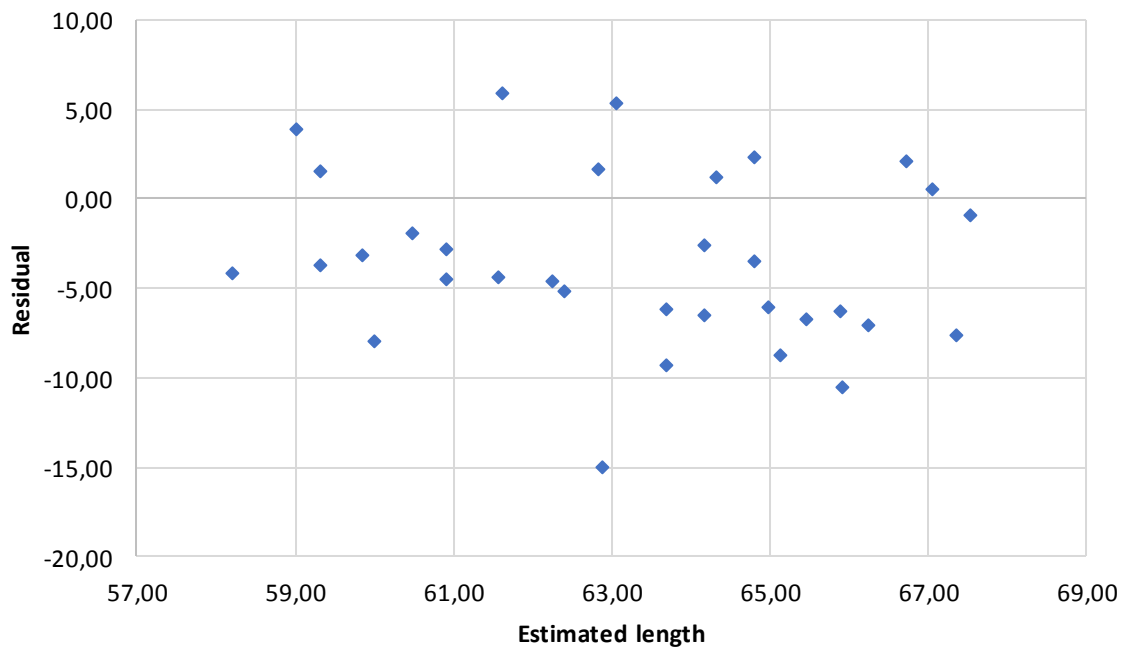


Figure 4.27 Accuracy of estimated ear length utilising Guyomarc'h & Stephan RF10 as indicated by residuals versus actual ear length

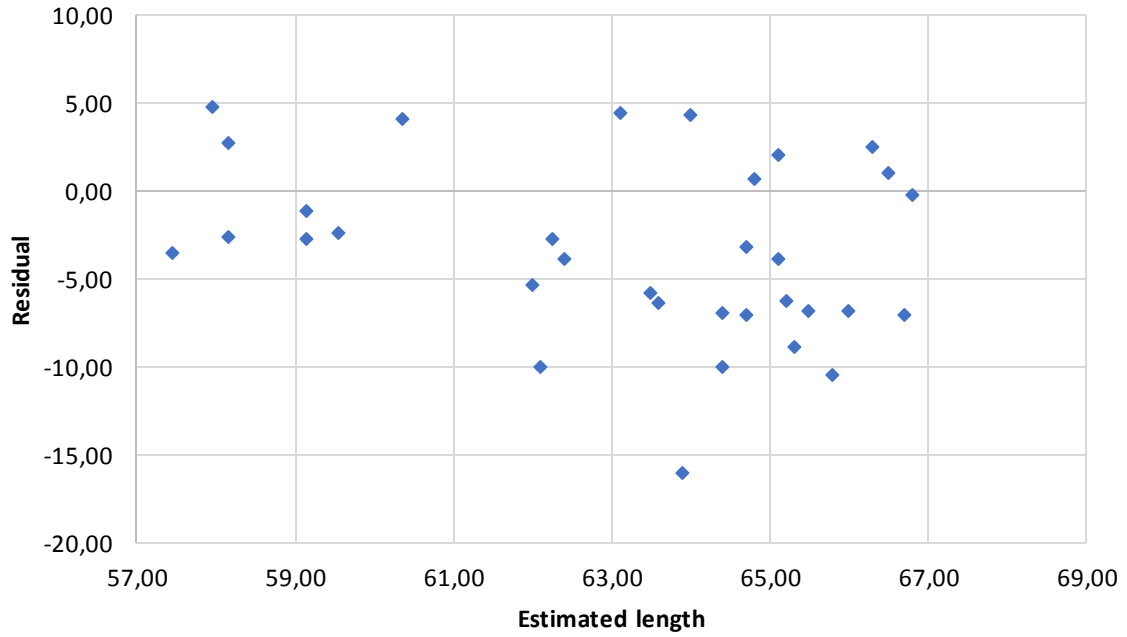


Figure 4.28 Accuracy of estimated ear length utilising Guyomarc'h & Stephan RF12 as indicated by residuals versus actual ear length

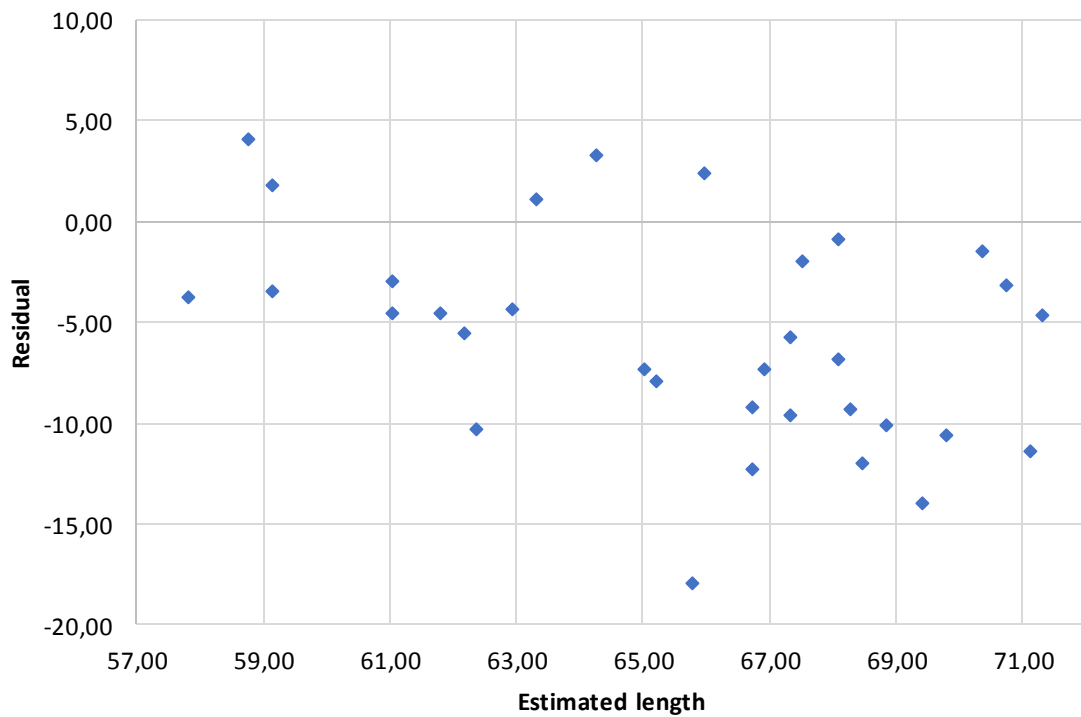


Figure 4.29 Accuracy of estimated ear length utilising Guyomarc'h & Stephan RF18 as indicated by residuals versus actual ear length

## 5. DISCUSSION

The purpose of this study was to assess aspects of facial features of black South Africans. An integrated FA model for this population is proposed by reflecting on existing FA guidelines as well as the results from this study. The various features assessed were the eyes, the mouth, the nose and the ears (refer to Appendix A).

In this discussion, repeatability assessments for qualitative and quantitative parameters are firstly discussed, as this is a reflection of the accuracy and the wider applicability of the results of this study. Following this, each individual feature is discussed with regard to the relationship between the soft tissue and the underlying bone and variations between the sexes (if at all) are put into context. The size of the eyeball and the ears are also addressed. These results are then compared to similar results published in the literature and suggestions made for appropriate guidelines to be used for FAs in this population.

### 5.1. Intra- and inter-observer repeatability

All cadaver-based measurements performed well. The intra- and inter-observer tests on quantitative parameters, similar to what is reported in the literature,<sup>61,91,92</sup> performed well indicating that the landmarks were readily identifiable and reliable. The majority of the measurements could be done with an acceptable degree of repeatability. Exceptions to the good repeatability of the quantitative measurements were the inter-observer results of the en-MOM and PhW dimensions. The en-MOM dimension, measured from the endocanthion to the medial orbital margin (MOM), displayed poor interobserver repeatability (ICC = 0.04). This observation might be explained by the exact placement of the MOM that is not clearly defined. Unlike the lateral orbital margin, the MOM is less well defined and quite rounded and irregular. The philtrum width also did not perform well for inter-observer repeatability (ICC = 0.23). Roelofse et al.<sup>91</sup> previously reported that most of the black South African population possessed a flat/absent philtrum (56%), while only 4% of the population had a deep philtrum. These factors could contribute to the difficulty in identifying the philtrum in black South Africans and may be related to why inter-observer tests for philtrum width performed poorly in the current study.

The qualitative parameters, on the other hand, did not perform as well as the majority of the quantitative parameters, as could be anticipated because of the subjective nature of these types of evaluations.

Inter-observer tests on the CBCT and CT scan measurements had a similar performance but were less well than expected (All ICC < 0.21) as compared to intra-observer tests. Mean values of most measurements, however, differed with less than 2 mm in general, which may be considered acceptable <sup>93</sup>. In general, lack of interobserver repeatability may primarily be related to the variability in interpretation of landmark locations <sup>94,95</sup>. Knowledge, experience and confidence in the use of the visualisation program used for measurements may also be responsible for the disagreement between observers. Image quality for instance, density and sharpness of the image, may cause difficulty in distinguishing between hard and soft tissues and so influence repeatability of manual measurements <sup>95</sup>.

The orbital depth measurement demonstrated the weakest repeatability, with the average difference between observers at approximately 4 mm for both CBCT and CT scans. The poor performance may be related to difficulty in identifying the optic foramen (the most anterior point of the optic canal), as this is not a clearly defined landmark. The optic foramen itself is on average almost 4 mm wide <sup>96</sup> and identified points along the foramen could vary in their distance from the landmark on the cornea. The variable localisation of the selected landmark on the optic foramen should therefore be taken into consideration when interpreting the orbital depth in this study. In future studies, attention should be given to define this landmark more precisely to improve greater interobserver repeatability.

## 5.2. Orbital and ocular dimensions

In this study, specific dimensions (absolute measurements and relationships between measurements) of the eye and orbit in South Africans were determined. Figure 5.1 graphically demonstrates the findings recorded in the literature (on the left) as opposed to findings observed in this study (on the right). Integration of the measurements obtained from the three modalities used (cadaver dissections, CT and CBCT) demonstrates that in black South Africans the exocanthion is positioned lower than the endocanthion, the orbit is rectangular-shaped and the transversely elongated or oval shaped eyeball is situated in the superolateral

aspect of the orbit. Findings regarding the shape of the orbit are in agreement with Krogman<sup>65</sup> and others stating that the orbits of skulls of Africans populations are more rectangular than those from other populations and the eyeball reflects this shape.

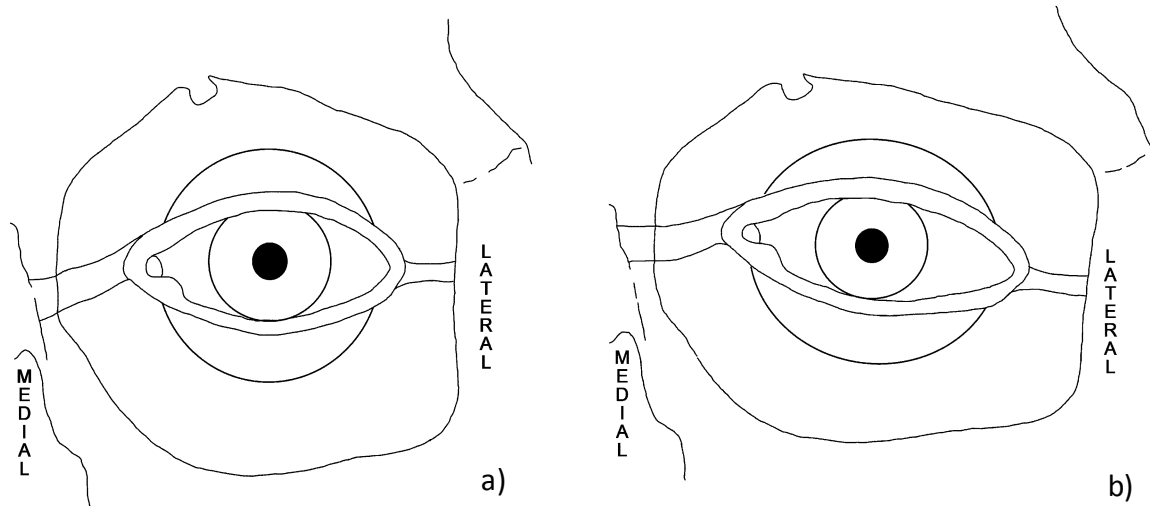


Figure 5.1 Graphic illustration of a) the findings from the literature<sup>19, 24</sup> and b) the mean dimensions of this study sample

Variations in the exact position of the endocanthion and exocanthion are reported in the literature. In most research done previously, the endocanthion was reported to be situated lower than the exocanthion. According to Stephan and Davidson<sup>19</sup>, the endocanthion in an Australian population lies approximately 19.5 mm below the superior orbital margin (SOM) reference plane and the exocanthion 18.5 mm below the SOM reference plane, while Kim et al.<sup>61</sup> reported that in their sample of Korean individuals, the endocanthion lies 22.8 mm and the exocanthion 20.2 mm respectively below the SOM. The findings of both these studies suggest an eye that slants slightly upwards in a lateral direction. However, in the current study, the opposite was true: the endocanthion was positioned 17.7 mm below the SOM reference plane and the exocanthion 19.8 mm indicating an eye that slants slightly downwards laterally. The lack of literature reports indicating a similar trend to that observed in this population group, seem to indicate that the inclination of the eye fissure is population specific. The differences in distances observed in populations may be related to the population specific variations in the morphology of the zygomatic bone as well as the zygomatic processes of the frontal and maxillary bones contributing to the margins of the orbit resulting in variations in the shape of the orbital border<sup>97</sup>.

Although outside the scope of this study, possible age related changes in the position of the endo -and exocanthion should be considered as reported by Sforza et al. <sup>98</sup>. These authors however suggest that although a decrease in height variation between the endo -and exocanthion does occur from the age of 30, major age-related changes in men only occur after the age of 64. As the mean age of the cadaver sample of the current study was 46.8 years, age should not play an important role in the variation noted in the height of the canthi. Future research considering the influence of aging should be conducted to verify this impression.

Reports regarding the distance of the exocanthion from the lateral orbital margin are remarkably similar in all populations at 4.5 mm <sup>19</sup>, 4.7 mm <sup>61</sup> and 5.0 mm medial to the malar tubercle <sup>26</sup>, and are comparable to findings in this study (5.0 mm). The distance from the medial orbital margin to the endocanthion is more variable: 4.8 mm <sup>19</sup>, 9.8 mm <sup>61</sup>, approximately 2 mm <sup>26</sup> and 4.8 mm (current study). The variation noted in the Korean sample <sup>61</sup> may be due to the presence of epicanthal folds in people of Asian descent. Epicanthal folds that cover the endocanthion may influence the inclination of the eye fissure in the longitudinal axis, essentially by masking the endocanthion and moving the medial end of the eye fissure downwards. The variation in the position of the canthi noted in the Korean sample may also be influenced by the size and shape of the nasal root <sup>59</sup>.

Considering the position of the eyeball in the orbit, measurements found in this study are consistent with many previous studies indicating that the eyeball is not centrally located within the orbit <sup>19, 22, 28-32, 61</sup>. Most of these studies report a supero-lateral position. In comparison to other studies (e.g., <sup>19, 29-31</sup>) however, the current sample showed a greater periorbital space in the transverse axis (i.e. the medial equator to medial orbital margin (MOM) and lateral equator to lateral orbital margin (LOM)), while a smaller periorbital space was observed in the vertical axis (i.e. the superior equator to SOM and inferior equator to IOM). Distances observed in this population group were measured as 3.4 mm from the SOM, 6.1 mm from the IOM, 8.3 mm from the MOM and 4.2 mm from the LOM. Specific distances reported by other authors, Stephan et al. <sup>29</sup> for instance, are as follows: 4.0 mm from the SOM, 6.9 mm from the IOM, 8.0 mm from the MOM and 3.9 mm from the LOM. Whitnall <sup>30, 31</sup> reported distances of 4.0 mm from the SOM, 6.8 mm from the IOM, 6.5 mm MOM and 4.5

mm from the LOM. These greater distances in the transverse axis in the black South African group is probably related to the more rectangular shape of the orbit in this group.

Interestingly, however, Kim et al.<sup>61</sup> on an Asian sample reported an infero-laterally positioned eyeball within the orbit. These authors suggest that the variable location of the eyeball may be partly attributed to differences in the ancestral origin of the subjects compared to previous studies, but is more likely due to the difference in the modalities used to obtain the measurements. Stephan and Davidson<sup>19</sup> and Stephan et al.<sup>29</sup> used cadaver samples, while Guyomarc'h et al.<sup>22</sup> made use of CT scans. Both these modalities might have been influenced by gravity in the supine position. Kim et al.,<sup>61</sup> however, utilised CBCT scans, where the patients were positioned in an upright position. While this argument is most definitely valid and should be investigated in future, the effects of inter-population morphological differences in the orbital margin should also be taken into consideration<sup>97</sup>.

Evaluation of the diameters of the eyeball in the current study (cadavers, CT and CBCT) indicates an oval shape (elongation in the transverse axis), which has also been observed by clinicians<sup>62</sup>. The medio-lateral diameter of the eye in this study is slightly greater than the supero-inferior diameter, but is also to a small extent (approximately 1 mm) larger than in other population groups<sup>22,62</sup>. In the current study, all diameters were marginally greater on CBCT than those reported on other modalities and other groups, while the CT findings were more in agreement with previous findings<sup>15,22,62,63</sup>. A comparison between the findings of this study and those in the literature are summarised in Table 1 of Appendix B. In essence, the eyeball in the current study population group is slightly larger and more oval shaped than that of other population groups and may be a reflection of the shape of the orbit, which is more rectangular in this population group<sup>65</sup>.

In general, when comparing the different modalities to one another, the CBCT and cadaver dissections agreed to a greater extent with each other than the CBCT and CT scans. This discrepancy between modalities could be due to the variation in resolution of the scans and the possible effect of gravity in the supine position. In general, variations noted on CBCT could be important as this modality is often considered superior, especially for studies with FA implications, because of higher resolution and more natural effect of gravity on the face<sup>54,99-105</sup>. It is recommended that CBCT scans should be used as the modality of choice when conducting studies with application to FAs.

Although difference between the sexes for Meq-Leq was statistically significant, the actual difference in real terms was minute (difference between mean values: 0.29 mm). The orbital depth variation between sexes was slightly greater with the difference between mean values being 2.17 mm. It was interesting to note that despite minute or non-significant sexual differences in the eyeball dimensions, variations in the orbital depth did exist. This may be explained by the uniform function of the eyeball to focus light rays that is similar between sexes despite the generally more gracile skull dimensions in females. However, the relative orbital dimensions to the rest of the skull have been described as greater in females than in males, but this could possibly not be quite adequate to compensate for the general greater skull robusticity in males<sup>56</sup>. In the presence of greater skull dimension in males, the orbit also tends to be greater in absolute size<sup>56,92,106</sup>. Despite a larger orbit in males (compared to females), and non-statistically significant differences between sexes regarding the size of the eyeball, females possess an eyeball that occupies 34% of the orbit compared to only 29.1% in males<sup>106</sup>. Masters reported that this difference of 4.9% was comparable to reports by another study that found the eyeball in females to occupy 5.7% more of the orbit than that in males. It may be possible that to ensure optimal focusing power of the eye, females need to compensate for the relatively greater volume of the orbit that is occupied and this may be achieved by the orbit being relatively larger than the rest of the upper facial skeleton<sup>56</sup>. It seems that the difference between the sexes is effectively cancelled out by the female orbit being larger in comparison to the rest of the skull, combined with an eyeball that fills more of the orbit.

The orbital depth may be influenced by the population group studied or the modality used for obtaining measurements. The mean depth measured on CBCT and CT scans for this population group was approximately 51 mm. The median value of the orbital depth measured on CBCT, similar to the current study, was approximately 48 mm on a mixed ancestral group (including Africans) from Tel Aviv, Israel<sup>62</sup>. A study by Wilkinson and Mautner<sup>15</sup> on MRI scans on a group from Manchester, UK, reported a composite distance of approximately 40 mm when adding two distances determined by the authors.

The findings of this study suggest that approximations of the eyeball and orbital area for the black South African population should accommodate for a more rectangular shaped orbit with a slightly larger, supero-laterally placed and transversely elongated or oval-shaped eyeball.

The eye fissure is sloped slightly downward laterally with the endocanthion at approximately 17.7 mm below the SOM reference plane and the exocanthion at approximately 19.8 mm from the SOM reference plane.

### 5.3. Nasal dimensions

Regarding the nasal tip and anterior nasal spine (ANS) shape, fewer variations existed than anticipated. The most prevalent shapes were the spatulate shaped ANS and the bulbous nasal tip shape. The sharp tip nose shape was not observed in this study sample. Furthermore, the presence of a sharp anterior nasal spine, which has been associated with a sharp nasal tip<sup>38</sup>, could not be documented in this study despite the low occurrence of sharp anterior nasal spines in this sample. Overall, the ANS predicted the nasal tip shape in only 62% of cases. The position of the nasal tip, as seen in profile with the Gerasimov two-tangent method, was as often overestimated (44%) as correctly estimated (44%). This finding was in conflict with previous described reports considering this method to have some value to predict a point on the external nasal surface (Rynn and Wilkinson, 2006).

Other methods of predicting the position of the nasal tip have been reported<sup>16, 36, 37, 39</sup>, but fell outside of the scope of this study. Future studies may assess if these provide better results. As far as the methods tested in this study are concerned, it therefore seems that there is no clear and consistent information that could be obtained from the skeleton to help predict nasal shapes. In the FA context, this lack of associations between the skeletal and surface features suggests that the most common observations for this population should be used. In this case, that implies a non-projecting nose with a bulbous shaped nasal tip.

### 5.4. Oral measurements and relationships

In the absence of other bony landmarks, the teeth and their positions are considered to be associated with the soft tissue landmarks of the mouth<sup>10, 107</sup>. In this study the position and distance between the cheilia (corners of the mouth) as well as the philtrum width were considered and related to teeth.

The positions of the cheilia were often found to be asymmetrical and most often occurred at the maxillary canine/first-premolar junction. However, they only showed a mild to moderate statistically significant correlation to the inter-canine width. Asymmetries of the mouth reported in the literature occurred in 23% of a female Chinese population, comparable to this study (27% male/female pooled), however in an African American population, it occurred in only 10% of males and 18% of females <sup>59</sup>. It has been suggested that asymmetry increases with ageing in other soft-tissue structures, e.g. the nose <sup>108</sup>.

When compared to other studies, the mouth corners were slightly further apart than expected (see Table 2 in Appendix B) and the inter-canine distance contributed to a smaller component of the mouth width (60% vs 75%; <sup>17</sup>. African populations display midfacial protrusion <sup>56</sup> which may influence various relationships between relevant structures.

The 75% rule of Stephan and Henneberg <sup>17</sup>, where the inter-canine width is considered to be approximately 75% of the mouth width, may be a useful guideline for estimating the mouth width in other groups, however it is clearly not applicable in this population as the average ratio calculated was 0.61. A more accurate guideline would thus be where the inter-canine width constitutes 60% of the total mouth width.

Fedosyutkin and Nainys <sup>25</sup> also stated that the philtrum width corresponds to the distance between the midpoints of the upper central incisors. This statement was corroborated by an Indian study, where a direct statistically significant correlation was found between the width of the central incisors and the philtrum in 200 subjects <sup>88</sup>. It was unclear, however, if the study correlated the distance between the midpoints of the upper central incisors to the philtrum width, or merely the tooth width. This guideline for estimating philtrum width from the teeth was, however, found to not be applicable to this population group, as only a mild, non-statistically significant correlation existed between the philtrum width and the distance between the midpoints of the upper central incisors. The inability to estimate the philtrum width could possibly be due to the flat/absent philtrum in most of the black South Africans <sup>91</sup>.

When estimating the dimensions of the mouth for approximations in the South African population, it is thus proposed to utilise the inter-canine width to constitute 60% of the mouth width. A flat/absent philtrum may be modelled with the cheilia corresponding to the maxillary canine/first-premolar junction.

## 5.5. Auricular dimensions

In this study, factors associated with the variation of the size of the ear were taken into consideration when evaluating formulae designed for this population group specifically, as well as the applicability of other previously published <sup>23</sup> regression formulae.

Variation between the sexes in this population was not statistically significant ( $p = 0.8000$ ), however variations between sexes may become significant when the sample size, especially that for females, is increased. When comparing the mean length of the ear between males and females in this population group, it can be noted that men do tend to have larger ears than women (means of 60.58 mm vs 57.24 mm). The literature reports also indicate this trend <sup>59, 69, 70, 72, 109, 110</sup>. It would thus be good practice to take this into consideration when creating approximations from the skull.

Another factor that has been reported to influence the size of the ear is aging <sup>71, 109-112</sup>. Ordinary Least Squares Regression between the pooled ear length and aging showed a small but statistically significant correlation ( $r^2 = 0.1430$  and  $p = 0.0300$ ). Aging therefore seems to have had an effect on ear length, but other factors could have been involved as well, e.g. sex and individual variations.

A formula based on this data set was constructed which considers the effects of sex and age:

$$L = 0.1307 * \text{Age} + 0.4243 * \text{Sex} + 53.3008$$

As sex was not regarded as having a statistically significant influence on ear size in this study, another formula was designed only taking age into account:

$$L = 0.1336 * \text{Age} + 53.4728$$

These formulae were considered more relevant (than other previously reported existing formulae) to the population group studied, however its applicability is limited to those with known age and/or sex. More research should be conducted on a greater sample size to verify the significance of these findings.

As both sex and aging had an effect on ear size, the applicability of existing regression formulae taking these two factors into account were evaluated <sup>23</sup>. The formula labelled no.

12 ( $L = 4.85 \cdot \text{sex} + 0.10 \cdot \text{age} + 54.95$ ) was considered most applicable by Guyomarc'h and Stephan 23, because, so far as the data suggest, it provides the greatest generality that has been verified by cross-validation. The study on the current sample indicated that the formula labelled as no. 10 ( $L = 4.85 \cdot \text{sex} + 0.10 \cdot \text{age} + 54.95$ ) by these authors could be considered most applicable to the current sample group. However, while the residual plots were mostly randomly distributed around zero, all were more weighted towards negative values, implying that ear length is being overestimated with these formulae. It is of great importance to remember that when using these formulae, an incorrect age or sex estimation from the skeleton can thus influence (compound) errors in ear length estimation and as such limits the use of such formulae in the approximation of ears.

It is interesting to note that the population groups (see Table 3 in Appendix B) show some geographical clustering – e.g. Europeans where almost all ear lengths reported in the literature are similar (males  $\pm 62 - 64$  mm, females  $\pm 58 - 60$  mm). Our sample presented with ear lengths greater than other African populations: (males: 60.58 and females: 57.24), but in general smaller than other groups from other geographical areas.

Approximations of ear length should take into consideration the influence of sex and age. Population specific formulae incorporating these factors should be used when possible. The formula indicated to be the most applicable to this specific sample was ( $L = 0.1336 \cdot \text{Age} + 53.4728$ ), however further research should be conducted on a greater sample size, specifically that of females, to determine if the influence of sex may be statistically significant.

## 5.6. Limitations and shortcomings

### 5.6.1. Sample size

A total number of 49 cadaver specimens were included in this study. Although this is a relatively large sample size in terms of cadaver studies, of this number only 11 were female. Small sample sizes may influence statistical significance to a degree and increase the risk of assuming a false premise as true <sup>113</sup>. The same applies for both CT and CBCT scan samples, where 30 scans each with 23 males and 7 females, and 17 males and 13 females, respectively were included in this study.

The effects of age on some of the facial features assessed may influence the significance of some measurements taken (e.g. the size of the ear, the position of the canthi). Some of the specimens were of unknown age and had to be excluded from statistical age analyses, which further reduced the sample size. The influence of age may be over- or underestimated due to a limited sample size.

### 5.6.2. Inter-observer correlations

Inter-observer correlations on cadavers for qualitative and some of the quantitative parameters (en-MOM and PhW) were relatively low. In future research, subjective assessments (such as determining the shape of the nose tip) should be avoided and rather quantified if possible. As discussed in the relevant sections, the poor performance of some quantitative parameters may be due to difficulty in identifying relevant landmarks/features and could be improved by revising the definition or choice of the landmarks. Further research should be conducted to determine more appropriate methodology for identifying and measuring these features.

The inter-observer repeatability on the scan samples, especially the orbital depth, was also low. One possible reason may be related to observers' interpretation of landmark locations<sup>94,95</sup>. The visualisation program used for measurements lacked the capability for automated identification of landmarks which may improve repeatability between observers.

### 5.6.3. Individual features

When considering each feature assessed in this study, possible shortcomings should be mentioned. Regarding the eyeball and orbits, further research should be conducted to include the effects of age on the position of the canthi. Findings on the position of the canthi should be verified on other modalities e.g. CBCT (and/or other modalities) if possible. Many other methods (besides Gerasimov's two-tangent method) for determining the projection of the nose have been reported in the literature. It would be of value to explore their applicability to the South African population as well. Rynn et al.<sup>16</sup> conducted a novel and comprehensive study to predict the nasal morphology from the skulls of various ancestry groups. The

applicability of these methods to the South African population should be investigated further to assess if it may be of value. Methods evaluated in this study for determining the mouth width was restricted to those directly related to the teeth. Further research should be considered to evaluate mouth width in edentulous persons. Regarding the ear, the focus of this study was only related to ear length. Further research should be conducted to include prediction guidelines for ear width, and incorporate measurements obtained from various modalities (not only cadaver samples).

## 6. CONCLUSION

In South Africa, facial approximation plays an important role in the identification of unknown remains. In this study certain aspects of facial features were investigated in order to provide guidelines to be used in facial approximations on black South Africans. Facial features studied included the eyes, the nose, the mouth and the ears. The findings of this study were used to reflect on previously published guidelines. An integrated summary is visualised in Appendix A.

1. Guidelines for the approximation of the eyes should include:
  - 1.1. a slightly larger (as compared to previous studies), supero-laterally placed and transversely elongated or oval-shaped eyeball.
  - 1.2. a laterally downward sloped eye fissure (endocanthion slightly higher than the exocanthion).
2. Guidelines for the approximation of the nose should take into account that:
  - 2.1. no clear and consistent information on predicting the nasal projection as described by the two-tangent method of Gerasimov <sup>35</sup> existed.
  - 2.2. the most common observation was a non-projecting nose with a bulbous shaped nasal tip.
3. Guidelines for the approximation of the mouth should take into account that:
  - 3.1. the inter-canine width constituted 60% of the mouth width.
  - 3.2. a flat/absent philtrum may be modelled with the cheilia corresponding to the maxillary canine/first-premolar junction.
4. Guidelines for the approximation of the ear should take into account that:
  - 4.1. sex and age might influence the approximations of ear length
  - 4.2. the most applicable formula to this specific sample was:

$$L = 0.1336 * \text{Age} + 53.4728$$

### 5. Future prospects

Possible limitations of the current study, might firstly be addressed in future studies by increasing the sample size as well as the following specific suggestions:

- 5.1. The influence of aging on the position of the canthi should be considered. Findings on the position of the canthi should be verified on other modalities e.g. CBCT if possible.
- 5.2. The landmarks pertaining to the orbital canal, medial orbital margin and the philtrum should be revised
- 5.3. Other methodologies (besides Gerasimov's two-tangent method), for instance the study by Rynn et al. <sup>16</sup>, should be explored to determine the projection and other features of the nose in this population group.
- 5.4. Other methods, not involving the teeth, should be conducted to evaluate mouth width in edentulous persons.
- 5.5. A greater sample size might elicit significant variations between the sexes in ear length estimation.
- 5.6. Further research should be conducted to include prediction guidelines for ear width, and to incorporate measurements obtained from various other modalities (not only cadaver samples).

## 7. REFERENCES

1. L'Abbé EN, Loots M and Meiring JH. The Pretoria Bone Collection: a modern South African skeletal sample. *HOMO - Journal of Comparative Human Biology*. 2005; 56: 197-205.
2. Cavanagh D and Steyn M. Facial reconstruction: soft tissue thickness values for South African black females. *Forensic Science International*. 2011; 206: 215. e1-. e7.
3. Stephan CN. Facial Approximation—From Facial Reconstruction Synonym to Face Prediction Paradigm. *Journal of Forensic Sciences*. 2015; 60: 566-71.
4. Stephan CN and Henneberg M. Building faces from dry skulls: are they recognized above chance rates? *Journal of Forensic Sciences*. 2001; 46: 432-40.
5. De Greef S and Willems G. Three-dimensional cranio-facial reconstruction in forensic identification: latest progress and new tendencies in the 21st century. *Journal of Forensic Science*. 2005; 50: JFS2004117-6.
6. Kollmann J and Büchly W. Die persistenz der raassen und die reconstruction der physiognomie prahistorischer Schädel. *Arch Kriminol*. 1898; 25: 329-59.
7. Rynn C and Wilkinson CM. Appraisal of traditional and recently proposed relationships between the hard and soft dimensions of the nose in profile. *American Journal of Physical Anthropology*. 2006; 130: 364-73.
8. Stephan CN. Beyond the sphere of the English facial approximation literature: ramifications of German papers on western method concepts. *Journal of forensic sciences*. 2006; 51: 736-9.
9. Gibson L. *Forensic art essentials: a manual for law enforcement artists*. Academic Press, 2010.
10. Wilkinson C and Rynn C. *Craniofacial Identification*. Cambridge University Press, 2012.
11. Stephan CN. Do resemblance ratings measure the accuracy of facial approximations? *Journal of Forensic Science*. 2002; 47: 239-43.
12. Stephan CN. Facial approximation: globe projection guideline falsified by exophthalmometry literature. *Journal of Forensic Science*. 2002; 47: 1-6.
13. Stephan CN, Henneberg M and Sampson W. Predicting nose projection and pronasale position in facial approximation: a test of published methods and proposal of new guidelines. *American Journal of Physical Anthropology*. 2003; 122: 240-50.
14. Tyrrell A, Evison MP, Chamberlain AT and Green MA. Forensic three-dimensional facial reconstruction: historical review and contemporary developments. *Journal of Forensic Science*. 1997; 42: 653-61.
15. Wilkinson CM and Mautner SA. Measurement of eyeball protrusion and its application in facial reconstruction. *Journal of Forensic Sciences*. 2003; 48: 12-6.
16. Rynn C, Peters HL and Wilkinson CM. Prediction of nasal morphology from the skull. *Forensic Science, Medicine and Pathology*. 2010; 6: 20-34.
17. Stephan CN and Henneberg M. Predicting mouth width from inter-canine width - a 75% rule. *Journal of Forensic Sciences*. 2003; 48: 1-3.
18. Stephan CN. Facial approximation: an evaluation of mouth-width determination. *American Journal of Physical Anthropology*. 2003; 121: 48-57.
19. Stephan CN and Davidson PL. The placement of the human eyeball and canthi in craniofacial identification. *Journal of Forensic Sciences*. 2008; 53: 612-9.
20. Wilkinson CM, Manish Motwani M and Chiang E. Relationship Between the Soft Tissues and the Skeletal Detail of the Mouth. *Journal of Forensic Sciences*. 2003; 48: 728-32.
21. Dias PEM, Miranda GE, Beaini TL and Melani RFH. Practical Application of Anatomy of the Oral Cavity in Forensic Facial Reconstruction. *PloS one*. 2016; 11: e0162732.
22. Guyomarc'h P, Dutailly B, Couture C and Coqueugniot H. Anatomical placement of the human eyeball in the orbit—validation using CT scans of living adults and prediction for facial approximation. *Journal of forensic sciences*. 2012; 57: 1271-5.

23. Guyomarc'h P and Stephan CN. The Validity of Ear Prediction Guidelines Used in Facial Approximation\*, †, ‡. *Journal of Forensic Sciences*. 2012; 57: 1427-41.
24. Kim S-R, Lee K-M, Cho J-H and Hwang H-S. Three-dimensional prediction of the human eyeball and canthi for craniofacial reconstruction using cone-beam computed tomography. *Forensic Science International*. 2016; 261: 164.e1-.e8.
25. Fedosyutkin BA and Nainys JV. The relationship of skull morphology to facial features. In: Iscan MY and Helmer RP, (eds.). *Forensic analysis of the skull - craniofacial analysis, reconstruction and identification*. New York: Wiley-Liss, 1993, p. 202,5,8.
26. Balueva T, Veselovskaya E and Kobylansky E. Craniofacial reconstruction by applying the ultrasound method in live human populations. *International Journal of Anthropology*. 2009; 24: 87-111.
27. Herrera LM, Strapasson RAP, Zanin AA, Silva JVL and Melani RFH. Comparison Among Manual Facial Approximations Conducted by Two Methodological Approaches of Face Prediction. *Journal of Forensic Sciences*. 2017; 62: 1279-85.
28. Bron A, Tripathi R and Tripathi B. *Wolff's anatomy of the eye and orbit, 8Ed*. Taylor & Francis, 1998.
29. Stephan CN, Haung AJR and Davidson PL. Further evidence on the anatomical placement of the human eyeball for facial approximation and craniofacial superimposition. *Journal of Forensic Sciences*. 2009; 54: 267-9.
30. Whitnall SE. *The anatomy of the human orbit and accessory organs of vision*. London: Oxford University Press, 1932.
31. Whitnall SE. *The anatomy of the human orbit and accessory organs of vision*. London: Oxford Medical Publications, 1921.
32. Goldnamer WW. *The anatomy of the human eye and orbit*. Professional Press, 1923.
33. Taylor KT. *Forensic art and illustration*. CRC Press, 2000.
34. Krogman W and Iscan M. *Human Skeleton in Forensic Medicine*. Illinois, USA: Thomas Publishers, 1986.
35. Gerasimov MM. *The reconstruction of the face from the basic structure of the skull*. Russia: Unknown, 1955.
36. Prokopec M and Ubelaker DH. *Reconstructing the shape of the nose according to the skull*. 2002.
37. George RM. The lateral craniographic method of facial reconstruction. *J Forensic sci*. 1987; 32: 1305-30.
38. Wilkinson C. *Forensic facial reconstruction*. Cambridge University Press, 2004.
39. Krogman WM. *The human skeleton in forensic medicine*. Springfield, IL: 1962.
40. Prag J and Neave R. Making faces: using forensic and archaeological evidence *London: British Museum, ISBN 0-7141-1743-9*. 1997.
41. Mala PZ and Veleminska J. Vertical Lip Position and Thickness in Facial Reconstruction: A Validation of Commonly Used Methods for Predicting the Position and Size of Lips. *Journal of Forensic Sciences*. 2016; 61: 1046-54.
42. Porter JP and Olson KL. Anthropometric facial analysis of the African American woman. *Archives of facial plastic surgery*. 2001; 3: 191-7.
43. Choe KS, Sclafani AP, Litner JA, Yu G-P and Romo T. The Korean American woman's face: anthropometric measurements and quantitative analysis of facial aesthetics. *Archives of facial plastic surgery*. 2004; 6: 244-52.
44. Arslan SG, Genç C, Odabaş B and Kama JD. Comparison of facial proportions and anthropometric norms among Turkish young adults with different face types. *Aesthetic plastic surgery*. 2008; 32: 234-42.
45. Ngeow W and Aljunid S. Craniofacial anthropometric norms of Malaysian Indians. *Indian journal of dental research*. 2009; 20: 313.
46. Briers N, Briers T, Becker PJ and Steyn M. Soft tissue thickness values for black and coloured South African children aged 6–13 years. *Forensic Science International*. 2015; 252: 188. e1-. e10.

47. Caldwell MC. The relationship of the details of the human face to the skull and its application in forensic anthropology. Arizona State University, 1981.
48. Ellis HD, Shepherd JW and Davies GM. Identification of familiar and unfamiliar faces from internal and external features: some implications for theories of face recognition. *Perception*. 1979; 8: 431-9.
49. O'Donnell C and Bruce V. Familiarisation with Faces Selectively Enhances Sensitivity to Changes Made to the Eyes. *Perception*. 2001; 30: 755-64.
50. Young AW, Hay DC, McWeeny KH, Flude BM and Ellis AW. Matching Familiar and Unfamiliar Faces on Internal and External Features. *Perception*. 1985; 14: 737-46.
51. Standring S. Gray's Anatomy: The Anatomical Basis of Clinical Practice. 40th edition ed.: Churchill Livingstone/Elsevier, 2008.
52. Clement JG and Ranson DL. *Craniofacial identification in forensic medicine*. Taylor & Francis, 1998.
53. Whitnall S. On a tubercle on the malar bone, and on the lateral attachments of the tarsal plates. *Journal of anatomy and physiology*. 1911; 45: 426.
54. Short LJ, Khambay B, Ayoub A, Erolin C, Rynn C and Wilkinson C. Validation of a computer modelled forensic facial reconstruction technique using CT data from live subjects: a pilot study. *Forensic Science International*. 2014; 237: 147. e1-. e8.
55. Angel J. Restoration of head and face for identification. *Proceedings of Meetings of American Academy of Forensic Science*. 1978.
56. İşcan MY and Steyn M. *The human skeleton in forensic medicine*. Charles C Thomas Publisher, 2013.
57. Moore KL, Dalley AF and Agur AMR. *Clinically Oriented Anatomy*. 5th ed.: Lippincott Williams & Wilkins, 2006.
58. Dunn KW and Harrison RK. Naming of parts: a presentation of facial surface anatomical terms. *British Journal of Plastic Surgery*. 1997; 50: 584-9.
59. Farkas L. *Anthropometry of the head & face*. 2nd ed. New York: Raven Press, 1994.
60. Gatliff BP. Facial sculpture on the skull for identification. *The American journal of forensic medicine and pathology*. 1984; 5: 327-32.
61. Kim S-R, Lee K-M, Cho J-H and Hwang H-S. Three-dimensional prediction of the human eyeball and canthi for craniofacial reconstruction using cone-beam computed tomography. *Forensic Science International*.
62. Bekerman I, Gottlieb P and Vaiman M. Variations in eyeball diameters of the healthy adults. *Journal of ophthalmology*. 2014; 2014.
63. Özer CM, Öz II, Serifoglu I, Büyükuysal MÇ and Barut Ç. Evaluation of Eyeball and Orbit in Relation to Gender and Age. *Journal of Craniofacial Surgery*. 2016; 27: e793-e800.
64. Broadbent T and Mathews V. Artistic relationships in surface anatomy of the face: application to reconstructive surgery. *Plastic and reconstructive surgery (1946)*. 1957; 20: 1-17.
65. Krogman W. The human skeleton in forensic medicine. I. *Postgraduate medicine*. 1955; 17: A-48; passim.
66. Haig ND. Exploring recognition with interchanged facial features. *Perception*. 1986; 15: 235-47.
67. Haig ND. The effect of feature displacement on face recognition. *Perception*. 1984; 42: 1158-65.
68. Wilkinson C. Facial reconstruction – anatomical art or artistic anatomy? *Journal of Anatomy*. 2010; 216: 235-50.
69. Kalcioğlu MT, Miman MC, Toplu Y, Yakinci C and Ozturan O. Anthropometric growth study of normal human auricle. *International journal of pediatric otorhinolaryngology*. 2003; 67: 1169-77.
70. Alexander KS, Stott DJ, Sivakumar B and Kang N. A morphometric study of the human ear. *Journal of Plastic, Reconstructive & Aesthetic Surgery*. 2011; 64: 41-7.
71. Asai Y, Yoshimura M, Nago N and Yamada T. Why do old men have big ears? Correlation of ear length with age in Japan. *BMJ: British Medical Journal*. 1996; 312: 582.

72. Bozkır MGI, Karakaş P, Yavuz M and Dere F. Morphometry of the External Ear in Our Adult Population. *Aesthetic Plastic Surgery : Official Journal of the International Society of Plastic Surgery*. 2006; 30: 81-5.
73. Evison M and Vorder Bruegge R. Computer-aided forensic facial comparison. Taylor and Francis Group, 2010.
74. Balueva T, Veselovskaya E and Rasskazova A. A comparison of the medieval and modern populations of the Novgorod region, based on facial reconstruction. *Archaeology, Ethnology and Anthropology of Eurasia*. 2010; 38: 135-44.
75. Heathcote JA. Why do old men have big ears? *BMJ*. 1995; 311: 1668.
76. Stephan CN. Craniofacial identifications: techniques of facial approximation and craniofacial superimposition. In: Blau S and Ubelaker DH, (eds.). *Handbook of forensic anthropology and archaeology*. California: Left Coast Press, 2009, p. 304-21.
77. Goldberg R, Relan A and Hoenig J. Relationship of the eye to the bony orbit, with clinical correlations. *Clinical & Experimental Ophthalmology*. 1999; 27: 398-403.
78. Drews LC. Exophthalmometry. *American journal of ophthalmology*. 1957; 43: 37-58.
79. Dunskey IL. Normative data for hertel exophthalmometry in a normal adult black population. *Optometry & Vision Science*. 1992; 69: 562-4.
80. Barretto RL and Mathog RH. Orbital measurement in black and white populations. *The Laryngoscope*. 1999; 109: 1051-4.
81. Stewart T. The points of attachment of the palpebral ligaments: their use in facial reconstructions on the skull. *Journal of Forensic Science*. 1983; 28: 858-63.
82. L'Abbé EN, Van Rooyen C, Nawrocki SP and Becker PJ. An evaluation of non-metric cranial traits used to estimate ancestry in a South African sample. *Forensic Science International*. 2011; 209: 195. e1-. e7.
83. Tobias PV. The biology of the southern African Negro. *The Bantu-speaking peoples of southern Africa*. 1974: 1-45.
84. De Villiers H. *The skull of the South African Negro: a biometrical and morphological study*. 1968.
85. Loth SR and Henneberg M. Mandibular ramus flexure: a new morphologic indicator of sexual dimorphism in the human skeleton. *American Journal of Physical Anthropology*. 1996; 99: 473-85.
86. Ribot I. Differentiation of modern sub-Saharan African populations: craniometric interpretations in relation to geography and history. *Bulletins et Mémoires de la Société d'Anthropologie de Paris*. 2004.
87. mediLexicon. Equator of Eyeball. *mediLexicon*. 2017.
88. Vuttiparum N and Benjakul C. Relationship between the width of maxillary central incisors and philtrum. *The Journal of the Dental Association of Thailand*. 1989; 39: 233-9.
89. Koo TK and Li MY. A guideline of selecting and reporting intraclass correlation coefficients for reliability research. *Journal of chiropractic medicine*. 2016; 15: 155-63.
90. Cardillo G. Fleiss' es kappa: compute the Fleiss' es kappa for multiple raters. 2007.
91. Roelofse MM, Steyn M and Becker PJ. Photo identification: Facial metrical and morphological features in South African males. *Forensic Science International*. 2008; 177: 168-75.
92. Ji Y, Qian Z, Dong Y, Zhou H and Fan X. Quantitative morphometry of the orbit in Chinese adults based on a three-dimensional reconstruction method. *Journal of Anatomy*. 2010; 217: 501-6.
93. Mala PZ. Pronasale Position: An Appraisal of Two Recently Proposed Methods for Predicting Nasal Projection in Facial Reconstruction. *Journal of Forensic Sciences*. 2013; 58: 957-63.
94. Subburaj K, Ravi B and Agarwal M. Automated identification of anatomical landmarks on 3D bone models reconstructed from CT scan images. *Computerized Medical Imaging and Graphics*. 2009; 33: 359-68.
95. Uysal T, Baysal A and Yagci A. Evaluation of speed, repeatability, and reproducibility of digital radiography with manual versus computer-assisted cephalometric analyses. *European Journal of Orthodontics*. 2009; 31: 523-8.

96. Liu X, Zhou C, Zhang G, Lin Y and Li S. CT anatomic measurement of the optic canal and its clinical significance. *Zhonghua er bi yan hou ke za zhi*. 2000; 35: 275-7.
97. Oettlé AC, Demeter FP and L'abbé EN. Ancestral Variations in the Shape and Size of the Zygoma. *The Anatomical Record*. 2017; 300: 196-208.
98. Sforza C, Grandi G, Catti F, Tommasi DG, Ugolini A and Ferrario VF. Age -and sex-related changes in the soft tissues of the orbital region. *Forensic Science International*. 2009; 185: 115. e1-. e8.
99. Baumgaertel S, Palomo JM, Palomo L and Hans MG. Reliability and accuracy of cone-beam computed tomography dental measurements. *American Journal of Orthodontics and Dentofacial Orthopedics*. 2009; 136: 19-25.
100. Machado GL. CBCT imaging – A boon to orthodontics. *The Saudi Dental Journal*. 2015; 27: 12-21.
101. Shah N, Bansal N and Logani A. Recent advances in imaging technologies in dentistry. *World Journal of Radiology*. 2014; 6: 794-807.
102. Claes P, Vandermeulen D, De Greef S, Willems G, Clement JG and Suetens P. Computerized craniofacial reconstruction: conceptual framework and review. *Forensic Science International*. 2010; 201: 138-45.
103. Hwang HS, Kim K, Moon DN, Kim JH and Wilkinson C. Reproducibility of Facial Soft Tissue Thicknesses for Craniofacial Reconstruction Using Cone-Beam CT Images. *Journal of forensic sciences*. 2012; 57: 443-8.
104. Hwang HS, Park MK, Lee WJ, Cho JH, Kim BK and Wilkinson CM. Facial soft tissue thickness database for craniofacial reconstruction in Korean adults. *Journal of forensic sciences*. 2012; 57: 1442-7.
105. Lee K-M, Lee W-J, Cho J-H and Hwang H-S. Three-dimensional prediction of the nose for facial reconstruction using cone-beam computed tomography. *Forensic Science International*. 2014; 236: 194. e1-. e5.
106. Masters MP. Relative size of the eye and orbit: An evolutionary and craniofacial constraint model for examining the etiology and disparate incidence of juvenile-onset myopia in humans. *Medical Hypotheses*. 2012; 78: 649-56.
107. George RM. The lateral craniographic method of facial reconstruction. *Journal of Forensic Science*. 1987; 32: 1305-30.
108. Schlager S. Soft-tissue reconstruction of the human nose: population differences and sexual dimorphism. Dissertation, Albert-Ludwigs-Universität Freiburg, 2013, 2013.
109. Meijerman L, Van Der Lugt C and Maat GJ. Cross-Sectional Anthropometric Study of the External Ear. *Journal of forensic sciences*. 2007; 52: 286-93.
110. Sforza C, Grandi G, Binelli M, Tommasi DG, Rosati R and Ferrario VF. Age -and sex-related changes in the normal human ear. *Forensic Science International*. 2009; 187: 110. e1-. e7.
111. Brucker MJ, Patel J and Sullivan PK. A morphometric study of the external ear: age -and sex-related differences. *Plastic and reconstructive surgery*. 2003; 112: 647-52; discussion 53-4.
112. Gualdi-Russo E. Longitudinal study of anthropometric changes with aging in an urban Italian population. *Homo*. 1998; 49: 241-59.
113. Faber J and Fonseca LM. How sample size influences research outcomes. *Dental Press J Orthod*. 2014; 19: 27-9.

APPENDIX A

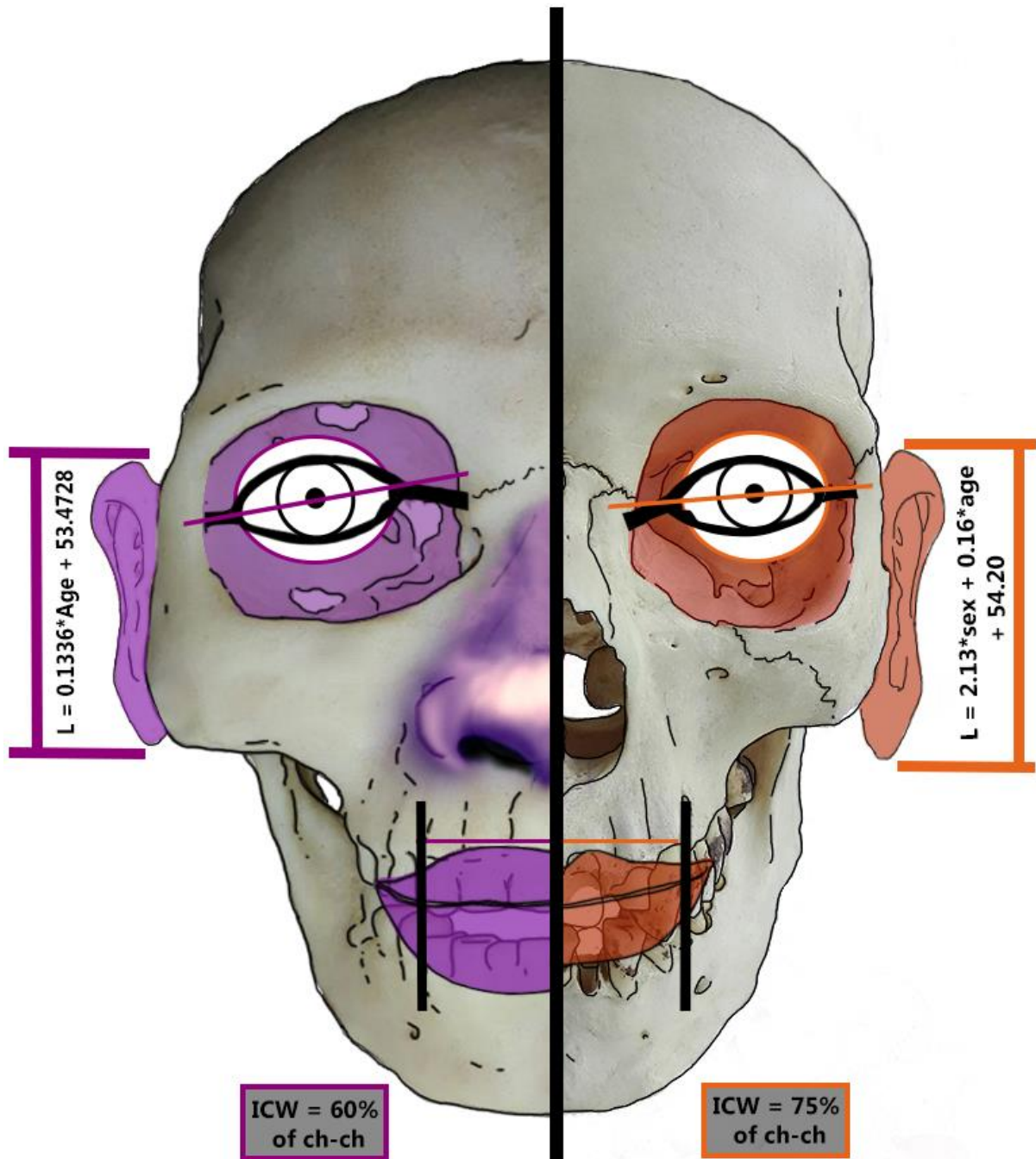


Figure 1. Integrated summary of findings (as discussed in conclusion)

## APPENDIX B

Table 1. Summary of variations in eyeball diameters in the literature

<i>Author(s)</i>	<i>Modality</i>	<i>N</i>	<i>Population</i>	<i>Antero-posterior diameter</i>	<i>SD</i>	<i>Medio-lateral diameter</i>	<i>SD</i>	<i>Supero-inferior diameter</i>	<i>SD</i>
<i>Wilkinson &amp; Mautner (2003)</i>	MRI	39	European	23.3	1.6	-	-	-	-
<i>Guyomarc'h et al. (2012)</i>	CT	375	French	23.7	-	24.3	-	24.6	-
<i>Bekerman et al. (2014)</i>	CT	500	Mixed ancestral groups	22.1 – 24.9		24.1 – 24.3		23.7 – 23.8	
<i>Özer et al. (2016)</i>	CT	198	Turkish	22.7 (F) 23.3 (M)	6.38 (F) 0.88 (M)	-	-	-	-
<i>This study</i>	Dissections	36	SA	-	-	25.2	1.42	23.6	1.29
<i>This study</i>	CT	30	SA	23.2	1.07	24.1	0.73	23.1	0.75
<i>This study</i>	CBCT	30	SA	25.1	0.56	25.4	0.38	24.1	0.64

Table 2. Mean mouth and inter-canine widths reported in the literature

Author	Population	Age range	M n	M ch-ch	M SD	ch-ch	M ICW	M SD	ICW	F n	F ch-ch	F SD	ch-ch	F ICW	F ICW SD
(Stephan and Murphy, 2008)*	European	62 – 94	6	55.1	4.4		40.8	0.8		3					
	South East Asian	-	12	54.2	5.6		41.2	1.5		15	51.2	3.5		40.8	1.9
(Stephan and Henneberg, 2003)*	European	-	17	55.0	3.2		41.2	1.5		44	51.4	3.3		38.3	1.7
	Other	-	4	52.5	4.4		38.4	3.2							
(Wilkinson et al., 2003)*	UK	20 – 60	64	48.8	3.7		-	-							
	Indian	20 – 60	32	49.0	4.1		-	-							
(Ferrario et al., 2000)	Italian	18 – 32	90	55.7	3.8		-	-		90	50.8	3.8		-	-
(Dias et al., 2016)	Brazilian	11 – 76	137	50.1	3.8		37.9	2.9		185	45.8	4.5		36.2	2.3
(Porter and Olson, 2001)*	African American	18 – 30	108	51.6	0.3		-	-							
	NA Caucasian	18 – 25	52	49.8	3.2		-	-		51	53.3	3.3		-	-
(Farkas, 1994)	German	18 – 25	60	51.6	3.2		-	-		60	48.7	2.7		-	-
	Czech	18 – 25	57	52.5	3.6		-	-		52	48.6	2.7		-	-
(Farkas et al., 2005)	NA Caucasian	18 – 30	<b>275</b>	53.3	-		-	-		<b>411</b>	49.8	-		-	-
	Azerbaijan	18 – 30	<b>30</b>	53.4	-		-	-		<b>30</b>	49.7	-		-	-
	Bulgarian	18 – 30	<b>30</b>	49.8	-		-	-		<b>30</b>	46.2	-		-	-
	Czech	18 – 30	<b>30</b>	53.8	-		-	-		<b>30</b>	50.2	-		-	-
	Croatian	18 – 30	<b>30</b>	50.5	-		-	-		<b>30</b>	46.9	-		-	-
	German	18 – 30	<b>30</b>	50.9	-		-	-		<b>30</b>	48.2	-		-	-
	Greek	18 – 30	<b>30</b>	51.8	-		-	-		-	50.3	-		-	-
	Hungarian	18 – 30	<b>30</b>	57.0	-		-	-		<b>30</b>	51.6	-		-	-
	Italian	18 – 30	<b>30</b>	50.8	-		-	-		-	47.7	-		-	-
	Polish	18 – 30	<b>30</b>	52.5	-		-	-		<b>30</b>	49.0	-		-	-
	Portuguese	18 – 30	<b>30</b>	50.0	-		-	-		<b>30</b>	45.3	-		-	-
	Russian	18 – 30	<b>30</b>	52.5	-		-	-		<b>30</b>	48.1	-		-	-
	Slovak	18 – 30	<b>30</b>	53.2	-		-	-		<b>30</b>	48.9	-		-	-
	Slovenian	18 – 30	<b>30</b>	53.0	-		-	-		<b>30</b>	49.2	-		-	-
	Iranian	18 – 30	<b>30</b>	50.3	-		-	-		<b>30</b>	45.0	-		-	-
	Turkish	18 – 30	<b>30</b>	53.0	-		-	-		<b>30</b>	47.6	-		-	-
	Egyptian	18 – 30	<b>30</b>	61.0	-		-	-		<b>30</b>	46.7	-		-	-
	Indian	18 – 30	<b>30</b>	51.0	-		-	-		<b>30</b>	46.5	-		-	-
	Singaporean Chinese	18 – 30	<b>30</b>	49.6	-		-	-		<b>30</b>	47.3	-		-	-
	Vietnamese	18 – 30	<b>30</b>	47.5	-		-	-		<b>30</b>	48.5	-		-	-
	Thai	18 – 30	<b>30</b>	50.3	-		-	-		<b>30</b>	45.4	-		-	-
	Japanese	18 – 30	<b>30</b>	48.4	-		-	-		<b>30</b>	46.5	-		-	-
	Angolan	18 – 30	<b>30</b>	54.4	-		-	-		<b>30</b>	52.9	-		-	-
	Tonga	18 – 30	<b>30</b>	53.2	-		-	-		-	-	-		-	-
	Zulu	18 – 30	<b>30</b>	56.2	-		-	-		<b>30</b>	52.2	-		-	-
	Afro-American	18 – 30	<b>30</b>	54.6	-		-	-		<b>30</b>	53.6	-		-	-
This study*	SA Africans	22 - 73	<b>36</b>	67.3	5.9		40.9	2.6							

\* Studies where samples were pooled: results for both males and females reported under males

n = sample size  
M = male  
F = female

ICW = inter-canine width  
SD = standard deviation  
ch-ch = mouth width

Table 3. Mean adult ear heights (mm) published in the literature. Where sides were not combined, information on the left has been reported

<i>Author</i>	<i>Population</i>	<i>Ages</i>	<i>Male sample</i>	<i>Male ear length (height)</i>	<i>SD</i>	<i>Female sample</i>	<i>Female ear length (height)</i>	<i>SD</i>
<i>(Kalcioğlu et al., 2003)</i>	Turkish	-	± 30*	64.5	-	± 30*	60.3	-
<i>(Porter and Olson, 2001)</i>	African American	18 – 30	-	-	-	108	57.4	0.39
	North American Whites	18 – 25	52	62.4	3.7	51	<b>59.0</b>	3.6
<i>(Farkas, 1994)</i>	Chinese	18 – 25	30	60.7	3.8	30	57.6	3.9
	African American	18 – 25	50	59.8	4.0	50	57.0	3.3
	Indian	15 – 29	10	68.9	3.9	14	60.9	3.7
<i>(Alexander et al., 2011)</i>	Caucasian	15 – 29	36	65.2	4.2	32	60.4	3.2
	African/Afro-Caribbean	15 – 29	10	62.7	2.8	5	60.4	2.1
<i>(Bozkır et al., 2006)</i>	Turkish	18 – 25	191	63.1	3.6	150	59.7	3.0
<i>(Asai et al., 1996)</i>	Japanese	21 – 94	400*	70.1	-	400*	70.1	-
<i>(Sforza et al., 2009)</i>	Italian	18 – 30	126	62.19	4.08	66	56.36	4.05
<i>(Meijerman et al., 2007)</i>	Dutch	20 – 90	1823	71.0	5.5	863	64.0	5.4
<i>(Farkas et al., 2005)</i>	North American Whites	18 – 30	275	62.4	-	411	58.5	-
	Azerbaijan	18 – 30	30	65.6	-	30	62.1	-
	Bulgarian	18 – 30	30	64.4	-	30	59.0	-
	Czech	18 – 30	30	64.3	-	30	61.7	-
	Croatian	18 – 30	30	63.6	-	30	59.1	-
	German	18 – 30	30	63.1	-	30	58.4	-
	Hungarian	18 – 30	30	63.9	-	30	60.2	-
	Polish	18 – 30	30	63.3	-	30	58.6	-
	Portuguese	18 – 30	30	60.9	-	30	55.4	-
	Russian	18 – 30	30	63.1	-	30	59.2	-
	Slovak	18 – 30	30	63.9	-	30	59.3	-
	Slovenian	18 – 30	30	63.3	-	30	59.6	-
	Iranian	18 – 30	30	61.2	-	30	59.0	-
	Turkish	18 – 30	30	64.8	-	30	60.0	-
	Egyptian	18 – 30	30	61.0	-	30	57.8	-
	Indian	18 – 30	30	61.1	-	30	57.1	-
	Singaporean Chinese	18 – 30	30	60.7	-	30	57.6	-
	Vietnamese	18 – 30	30	59.9	-	30	59.8	-
	Thai	18 – 30	30	62.4	-	30	60.3	-
	Japanese	18 – 30	30	65.6	-	30	61.9	-
	Angolan	18 – 30	30	57.5	-	30	55.0	-
	Tonga	18 – 30	30	55.8	-	-	-	-
	Zulu	18 – 30	30	57.8	-	30	56.2	-
	Afro-American	18 – 30	30	59.8	-	30	57.0	-
<i>This study</i>	SA Africans	22 – 73	38	60.58	5.24	11	57.24	4.68

\* Male and female samples pooled, no separate sample size indicated

## APPENDIX C

### Facial approximations: Characteristics of the Eye in a South African Sample

#### Abstract

Although guidelines for facial approximations, including those for the eye, are in use in South Africa, limited data on African populations exist to confirm its validity. As precise placement of the eyes in facial approximations is of importance for facial recognition, this study tested established guidelines by measuring specific instrumental dimensions. Forty-nine cadavers from the Sefako Makgatho Health Sciences University and the University of Pretoria were dissected to determine the position of the canthi and the size and position of the eyeball in the orbit. Thirty cone beam computer tomography scans and 30 computer tomography scans from the Oral and Dental and Steve Biko Hospitals respectively were used to determine the size of the eyeball. Results from this study were compared to the published guidelines. The most prominent discrepancies included a more rectangular shape of the orbit, an oval shaped eyeball and a different position of the canthi. In African faces, the medial canthus was found to be located higher than the lateral canthus. The distance between the endocanthion and superior orbital margin was 17.7 mm and the exocanthion and superior orbital margin 19.5 mm. Inter-population differences may have an effect on facial approximations and its accuracy as is often demonstrated in practice. The findings of this study should be taken into consideration when designing population specific guidelines for reconstruction of the eye in South Africans of African ancestry.

#### Key words:

Facial approximations, Canthi, Eyeball, Orbit.

#### Highlights:

- Dimensions of the eye and orbit in South Africans varies from published guidelines
- A more rectangular orbit results in a more transversely elongated eyeball
- The eyeball is located supero-laterally within the orbit (Leq-LOM = 4.2 mm vs Meq-MOM = 8.4 mm and Seq-SOM = 3.4 mm vs leq-IOM = 6.1 mm)
- The exocanthion is situated lower than the endocanthion (ex-SOM = 19.5 mm vs en-SOM = 17.7 mm)

## Introduction

Identification of unknown individuals is a challenge in the South African context. In cases where there is a strong suspicion regarding the identity of the unknown individual and a close relative is available, methods such as DNA comparison and dental record comparison are useful. However, because of socio-economic and other reasons in the South African context, unidentified individuals without known relationships are commonplace [1]. In these cases, it is not possible to identify unknown individuals with primary identifiers and therefore forensic facial reconstruction/approximation is often used to obtain information on a case [1, 2].

The facial reconstruction/approximation process always begins with the placement of the eyes. Facial recognition (especially of familiar individuals) is dependent on the morphology of the orbital area [3-7], therefore it is important to be precise and correct in placing the eyes [8] and associated features. The eyes are to be positioned supero-laterally in the orbit according to guidelines established by expert studies [9-11]. Although conflicting findings on the position of the eyes have been reported, several studies [8, 10-12] provide strong evidence of a more superior and lateral placement of the eyeball in the orbit. Specific distances of this position have been established for some populations [12], but it is uncertain how applicable these absolute values are in the South African context.

Variations in the position of the endocanthion and exocanthion are also reported in the literature. Although all researchers did not use directly comparable landmarks to define the position of the endocanthion and the exocanthion, the general trend indicates that the endocanthion is positioned lower than the exocanthion [8, 13]. A study by Stewart [14], however, found the endocanthion and exocanthion to be on the same level. It would therefore be of value to determine the position of these landmarks in South African groups.

Similarly, variations have been reported in the dimensions of the eyeball. Although the eyeball is often considered as almost spherical [15], slight elongation in certain axes has been reported in the literature [15, 16]. The medio-lateral axis was found to often be longer than the supero-inferior axis [16].

In South Africa, guidelines created for and based on other populations are often applied in facial approximations (Capt. T.M. Briers, personal communication, 2014). However, these guidelines may not necessarily be applicable in the South African context as a degree of inter-

population variation exists in facial features. It is postulated that these inter-population differences may have an effect on facial approximations and its accuracy, as is often demonstrated in practice. The less accurate a facial representation, the smaller the likelihood of an unknown individual being recognised and identified.

The purpose of this study was to assess specific features related to the eye in South Africans and compare it to established guidelines commonly used in the facial approximation process. The features assessed included the position of the eyeball within the orbit, the size of the eyeball and the position of the canthi.

## Materials & Methods

A total of 49 adult cadavers (38 males and 11 females, age range 22 – 73 years, mean age 47 years) from the dissection halls of two South African universities, namely Sefako Makgatho Health Sciences University (SMU) and the University of Pretoria (UP), were used in this study. Bodies at UP generally had their origins from local hospitals in Pretoria [1], while those at SMU originated from a wider area of the Gauteng Province and some areas in the North West Province. Samples demonstrating damage, distortion, or any effects of desiccation due to embalming were excluded.

A total of 30 computer tomography (CT) scans (23 males, 7 females, age range 21 – 84 years, mean age 42 years) from Steve Biko Academic Hospital affiliated with UP and 30 cone beam computer tomography (CBCT) scans (17 males and 13 females, age range 18 – 64 years, mean age 33) from the Oral and Dental Hospital, UP, were also used for measurement and analyses. These hospitals service the greater Gauteng area, as well as parts of the Limpopo and North West provinces. Patients' heads were orientated in the standard natural head position for scanning – supine in the case of CT and sitting in the case of CBCT. The CT scans slices taken by a Siemens SOMATOM Sensation 64 scanner were 2 mm thick. CBCT scans were obtained using a Planmeca ProMax 3D scanner with a voxel size of 0.4 mm. Scans were retrospectively analysed and excluded if not orientated in the desired plane, the implicated structures could not be clearly identified or injury to the orbital area was present. All cadavers and scans were of South Africans of African ancestry (hereafter referred to as South Africans (SA)).

Ethics clearance was obtained from the Main Ethics and Research Committee, Faculty of Health Science, University of Pretoria (Cadaver sample: 8/2016; Scan sample: 183/2016) prior

to commencement of this study. The Faculty of Health Sciences Research Ethics Committee complies with the SA National Act no. 61 of 2003 as it pertains to health research.

The orbital regions of 49 cadavers were dissected and measured to determine the position of the canthi, the position of the eyeball in the orbit and the diameters of the eyeball. A non-parametric Wilcoxon Rank Sum test (2-sided) was used to investigate whether differences occurred between sexes. As the p values for all individual measurements were non-significant ( $p > 0.05$ ), male and female samples were pooled for the remainder of the analyses.

The position of the canthi was determined on cadavers by pinning the Frankfort Horizontal Plane (FHP) from porion to orbitale and marking a reference plane parallel to the FHP and tangent to the most superior point on the superior orbital margin (SOM). This is similar to the methodology followed by Stephan & Davidson [8] and Stephan et al.[12]. The endo -and exocanthion were identified and pinned and four distances were measured namely (1) between the endocanthion and medial orbital margin (MOM), (2) between the endocanthion and SOM, (3) between the exocanthion and lateral orbital margin (LOM) and (4) between the exocanthion and SOM (Fig. 1a).

To determine the position of the eyeball in the orbit of each cadaver, a circular cut was made approximately 5 mm outside of the orbital margin. The skin and orbicularis oculi muscle were removed, and the entire eyeball exposed by careful blunt dissection and removal of peri-orbital fat and tissue. Pins were placed perpendicular to the surface of the bone at the most extreme points on the LOM, MOM, IOM and SOM. Another set of four pins were placed at the shortest distances respectively from the LOM, MOM, IOM and SOM on the equator of the eyeball (an imaginary line encircling the globe of the eye equidistant from the anterior and posterior poles) [17]. Four distances were measured between the pins, namely (1) inferior equator to IOM, (2) superior equator to SOM, (3) lateral equator to LOM and (4) medial equator to MOM (Fig. 1b).

Two measurements were taken on the cadavers to determine the diameters of the eyeball, namely (1) medio-lateral diameter (distance between pins at medial and lateral equators) and (2) supero-inferior diameter (distance between pins at superior and inferior equators) (Fig. 1c). Individual measurements (as shown in Fig. 1 b and c) were used to obtain the horizontal and vertical diameters of the orbit. For the horizontal diameter, the distances considered

were the distance between the medial equator of the eye and the MOM (Fig. 1b (4)); the medio-lateral diameter of the eye (Fig. 1c (1)); and the distance between the lateral equator of the eye and the LOM (Fig. 1b (3)). To obtain the vertical diameter of the orbit, the distances added together were the distance between the superior equator of the eye and the SOM (Fig. 1b (2)); the supero-inferior diameter of the eye (Fig. 1c (2)); and the distance between the inferior equator of the eye and the IOM (Fig. 1b (1))

CBCCT and CT scans were imported into MevisLab as DICOM (.dcm) files for measurements regarding the diameter of the eyeball. ExaminerViewer was used to visualise the 3D reconstruction of the files to ensure the correct voxel size and reconstruction. ROI Select was used to select a specific region of interest, enlarging the relevant areas, in this case the orbital area (Fig. 2). OrthoView2D was then used to visualise the region of interest and identify two points corresponding in all three planes (coronal, sagittal and transverse). The relevant points to determine the diameter of the eyeball were the most inferior, superior, medial, lateral, anterior and posterior points on the equator of the eyeball. Lastly, XMarkerListMaxDistance was used to measure the distance between the identified points. Scans were orientated, points identified and measurements taken on a multiplanar level as the relevant landmarks and distances were not necessarily visible on a single plane simultaneously. The points, however, retained their respective three-dimensional (3D) positions regardless of scrolling through the slices. The dimensions reflecting the size and shape of the eyeball included the antero-posterior diameter (Fig. 3a), the medio-lateral diameter (Fig. 3b) and the supero-inferior diameter (Fig. 3c). Although visualisation of the eyeball on the 2D figure is not that clear, by scrolling up and down on the 3D image, the borders of the eyeball could be more readily identified thus enabling measurements. Non-parametric Wilcoxon Rank Sum tests (2-sided) once again determined non-significant variations ( $p > 0.05$ ) between male and female, thus samples were pooled.

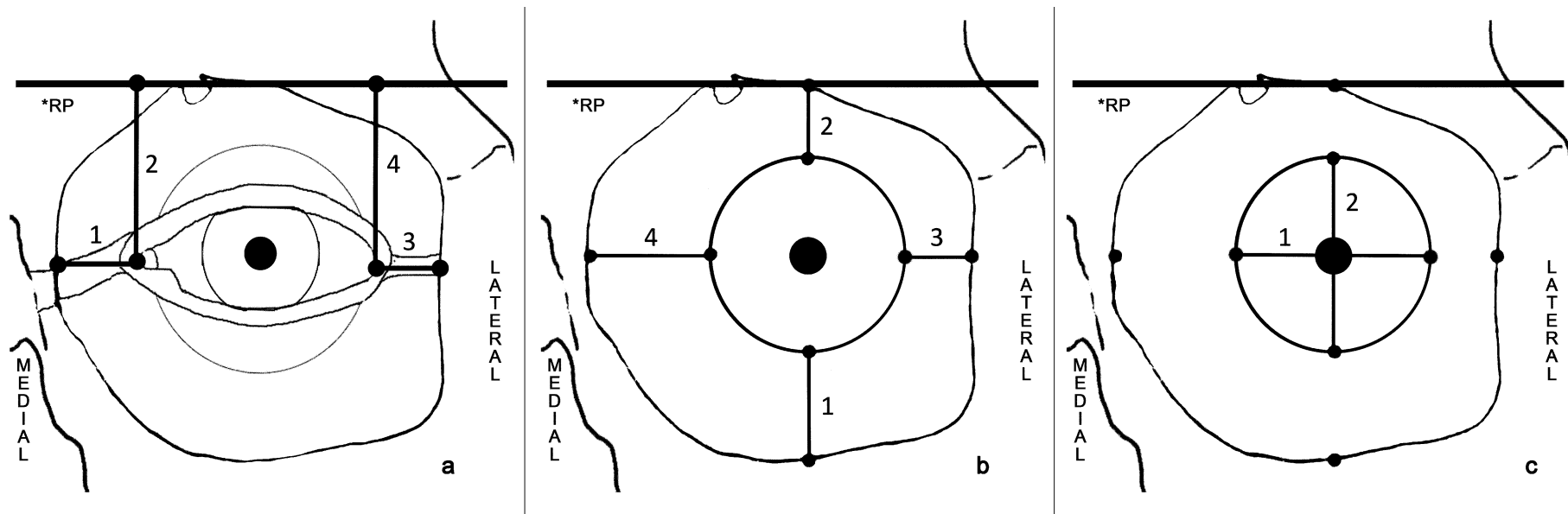


FIG. 1: *Orbital and optic measurements. \*RP: Reference plane parallel to FHP*

*a) Position of the canthi:*

- 1: distance between the medial canthus and MOM*
- 2: distance between the medial canthus and SOM reference plane*
- 3: distance between the lateral canthus and LOM*
- 4: distance between the lateral canthus and the SOM reference plane*

*b) Position of the eyeball in the orbit*

- 1: distance between the inferior equator and the IOM*
- 2: distance between the superior equator and SOM*
- 3: distance between the lateral equator and LOM*
- 4: distance between the medial equator and MOM*

*c) Size of the eyeball*

- 1: medio-lateral diameter distance from the medial equator to the lateral equator*
- 2: supero-inferior diameter (distance from the superior to inferior equator)*

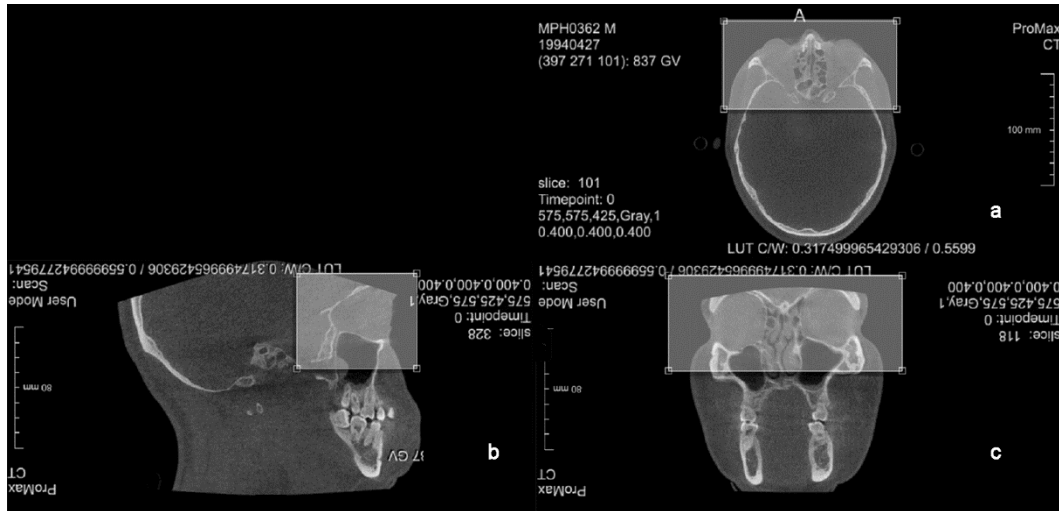


FIG. 2: Selecting the region of interest on MevisLab.  
 a) Transvers plane; b) Sagittal plane and c) Coronal plane

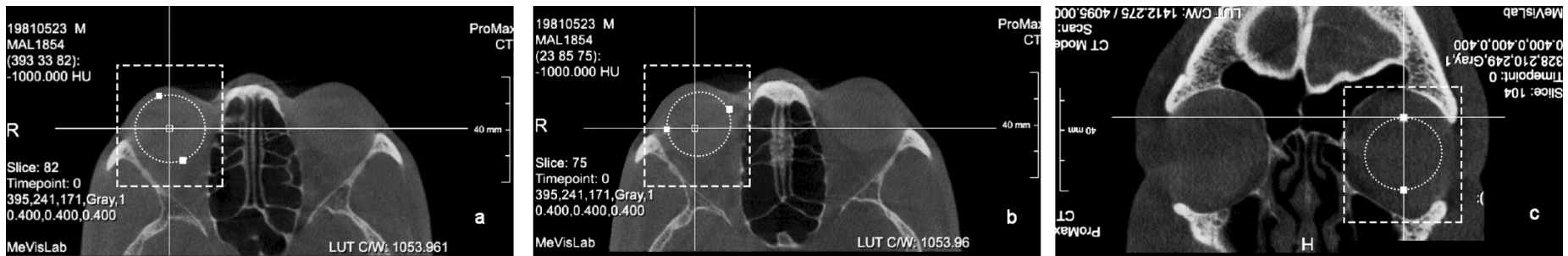


FIG. 3: Measuring the diameters of the eyeball between white squares.  
 a) Antero-posterior diameter; b) Medio-lateral diameter; c) Supero-inferior diameter

The data were tested for variations between the sexes by means of a non-parametric Wilcoxon Rank Sum test (2-sided). Male and female samples were pooled together as there were no statistical differences between the sexes (except CBCT Meq-Leq where  $p < 0.05$ ).

Comparisons were conducted between the measurements of the eyeball for all three modalities (dissection, CT and CBCT) utilising the Kruskal-Wallis test. The Kruskal-Wallis test is a non-parametric version of the classical one-way ANOVA, and an extension of the Wilcoxon Rank Sum test to more than two groups. Further comparisons on the medio-lateral and supero-inferior diameters were done between two modalities at a time by means of the non-parametric Wilcoxon Rank Sum test, i.e. CT vs CBCT; CT vs dissection and dissections vs CBCT.

Intra-observer repeatability was assured for all measurements by obtaining three measurements for each dimension and calculating the standard deviations (Table 1). As the average standard deviations were very small (between 0.01 and 0.30), the average of the three measurements were used for further statistical analyses. Inter-observer repeatability testing was performed by obtaining measurements from one other observer. A total of 38 cadavers as well as all CT and CBCT scans were re-measured for all parameters. Interclass Correlation Coefficient A-1 (ICC) testing was done to compare measurements obtained by the two different observers.

## Results

The results for all observational errors (or standard deviations) calculated are summarised in Table 1. All average standard deviations were below 0.2, with some as low as 0.01. The accuracy of the measurements, when repeated by the same researcher, was considered higher the closer the standard deviation average was to zero. Therefore, due to such small standard deviations, the average measurement for each parameter was used for all further statistical analyses.

Descriptive statistics of the dimensions describing specific features of the eye including the position of the canthi, the position of the eyeball and the size of the eyeball were calculated and are summarised in Figures 4, 5 and 6 respectively.

Regarding the position of the canthi (Fig. 4), the endocanthion was found to be located higher and closer to the orbital margin than the exocanthion. Distances between ex-SOM (4) were

found to be greater than the en-SOM (2) ( $p < 0.01$ ), indicating that the exocanthion is located lower than the endocanthion in relation to the SOM reference plane.

From Fig. 5 it can be noted that the eyeball is positioned supero-laterally within the orbit. A statistically significant difference between the distances of the Seq-SOM and leq-IOM ( $p < 0.01$ ) and the Meq-MOM and Leq-LOM ( $p < 0.01$ ) was found. Fig. 5 illustrates that the distances between Seq-SOM (2) and Leq-LOM (3) were smaller than the distances between leq-IOM (1) and Meq-MOM (4), indicating that the eyeball is located more supero-laterally within the orbit. The dimensions of the eyeball with all modalities demonstrated a transverse elongation. The diameter of the eyeball (Fig. 6) as measured on cadavers (1), indicated that the medio-lateral diameter was statistically significantly greater than the supero-inferior diameter ( $p < 0.01$ ). Similar results were found with CT (2) ( $p < 0.01$ ) and CBCT (3) ( $p < 0.01$ ) scans.

**Table 1 Observation errors calculated for all orbital and ocular measurements.**

<b>SD</b>	<b>Position of the Canthi (Cadavers)</b>				<b>Position of the Eyeball (Cadavers)</b>				<b>Eyeball diameters (CBCT)</b>			<b>Eyeball diameters (CT)</b>				
	<i>en-MOM</i>	<i>en-SOM</i>	<i>ex-LOM</i>	<i>ex-SOM</i>	<i>Meq-MOM</i>	<i>Leq-LOM</i>	<i>Seq-SOM</i>	<i>IOM</i>	<i>Meq-Leq</i>	<i>Seq-Ieq</i>	<i>Meq-Leq</i>	<i>Seq-Ieq</i>	<i>Aeq-Peq</i>	<i>Meq-Leq</i>	<i>Seq-Ieq</i>	<i>Aeq-Peq</i>
<b>MAX</b>	0.06	0.06	0.05	0.09	0.05	0.05	0.06	0.05	0.05	0.06	0.36	0.33	0.44	0.46	0.39	0.34
<b>MIN</b>	0.00	0.00	0.01	0.01	0.00	0.00	0.01	0.00	0.00	0.00	0.03	0.00	0.01	0.00	0.00	0.00
<b>AVE</b>	0.01	0.02	0.02	0.02	0.01	0.01	0.01	0.01	0.01	0.02	0.17	0.15	0.15	0.14	0.11	0.13

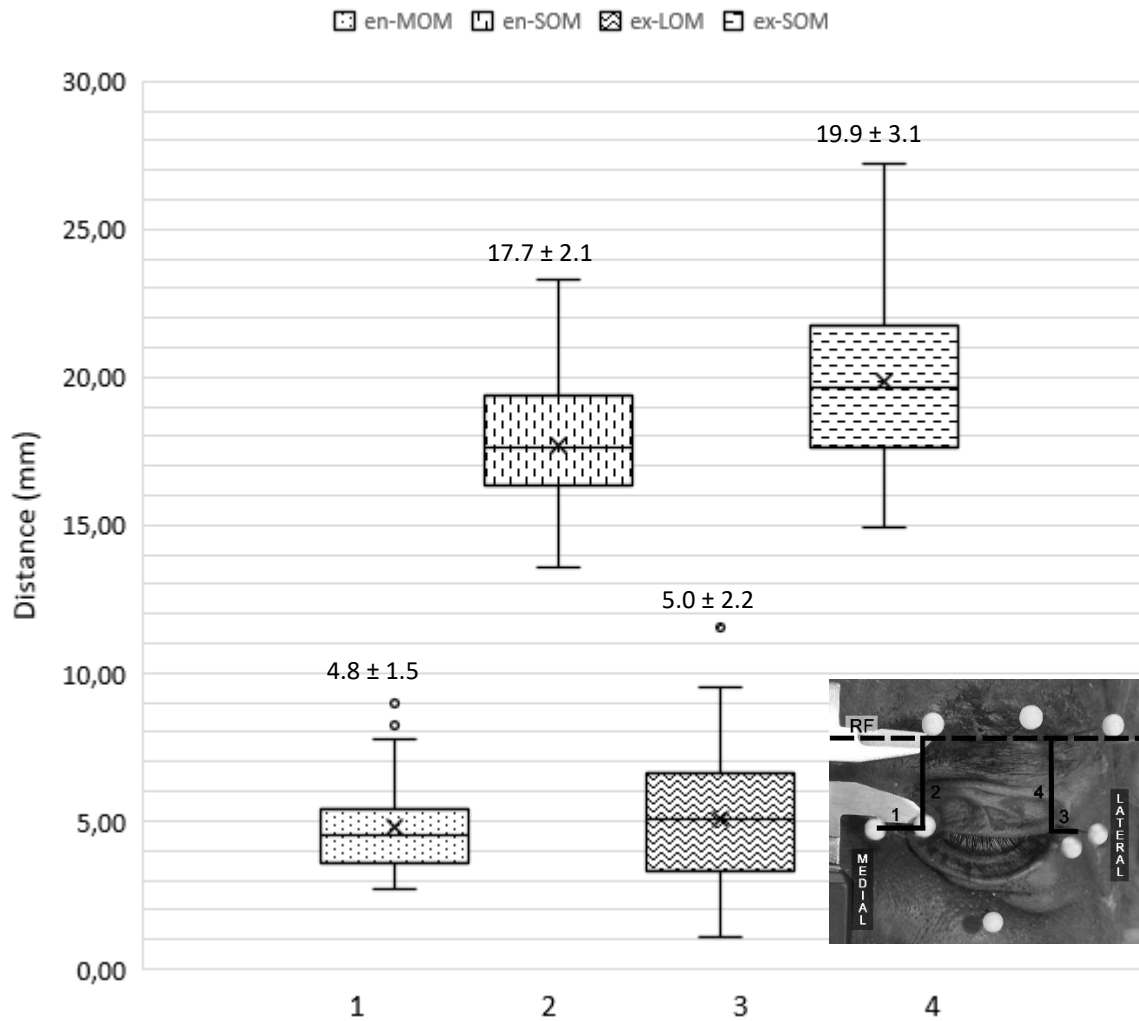


FIG. 4: Basic descriptive statistics for the measurements pertaining to the position of the canthi. (1) Distance between endocanthion and MOM, (2) distance between endocanthion and SOM, (3) distance between exocanthion and LOM and (4) distances between exocanthion and SOM

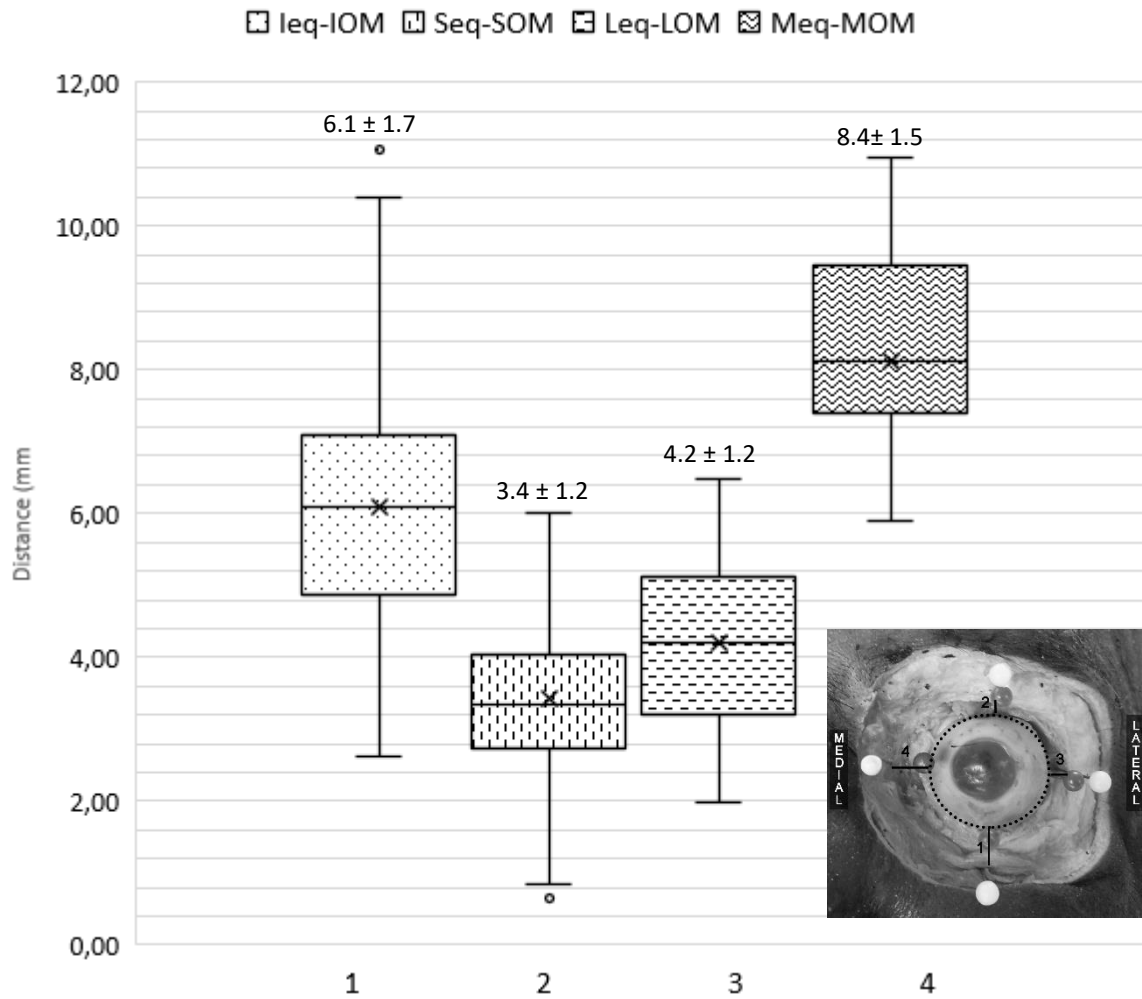


FIG 5: Basic descriptive statistics for measurements pertaining to the position of the eyeball in the orbit in dissections. (1) Distances between the inferior equator and the IOM, (2) distances between the superior equator and the SOM, (3) distances between the lateral equator and the LOM and (4) distances between the medial equator and the MOM

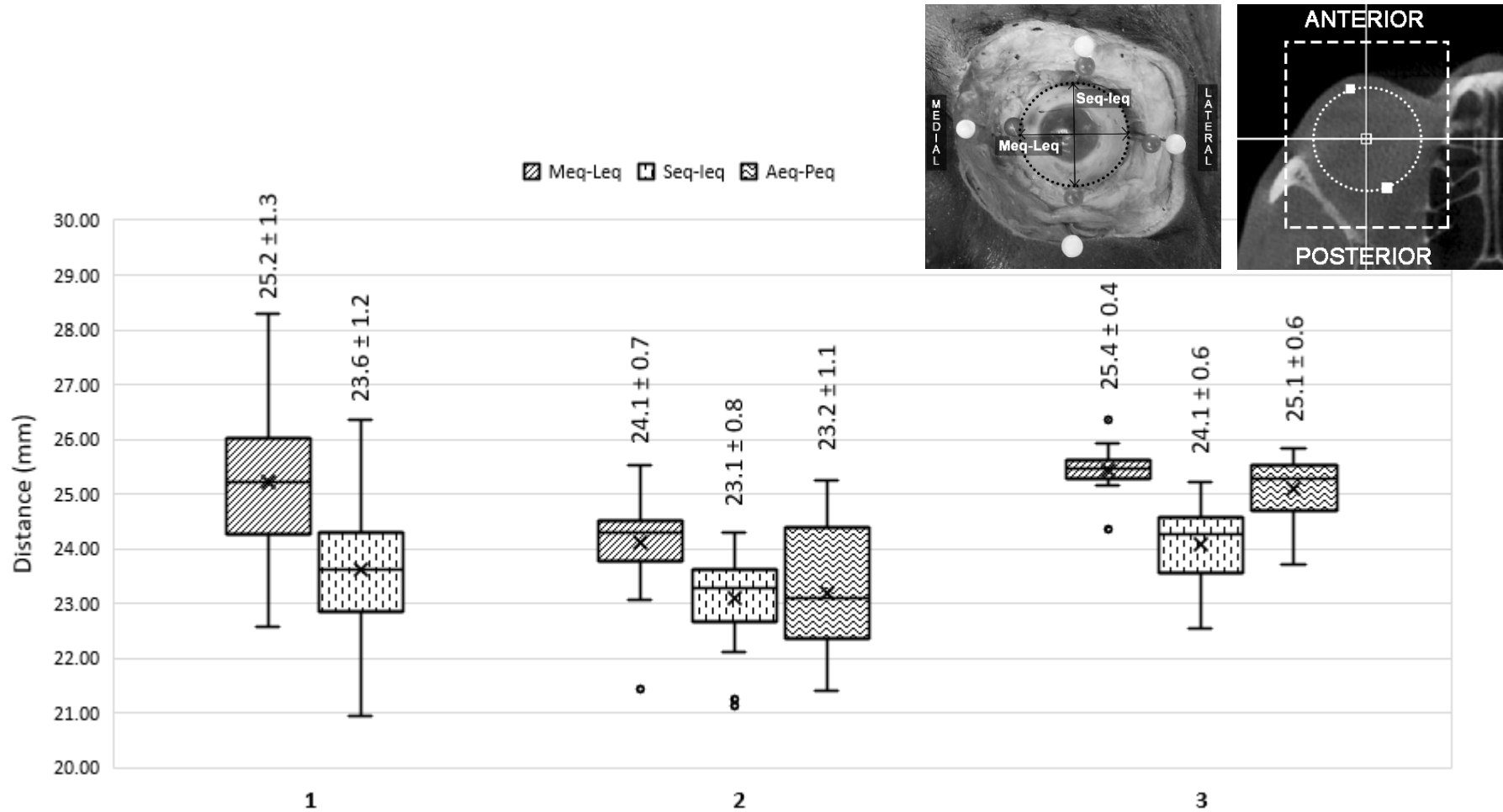


FIG. 6 Basic descriptive statistics for measurements pertaining to the size of the eyeball in all three modalities: (1) Dissections, (2) CT scans and (3) CBCT scans.

Kruskal-Wallis test (dissections vs CT vs CBCT) for medio-lateral diameter  $p$ -value  $< 0.01$

Kruskal-Wallis test (dissections vs CT vs CBCT) for supero-inferior diameter  $p$ -value  $< 0.01$

Wilcoxon Rank Sum test (CT vs CBCT) for antero-posterior diameter  $p$ -value  $< 0.01$

Calculations show that the width of the orbit is consistently greater than the height of the orbit, ( $p < 0.01$ ) indicating a more rectangular shaped orbit. The shape of the eyeball thus reflects the shape of the orbits.

#### *Statistical comparisons between modalities*

Comparisons between two modalities were performed by utilising a Wilcoxon Rank Sum test for each of the three diameters (medio-lateral, supero-inferior and antero-posterior) of the eyeball. Box-and-whisker plots illustrate the variations in measurements obtained by using the different modalities (Fig. 6).

The dissection and CBCT measurements of the medio-lateral and supero-inferior dimensions of the eyeball showed a greater agreement than did CT measurements vs. CBCT measurements. This is demonstrated in the non-statistically significant differences demonstrated in the CBCT vs dissection derived means ( $p = 0.39$ ), while the variation between CT vs dissection measurements concerning the medio-lateral diameter was statistically significant ( $p < 0.01$ ) and so was CBCT vs CT ( $p < 0.01$ ). When considering the supero-inferior diameter, a statistically significant difference existed when comparing CBCT and CT ( $p < 0.01$ ); however, this difference was less significant when comparing CBCT to cadaver measurements ( $p = 0.02$ ). The variation in the supero-inferior diameters when comparing CT to dissection measurements was not statistically significant ( $p = 0.05$ ). CBCT data had the highest mean values, followed by the dissection data and then the CT data. Dissection data, however, had the greatest range, followed by CT data and lastly CBCT data. When comparing CBCT to CT measurements for the antero-posterior diameter, a statistically significant difference was observed ( $p < 0.01$ ).

Table 2 summarises the descriptive relationships for measurements performed on dissections, CBCT and CT scans. From the relationship between measurements, it can be seen that the distance from the exocanthion to SOM was greater than the distance from the endocanthion to the SOM, indicating that the exocanthion was on average located lower than the endocanthion. The width of the orbit was greater than the height, indicating that the orbit was more rectangular shaped. It can also be seen that the distance of the medial equator to

the MOM and the distance of the inferior equator to the IOM was greater than the distance between the lateral equator to LOM and superior equator to SOM, demonstrating a more supero-laterally positioned eyeball. The medio-lateral diameter was also greater than the supero-inferior diameter, indicating that the eyeball is elongated or oval shaped in the transverse axis.

ICC tests for cadaver measurements performed consistently, with excellent agreement (ICC > 0.90; not considered due to chance) between observers for ex-SOM, Meq-MOM, Leq-LOM, leq-IOM, and Leq-Meq. Good agreement that was not considered due to chance (ICC > 0.85) was found between observers for en-SOM, Seq-SOM, Seq-leq, however the ex-LOM showed moderate agreement (ICC = 0.68) due to chance and the en-MOM dimension displayed poor inter-observer repeatability (ICC = 0.04). Inter-observer repeatability tests for all CT and CBCT scan measurements were reported as less than 0.21.

**Table 2 Descriptive relationships between measurements**

Measurements compared	Description	Result	Dissections (Wilcoxon Rank Sum Test)		CBCT (Signed Rank Test)		CT (Signed Rank Test)	
			Ratio	p-value	Ratio	p-value	Ratio	p-value
<b>en-SOM vs ex-SOM</b>	<b>Vertical position of the canthi</b>	ex-SOM > en-SOM	1.12	< 0.01				
<b>Width of orbit vs Height of orbit</b>	<b>Orbital shape</b>	Width > Height	1.14	< 0.01				
<b>Meq – MOM vs Leq – LOM</b>	<b>Horizontal position of eyeball in the orbit</b>	Meq – MOM > Leq – LOM	1.98	< 0.01				
<b>Seq – SOM vs leq – IOM</b>	<b>Vertical position of eyeball in the orbit</b>	leq – IOM > Seq – SOM	1.79	< 0.01				
<b>Medial – Lateral equators vs Superior – Inferior equators</b>	<b>Shape of eyeball</b>	Meq-Leq > Seq-leq	1.07	<0.01	1.05	< 0.01	1.04	< 0.01

## Discussion and conclusions

In this study, specific dimensions (absolute measurements and relationships between measurements) of the eye and orbit in South Africans were determined. Figure 7 summarises the findings recorded in the literature and mean dimensions observed in this study. Integration of the measurements obtained from the three modalities used (cadaver dissections, CT and CBCT) demonstrates that the exocanthion was positioned lower than the endocanthion, the orbit was rectangular-shaped and the oval shaped eyeball was situated in the superolateral aspect of the orbit. Findings regarding the shape of the orbit were in agreement with Krogman (1955) and others stating that the orbits of skulls of Africans are more rectangular than those from other populations.

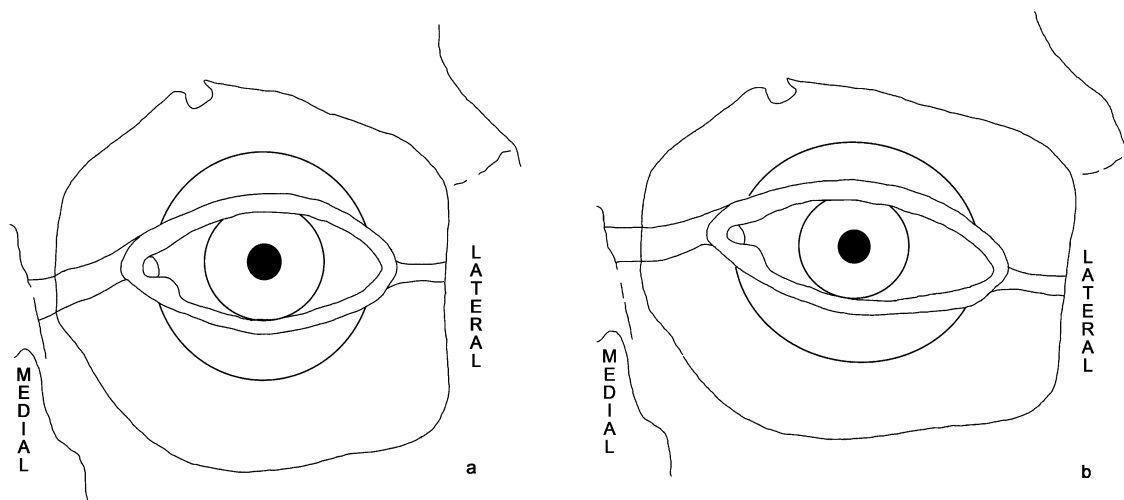


FIG 7. *Graphic illustration of a) the expected findings and b) the mean dimensions of this study sample*

While most of the cadaver measurements had good inter-observer repeatability, the en-MOM dimension displayed poorly (ICC = 0.04). This observation might be explained by the exact placement of the MOM that is not clearly defined. Unlike the lateral orbital margin, the MOM is less well defined, rounded and irregular. Inter-observer repeatability tests on CBCT and CT scan measurements had a similar performance but were less well than expected (All ICC < 0.21) as compared to intra-observer tests. Mean values of most measurements, however, differed with less than 2 mm in general, which may be considered acceptable [18]

Variations in the exact position of the endocanthion and exocanthion are reported in the literature. In most research done previously, the endocanthion was reported to be situated lower than the exocanthion. According to Stephan and Davidson [8], the endocanthion in an Australian population lies approximately 19.5 mm below the SOM reference plane and the exocanthion 18.5 mm below the SOM reference plane, while Kim et al. [13] reported that in their sample of Korean individuals, the endocanthion lies 22.8 mm and the exocanthion 20.2 mm respectively below the SOM. However, in the current study, the opposite was true: the endocanthion was positioned 17.7 mm below the SOM reference plane and the exocanthion 19.5 mm. It is reasonable to postulate that the differences in distances observed in this population may be related to the population specific variation in the morphology of the zygomatic bone as well as the zygomatic processes of the frontal and maxillary bones contributing to the margins of the orbit resulting in variations in the shape of the orbital border [19].

Reports regarding the distance of the exocanthion from the lateral orbital margin are remarkably similar at 4.5 mm [8], 4.7 mm [13] and 5 mm medial to the malar tubercle [20], and are comparable to our findings (5.0 mm). The distance from the medial orbital margin to the endocanthion is more variable: 4.8 mm [8], 9.8 mm (Kim et al., [13], approximately 2 mm lateral to the MOM [20] and 4.8 mm (current study). The variation noted in the Korean sample [13] might be due to the presence of epicanthal folds in people of Asian descent. Epicanthal folds that cover the endocanthion may influence the inclination of the eye fissure's in the longitudinal axis, by shifting the medial point of the axis from the endocanthion to a lower positioned point at the crossing of the epicanthus with the rim of the lower eyelid [21]. It may also be influenced by the size and shape of the nasal root [21].

Considering the position of the eyeball in the orbit, measurements found in this study are consistent with many previous studies, indicating a more supero-laterally placed eyeball [8, 10-12, 22, 23].. Distances observed in this population group were measured as 3.4 mm from the SOM, 6.1 mm from the IOM, 8.3 mm from the MOM and 4.2 mm from the LOM. Specific distances reported by other authors, Stephan et al. (2009) for instance, are as follows: 4.0 mm from the SOM, 6.9 mm from the IOM, 8.0 mm from the MOM and 3.9 mm from the LOM and Whitnall [10, 11]: 4.0 mm from the SOM, 6.8 mm from the IOM, 6.5 mm MOM and 4.5 mm from the LOM. Although some measurements are similar to other studies (e.g., [8, 10-

12]), small differences observed cumulatively in the transverse plane (i.e. the medial equator to MOM and lateral equator to LOM), are indicative of a greater periorbital space compared to a smaller periorbital space observed in the longitudinal axis (i.e. the superior equator to SOM and inferior equator to IOM). These greater distances in the transverse axis in the African group is probably related to the more rectangular shape of the orbit in this group.

Evaluation of the diameters of the eyeball (summarised in Table 3) indicate an oval shape (elongation in the transverse axis) which has also been observed by clinicians [16, 24]. The medio-lateral diameter of the eye in Africans is slightly greater than the supero-inferior diameter, but also to a small extent (approximately 1 mm) greater than in other population groups [15, 25]. All diameters were marginally greater on CBCT than reported on other modalities and other groups while the CT findings were more in agreement with previous findings [15, 24-26].

In conclusion, it was found that dimensions of the eye itself and its relative position in the orbit in South Africans varied minimally from the established guidelines. However, the more rectangular orbit resulted in a more transversely elongated eyeball which was located supero-laterally within the orbit. The exocanthion in this group was situated lower than the endocanthion, in contrast to what was found in other studies. These variations can have a significant impact on the approximation of this pivotal feature. The combined effect of these variations can influence the likelihood of an unknown individual being identified, and therefore population specific standards should be used in cases of facial approximation.

**Table 3. Summary of variations in eyeball diameters**

Author(s)	Year	Modality	n	Ancestry	Antero-posterior diameter	SD	Medio-lateral diameter	SD	Supero-inferior diameter	SD
<b>Wilkinson &amp; Mautner</b>	2003	MRI	39	European	23.28	1.66	-	-	-	-
<b>Guyomarc'h et al.</b>	2012	CT	375	French	23.7	-	24.3	-	24.6	-
<b>Bekerman et al.</b>	2014	CT	500	Mixed ancestral groups	22.1 – 24.9	-	24.1 – 24.3	-	23.7 – 23.8	-
<b>Özer et al.</b>	2016	CT	198	Turkish	22.7 (females) 23.3 (males)	6.38 (females) 0.88 (males)	-	-	-	-
<b>This study</b>	2017	Dissections	36	SA	-	-	25.2	1.42	23.6	1.29
<b>This study</b>	2017	CT	30	SA	23.2	1.07	24.1	0.73	23.1	0.75
<b>This study</b>	2017	CBCT	30	SA	25.1	0.56	25.4	0.38	24.1	0.64

## References

- [1] E.N. L'Abbé, M. Loots, J.H. Meiring, The Pretoria Bone Collection: a modern South African skeletal sample, *HOMO - Journal of Comparative Human Biology* 56 (2005) 197-205.
- [2] D. Cavanagh, M. Steyn, Facial reconstruction: soft tissue thickness values for South African black females, *Forensic Science International* 206 (2011) 215. e1-215. e7.
- [3] E. Hjelmas, J. Wroldsen, Recognizing faces from the eyes only, In *Proceedings of the 11th Scandinavian Conference on Image Analysis*, Citeseer, 1999.
- [4] H.D. Ellis, J.W. Shepherd, G.M. Davies, Identification of familiar and unfamiliar faces from internal and external features: some implications for theories of face recognition, *Perception* 8 (1979) 431-439.
- [5] S.J. McKelvie, The role of eyes and mouth in the memory of a face, *The American Journal of Psychology* (1976) 311-323.
- [6] N.D. Haig, Exploring recognition with interchanged facial features, *Perception* 15 (1986) 235-247.
- [7] N.D. Haig, The effect of feature displacement on face recognition, *Perception* 42 (1984) 1158-1165.
- [8] C.N. Stephan, P.L. Davidson, The placement of the human eyeball and canthi in craniofacial identification, *Journal of Forensic Sciences* 53 (2008) 612-619.
- [9] C. Wilkinson, C. Rynn, *Craniofacial Identification*, Cambridge University Press, 2012.
- [10] S.E. Whitnall, *The anatomy of the human orbit and accessory organs of vision*, Oxford Medical Publications, London, 1921.
- [11] S.E. Whitnall, *The anatomy of the human orbit and accessory organs of vision*, Oxford University Press, London, 1932.
- [12] C.N. Stephan, A.J.R. Haug, P.L. Davidson, Further evidence on the anatomical placement of the human eyeball for facial approximation and craniofacial superimposition, *Journal of Forensic Sciences* 54 (2009) 267-269.
- [13] S.-R. Kim, K.-M. Lee, J.-H. Cho, H.-S. Hwang, Three-dimensional prediction of the human eyeball and canthi for craniofacial reconstruction using cone-beam computed tomography, *Forensic Science International* 261 (2016) 164.e1-164.e8.
- [14] T. Stewart, The points of attachment of the palpebral ligaments: their use in facial reconstructions on the skull, *Journal of Forensic Science* 28 (1983) 858-863.
- [15] P. Guyomarc'h, B. Dutailly, C. Couture, H. Coqueugniot, Anatomical placement of the human eyeball in the orbit—validation using CT scans of living adults and prediction for facial approximation, *Journal of forensic sciences* 57 (2012) 1271-1275.
- [16] I. Bekerman, P. Gottlieb, M. Vaiman, Variations in Eyeball Diameters of the Healthy Adults, *Journal of Ophthalmology* 2014 (2014) 5.
- [17] mediLexicon, *Equator of Eyeball*, mediLexicon, 2017.
- [18] P.Z. Mala, Pronasale Position: An Appraisal of Two Recently Proposed Methods for Predicting Nasal Projection in Facial Reconstruction, *Journal of Forensic Sciences* 58(4) (2013) 957-963.
- [19] A.C. Oettlé, F.P. Demeter, E.N. L'abbé, Ancestral Variations in the Shape and Size of the Zygoma, *The Anatomical Record* 300 (2017) 196-208.
- [20] T. Balueva, E. Veselovskaya, E. Kobylansky, Craniofacial reconstruction by applying the ultrasound method in live human populations, *International Journal of Anthropology* 24 (2009) 87-111.
- [21] L. Farkas, *Anthropometry of the head & face*, 2nd ed., Raven Press, New York, 1994.
- [22] A. Bron, R. Tripathi, B. Tripathi, *Wolff's anatomy of the eye and orbit*, 8Ed, Taylor & Francis, 1998.
- [23] W.W. Goldnamer, *The anatomy of the human eye and orbit*, Professional Press, 1923.
- [24] C.M. Özer, I.I. Öz, I. Serifoglu, M.Ç. Büyükuysal, Ç. Barut, Evaluation of Eyeball and Orbit in Relation to Gender and Age, *Journal of Craniofacial Surgery* 27 (2016) e793-e800.
- [25] I. Bekerman, P. Gottlieb, M. Vaiman, Variations in eyeball diameters of the healthy adults, *Journal of ophthalmology* 2014 (2014).
- [26] C.M. Wilkinson, S.A. Mautner, Measurement of eyeball protrusion and its application in facial reconstruction, *Journal of Forensic Sciences* 48 (2003) 12-16.